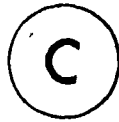


MODELLING SOLAR RADIATION TRANSMISSION  
IN CLOUDY ATMOSPHERES

By



JAMES E. HOWARD, B.Sc.

A Thesis

Submitted to the School of Graduate Studies  
in Partial Fulfilment of the Requirements

for the Degree

Master of Science

McMaster University

January 1982

MODELLING SOLAR RADIATION TRANSMISSION IN CLOUDY ATMOSPHERES

MASTER OF SCIENCE  
(Geography)

McMASTER UNIVERSITY  
Hamilton, Ontario

TITLE: Modelling Solar Radiation Transmission in Cloudy  
Atmospheres

AUTHOR: James E. Howard, B.Sc. (McMaster University)

SUPERVISOR: Professor J.A. Davies

NUMBER OF PAGES: XIII, 146

## Abstract

The transmission of solar radiation through cloudy atmospheres was examined using nine years of continuous hourly radiation and meteorological records. Transmittances of clouds were empirically determined using data from five stations in southern Canada. Statistical parameters were evaluated for exponential, linear and constant expressions for transmittance of global radiation. Parameters were also determined for global irradiances after correcting for multiple reflection between the surface and atmosphere. Exponential and linear uncorrected results compared well with previous work, however marked differences were noted in comparisons of constant transmittance values for Canada with those calculated for Hamburg, Germany and those for Blue Hill, Massachusetts. Multiple reflection effects were shown to enhance the surface irradiance by as much as 30%. Results of regression analysis indicated transmittance to be effectively independent of zenith angle.

Several expressions for estimating direct beam transmittance were tested in a numerical model using data from three stations in eastern Canada. Results showed the present form, the product of global radiation and one minus the total cloud opacity, performed best thereby justifying its further usage.

Results of direct beam and cloud transmittance analyses were combined to estimate direct, diffuse and global surface irradiances. Results were compared with measured fluxes for hourly, daily, monthly and monthly mean hourly time periods. Correcting for multiple reflection underestimated surface irradiances. No improvement in performance was obtained in models using uncorrected Canadian-derived parameters over existing parameters determined for Blue Hill. Underestimation of transmittance by the corrected parameters was attributed to the presence of undetected overlying cloud above the overcast deck. Although mean bias error values are better for global irradiances determined using the original Blue Hill parameters, it is shown that differences in model estimates which used Canadian data are within the range of uncertainties on the calculated values of the solar constant, aerosol transmission and surface albedo.

## Acknowledgements

This project was supported by contracts from the Atmospheric Environment Service.

I would like to express my sincere gratitude to Dr. J.A. Davies for his invaluable assistance and guidance throughout the project and his critical review of the text. Also, the aid of Dr. W.R. Rouse, Dr. J.J. Drake and Mr. Michael Yu of McMaster University and Dr. Don McKay of the Atmospheric Environment Service was appreciated. I am very grateful to fellow students Bruce McArthur, Rick Bello, Allan Sawchuk, Kathie Stewart and Johnny Forster for their helpful comments and good company. My gratitude also extends to my parents for their encouragement and allowing me the opportunity to pursue my education. Many of the plots were done using subroutine GRAFF by J.J. Drake and J.G. Cogley. Typing of the draft was done by Darlene Watson.

Finally, I wish to thank my wife Linda for her infinite patience and encouragement throughout.

## Table of Contents

	Page
DESCRIPTIVE NOTE	ii
ABSTRACT	iii
ACKNOWLEDGEMENTS	v
TABLE OF CONTENTS	vi
LIST OF ILLUSTRATIONS	ix
LIST OF TABLES	xii
LIST OF APPENDICES	xiv
CHAPTER ONE - INTRODUCTION	
1.1 Introductory Remarks	1
1.2 Treatment of Cloud	3
1.3 Aims of the Study	7
CHAPTER TWO - TRANSMISSION OF SOLAR RADIATION THROUGH CLOUDS	
2.1 Theoretical Background	8
2.2 Empirical Approach	13
CHAPTER THREE - DETERMINATION OF CLOUD PARAMETERS	
3.1 Data	18
3.2 Calculation of Relative Optical Air Mass	21
3.3 Re-evaluation of Cloud Transmittance Parameters using the Original Haurwitz Method	23
3.3.1 Results	23
3.4 Calculation of Transmittance Parameters after Correcting for Multiple Reflection	32

3.4.1	Results	36
3.5	Analysis of Seasonal Variation	45
3.5.1	Results	45
CHAPTER FOUR	- CLOUD TYPE TRANSMITTANCES	
4.1	Transmission Calculation	54
4.2	Results	54
4.2.1	Exponential Transmittance	54
4.2.2	Linear Transmittance	62
4.2.3	Constant Transmittance	62
4.3	Results of Seasonal Analysis	66
4.4	Variations in Transmittance Among Canadian Stations	68
4.5	Comparison of Empirical and Theoretical Cloud Transmissions	68
4.5.1	Results	70
CHAPTER FIVE	- MODEL CALCULATIONS OF SURFACE IRRADIANCE	
5.1	Direct Beam Radiation	73
5.1.1	Expressions for Transmittance	73
5.1.2	Performance Measures	76
5.1.3	Results	77
5.2	Global Radiation	80
5.2.1	MAC Model Transmittance Formulation	81
5.2.2	Results	82
5.3	Diffuse Radiation	92
5.3.1	Results	92
5.4	Discussion of Results	94
5.4.1	Solar Constant	95
5.4.2	Aerosol Parameterization	96
5.4.3	Water Vapour Absorption	98



	5.4.4	Surface Albedo	99
	5.4.5	Atmospheric Backscatter	100
CHAPTER SIX	-	SUMMARY AND CONCLUSIONS	
	6.1	Summary	102
	6.2	Conclusions	104
	6.3	Recommendations for Future Study	106
REFERENCES			108
APPENDIX	A	List of Symbols	114
APPENDIX	B	Formulation of the MAC Layer Model	119
APPENDIX	C.1	Description of Data	124
	C.2	Record Format Specification	124
	C.3	Required Data	125
APPENDIX	D	Listings of Computer Programs	126
APPENDIX	E.1	Cloud Transmission Results for Individual Stations	142
	E.2	Mean Seasonal Cloud Type Transmittances (uncorrected)	145
	E.3	Mean Seasonal Cloud Type Transmittances (corrected)	146

## List of Illustrations

Figure		Page
1.1	Solar radiation stations in the AES network as of January 1977. (Davies and Hay, 1980)	2
3.1	Global irradiance curves for altocumulus cloud for individual stations, pooled data and the Haurwitz transmittance parameters.	24
3.2	Global irradiance curves for altostratus cloud for individual stations, pooled data and the Haurwitz transmittance parameters.	25
3.3	Global irradiance curves for cirrostratus cloud for individual stations, pooled data and the Haurwitz transmittance parameters.	26
3.4	Global irradiance curves for cirrus cloud for individual stations, pooled data and the Haurwitz transmittance parameters.	27
3.5	Global irradiance curves for stratocumulus cloud for individual stations, pooled data and the Haurwitz transmittance parameters.	28
3.6	Global irradiance curves for stratus cloud for individual stations, pooled data and the Haurwitz transmittance parameters.	29
3.7	Global irradiance curves for fog for individual stations, pooled data and the Haurwitz transmittance parameters.	30
3.8	Schematic illustration of multiple reflection of transmitted radiation ( $t$ ) between ground surface ( $\alpha_s$ ) and atmosphere ( $\alpha_b$ ).	33
3.9	Global irradiance curves for altocumulus cloud after correcting for multiple reflection.	39
3.10	Global irradiance curves for altostratus cloud after correcting for multiple reflection.	39

3.11	Global irradiance curves for cirrostratus cloud after correcting for multiple reflection.	40
3.12	Global irradiance curves for cirrus cloud after correcting for multiple reflection.	40
3.13	Global irradiance curves for stratocumulus cloud after correcting for multiple reflection.	41
3.14	Global irradiance curves for stratus cloud after correcting for multiple reflection.	41
3.15	Global irradiance curves for fog after correcting for multiple reflection.	42
3.16a,b	Distribution of scatter in overcast global irradiance measurements of altocumulus (a) and cirrus (b) clouds.	43
3.17	Uncorrected seasonal and all-year global irradiance curves for altocumulus cloud.	50
3.18	Corrected seasonal and all-year global irradiance curves for altocumulus cloud.	50
3.19	Uncorrected seasonal and all-year global irradiance curves for altostratus cloud.	51
3.20	Corrected seasonal and all-year global irradiance curves for altostratus cloud.	51
3.21	Uncorrected seasonal and all-year global irradiance curves for stratocumulus cloud.	52
3.22	Corrected seasonal and all-year global irradiance curves for stratocumulus cloud.	52
3.23	Uncorrected seasonal and all-year global irradiance curves for stratus cloud.	53
3.24	Corrected seasonal and all-year global irradiance curves for stratus cloud.	53
4.1	Cloudless sky global irradiances of Blue Hill, Massachusetts and pooled data for Canada.	57
4.2	Transmittance curves of altocumulus cloud for Blue Hill and pooled Canadian data.	58
4.3	Transmittance curves of altostratus cloud for	

	Blue Hill and pooled Canadian data.	58
4.4.	Transmittance curves of cirrostratus cloud for Blue Hill and pooled Canadian data.	59
4.5	Transmittance curves of cirrus cloud for Blue Hill and pooled Canadian data.	59
4.6	Transmittance curves of stratocumulus cloud for Blue Hill and pooled Canadian data.	60
4.7	Transmittance curves of stratus cloud for Blue Hill and pooled Canadian data.	60
4.8	Transmittance curves of fog for Blue Hill and pooled Canadian data.	61

List of Tables .

Table		Page
3.1	Numbers of Observations with Overcast Conditions	20
3.2	Parameter Values for Haurwitz's Radiation Model	31
3.3	Data for Calculating Surface Albedo	37
3.4	Parameter values for Haurwitz's radiation model using corrected mean global irradiance data for Canada	44
3.5	Number of hours of data within each season at each station for each of four cloud types	46
3.6	Seasonal parameter values for four cloud types using uncorrected global irradiance data	48
3.7	Seasonal parameter values for four cloud types using corrected global irradiance data	49
4.1	Parameter Values for Cloudless Sky Global Irradiances	56
4.2	Cloud-Type Transmittance Parameters	56
4.3	Cloud Transmission Results	63
4.4	Mean Transmittance Values	64
4.5	Mean Seasonal Cloud Transmittances	67
4.6	Variation in Mean Transmittance Among Stations	69
4.7	Transmission of Solar Radiation Through Clouds	71
5.1	Formulations of Direct Beam Transmittance	74
5.2	Model Performance for Direct Beam Irradiance	78
5.3	Cloud Type Albedo	83
5.4	Cloud Transmittance Functions	83

5.5	Model Variants	84
5.6	Cloud-Type Groups	84
5.7	Parameter Values used in Model Variants	85
5.8	Model Performance for Global Irradiance	91
5.9	Model Performance for Diffuse Irradiance	93
5.10	Mean Bias Errors for $k = 1.0$ and $k < 1.0$	97
5.11	Errors in Precipitable Water Estimates	97

## CHAPTER ONE

### INTRODUCTION

#### 1.1 Introductory Remarks

Solar radiation is important to the environmental and agricultural sciences since it is the driving force for physical processes in the Earth-Atmosphere System. In addition, it is significant in the design and planning of solar energy systems. The availability of measured radiation data however is spatially and temporally limited. Although Canada's measurement network is extensive compared with many countries (Davies and Idso, 1979), large gaps exist throughout many parts of the country (Figure 1.1). Data for these areas can be provided by calculations using numerical models.

Calculation procedures range in complexity from regression equations which use either sunshine duration or cloud amount as predictors of surface irradiance to numerical solutions of the radiative transfer equation. The latter require large amounts of computer time since calculations must be made spectrally which limits widespread usage. Regression models, on the other hand, have generally been developed for a specific location and may not be

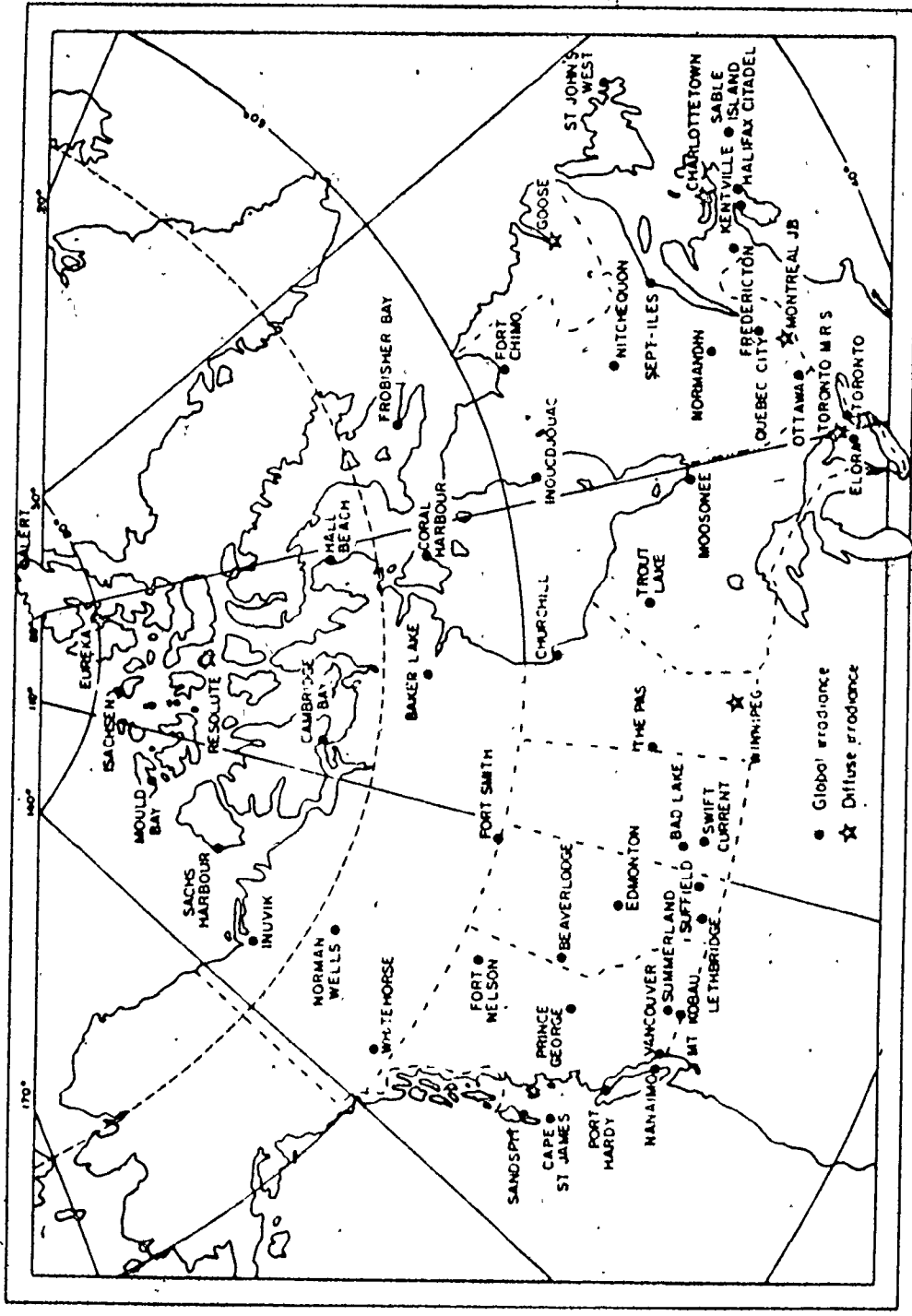


Figure 1.1 Solar radiation stations in the AES network as of January 1977. (Davies and Hay, 1980)



applicable elsewhere.

Between these two extremes are the "layer" models (Atwater and Brown, 1974; Davies et al., 1975 Suckling and Hay, 1977). These are simplified solutions to the radiative transfer equation which avoid detailed spectral calculations and use empirical expressions to calculation atmospheric attenuation processes.

## 1.2 Treatment of Cloud

Clouds exert the greatest control on the transfer of radiation and introduce the greatest uncertainty into model calculations. The uncertainty arises for several reasons. First, variable cloud geometry, size and structure produce large variations in optical properties even for clouds of the same type. Secondly, large changes in cloud cover often occur in a short period of time. Since clouds develop and disperse quickly, even hourly observations may not be sufficiently frequent to sample the variation in cloud conditions throughout the day. Thirdly, surface-based cloud observations of middle and upper level clouds are often restricted or prohibited altogether by the presence of lower cloud. Satellites can provide cloud information by remote sensing techniques but limitations in resolution, and confusion between ground and cloud reflection limit its usefulness at present. At best, the use of cloud cover data in layer models provides a crude

approximation of real atmospheric cloud conditions.

Layer models use mean transmission properties of clouds in their calculations. However, these properties have received little study. The most comprehensive study to date by Haurwitz (1948) used data collected at the Blue Hill Observatory in Massachusetts. He related measured hourly global radiation  $G$  under overcast skies at the surface to optical air mass  $m$ ,

$$G_c = a_j/m \exp(-b_j m) \quad 1.1$$

where  $a$  and  $b$  are statistically determined parameters for each cloud type,  $j$ . Only overcast conditions of one cloud type were considered. A similar analysis for cloudless skies allowed clear sky irradiances to be calculated from

$$G_0 = a_0/m \exp(-b_0 m) \quad 1.2$$

Haurwitz's parameter values have been used in all layer models.

Vowinckel and Orvig (1962) have provided the only study of cloud transmissions in Canada. They investigated the variability in transmittance of Arctic clouds. Results showed that transmission varied significantly with season, location and solar zenith angle. The variability in transmission of a particular cloud type with location was often greater than the variability in transmission between different cloud types at one location. Transmission increased with latitude, solar altitude and was

largest in winter. Seasonal and latitudinal variations were attributed to thinner clouds characteristic of colder environments. Arctic clouds tend to be thinner and more stratiform than clouds in temperate zones due to reduced convection. Optical depth and cloud top albedo increase with cloud depth thereby reducing the radiation which enters the cloud and attenuating more while passing through the cloud. Thus, less radiation is transmitted through thicker clouds formed in warmer environments where convective forces are stronger. Solar altitude determines the angle of incidence of direct beam radiation. As the angle of incidence decreases in summer, cloud top albedo decreases, thus transmitting more radiation. However, the thicker clouds in summer attenuate more radiation hence negating the effect of decreased cloud top albedo.

Schertzer (1975) attempted to redefine Haurwitz's cloud coefficients using the same method as Haurwitz with data for Southern Ontario collected during the International Field Year for the Great Lakes (IFYGL). Data for Kingston, Peterborough and Trenton were pooled to establish a large enough data base. There were, however, few observations of overcast cumuloform clouds. Results of a test with the revised cloud coefficients showed that transmissions were reduced suggesting cloud transmittances determined for the Canadian stations were smaller than those for Blue Hill.

Atwater and Brown (1974) used Haurwitz's data to express transmission  $t_j$  as a linear function of optical air mass.

$$t_j = c_j + d_j m$$

1.3

More recently Atwater and Ball (1980) obtained  $c$  and  $d$  values for cumuloform clouds using data from the Global Atmospheric Research Program's Atlantic Tropical Experiment (GATE). The data, obtained from ground-based, plane and satellite observations, were very limited (August 30-September 19, 1974). However, their results did show that cloud transmission is independent of solar zenith angle (and, therefore, of air mass) and a constant mean transmittance value could be applied to a specific cloud type. This air mass independence was also noted by Kasten and Czeplak (1980).

Cloud cover also determines the atmospheric transmission of direct beam radiation to the surface. Under cloudless skies, many models estimate surface irradiance to an accuracy within 5%, (Lacis and Hansen, 1974; Hottel, 1974; King and Buckius, 1979). Results are much poorer however, when cloud is present. Direct beam radiation has been calculated in the layer models from various measures of sky transmittance; (i)  $1-CA$ , where  $CA$  is the fractional cloud amount (Davies and Hay, 1978), (ii)  $1-CO$ ; where  $CO$  is the fractional cloud opacity (Davies, 1980), or (iii)  $s$ , the duration of sunshine (Suckling and Hay, 1977). Although sunshine duration should be directly related to the direct beam irradiance, results of layer models which use sunshine duration as an indicator of sky transmittance have been unimpressive. This may be due to the inability of the Campbell-

Stokes sunshine recorder to register weak irradiances at large zenith angles, thus underestimating sunshine duration and the recorder's tendency to "overburn" the recording paper when sunny and cloudy periods alternate quickly, hence overestimating sunshine.

### 1.3 Aims of the Study

This study examines the transmission of global and direct beam solar radiation through cloudy atmospheres. Nine years of hourly data records from 1968-1976 collected at five stations across Southern Canada were used to develop mean transmission properties of clouds for Canada. Analytical procedures identical or similar to those used in previous work are employed to evaluate cloud parameters for several transmission expressions. In addition, various methods of calculating the direct beam irradiance at the surface are tested. Revised beam and global radiation transmittances are then computed in a layer model and the results compared with those obtained with the Haurwitz cloud parameterization.

## CHAPTER TWO

### TRANSMISSION OF SOLAR RADIATION THROUGH CLOUDS

#### 2.1 Theoretical Background

The transmission of solar radiation through a cloud is determined by, optical depth, single scattering albedo of the cloud droplets and the asymmetry factor of those droplets. Specification of these variables is difficult since the geometry and microphysics of clouds are highly variable even for clouds of the same type. Theoretical transmissions can be calculated using the Mie theory for model clouds with specified boundary conditions.

Clouds are assumed to consist of spherical water droplets with geometrical cross-section  $G_X$  given by

$$G_X = \pi r^2 \quad 2.1$$

where  $r$  is the radius of the cloud droplet. The optical cross-section for extinction  $C_{ex}$  is the area normal to the incident beam which would attenuate the same amount of radiation as the spherical particle. The efficiency factor of extinction  $Q_{ex}$  is the ratio of optical to geometrical cross-sections of the

cloud droplet.

$$Q_{ex} = C_{ex}/GX \quad 2.2$$

It is a function of the radius of the droplet and the complex index of refraction,  $m_{IR}$ . The imaginary part of the index controls the fraction of the attenuation due to absorption ( $m_{IMAG}$ ) while the real part determines attenuation by scattering ( $m_{REAL}$ ). It is given by,

$$m_{IR} = m_{REAL} - m_{IMAG} i \quad 2.3$$

where  $i = \sqrt{-1}$ . If  $m_{IMAG} = 0$ , the particle only scatters. The efficiency factor is also a function of wavelength  $\lambda$ . The size of the droplet and wavelength of radiation are often combined into the Mie size parameter  $X$  given by,

$$X = 2\pi r/\lambda \quad 2.4$$

For a monodispersion of cloud droplets (all of the same particle size) the optical cross-section of extinction is

$$C_{ex} = GXQ_{ex}(m_{IR}, X) \quad 2.5$$

However, clouds are always a polydispersion (more than one particle size) hence, this expression must be integrated over the entire

range of radii. The total optical cross-section per unit volume is the extinction coefficient  $\beta_{ex}$  and is calculated from

$$\beta_{ex} = \int_0^{\infty} \pi r^2 Q_{ex}(m_{IR}, x) n(r) dr [km^{-1}] \quad 2.6$$

where  $n(r)$  is the number of particles per unit volume with radii in the interval defined by  $r$  to  $r + dr$ . The extinction coefficient is the sum of a scattering component  $\beta_{sc}$  and an absorption component  $\beta_{ab}$ ,

$$\beta_{ex} = \beta_{sc} + \beta_{ab} \quad 2.7$$

This applies to a specific height in the atmosphere. To determine the extinction coefficient for a layer (i.e. a cloud layer) within the atmosphere, Equation 2.6 must be integrated between the upper and lower boundaries,  $z_1$  and  $z_2$ . This is the spectral optical depth,  $\tau$  of the particular layer.

$$\tau(z_1 - z_2) = \int_{z_1}^{z_2} \beta_{ex} dz \quad 2.8$$

Single scattering albedo  $\bar{w}_0$ , is a measure of the effectiveness of scattering by the particle relative to total extinction. It is given by,

$$\bar{w}_0 = Q_{sc}/Q_{ex} = Q_{sc}/(Q_{sc} + Q_{ab}) \quad 2.9$$



The asymmetry factor  $g$  summarizes the distribution of light scattered by the particle. It is defined as the integral over all solid angles of  $P_F(\cos \gamma)$  where  $P_F$  is the phase function and  $\gamma$ , the scattering angle between an impinging and scattered ray.

$$g = \langle \cos \gamma \rangle = \int_{-1}^{+1} P_F(\cos \gamma) \cos \gamma d(\cos \gamma) \quad 2.10$$

This integral can be separated into two parts.

$$g = \int_0^1 (P_F(\cos \gamma) \cos \gamma) d(\cos \gamma) - \int_0^{-1} (P_F(\cos \gamma) \cos \gamma) d(\cos \gamma) \quad 2.11$$

These represent scattering in the forward and backward direction respectively. From this equation it can be shown that the ratio of backward to forward scatter  $bf$  is given by,

$$bf = 0.5 (1 - g) \quad 2.12$$

A value of  $g = 1$  indicates complete forward scatter;  $-1$  complete backward scatter; and  $0$ , isotropic scattering.

Following Paltridge and Platt (1976) transmission  $T_R$  through a homogeneous cloud layer can be determined from the two-stream approximation of the radiative transfer equation as,

$$T_R = 4u / [(u + 1)^2 \exp(\tau_{\text{eff}}) - (u - 1)^2 \exp(-\tau_{\text{eff}})] \quad 2.13$$

$$\text{where } u^2 = (1 - \bar{w}_0 + 2b\bar{w}_0) / (1 - \bar{w}_0) \quad 2.14$$

$$\text{and } \tau_{\text{eff}} = \sqrt{3} u (1 - \bar{w}_0) \tau \quad 2.15$$

These variables depend upon the drop-size distribution within the cloud and the physical geometry of the cloud, both of which can only be estimated. However, scattering by water droplets (and ice crystals) is known to be strongly anisotropic in the forward direction, hence the asymmetry factor  $g$  should be quite close to unity. Various theoretical studies have used the values 0.875 (Danielson and Moore, 1969), 0.80 and 0.95 (Joseph, Wiscombe, and Weinman, 1976), 0.786 (Shettle and Weinman, 1970; Irvine, 1968) and 0.75 (Liou, 1973). Because water and ice particles absorb very little in the visible and near infra-red range of the spectrum values of the single scattering albedo are generally assumed to be one or very close to one. Since the real and imaginary refractive indices of water are very similar to those of ice, the single scattering albedo changes little for different types of cloud consisting of ice or liquid water particles.

Optical depth of the cloud does vary significantly since it is a function of both the spectral extinction coefficient and the geometrical depth of the cloud. Theoretical values of extinction coefficients have been calculated by Carrier et al. (1967) for various types of water clouds. Liou (1973) determined values for cirriform clouds consisting mainly of ice particles. The

extinction coefficient for a particular cloud type changes very little over the range of solar wavelengths used. Hence optical depth is relatively independent of wavelength in the visible part of the spectrum.

## 2.2 Empirical Approach

Layer models use mean empirically determined cloud transmission properties. These are calculated from long-term records of surface-based observations for global irradiance and cloud type. The climatic-mean cloud type transmittance for a single layer of cloud is given by

$$t_i = 1/c_i \{ G(1 - \alpha_s \alpha_b) / G_0 - (1 - c_i) \} \quad 2.16$$

where  $c_i$  is the fractional cloud cover,  $G_c$  and  $G_0$  are the global irradiances under cloudy and cloudless skies respectively  $\alpha_s$  is the reflectivity of the surface and  $\alpha_b$ , the reflectivity of the atmosphere for surface reflected radiation. However, for partially clouded skies, fractional cloud cover is difficult to determine accurately. Hence, only cases of ten-tenths cloud have been considered (Atwater and Ball, 1981). Equation 2.16 then reduces to

$$t_i = G_c(1 - \alpha_s \alpha_b) / G_0 \quad 2.17$$

This expression removes the effects of multiple reflection between the surface and atmosphere. With the exception of the study by Atwater and Ball (1981) this correction has been neglected in previous studies even though it often significantly enhances surface fluxes. In the presence of snow-cover, especially in high latitudes, this effect becomes even more important. Holmgren and Weller (1973) noted that the incoming solar irradiance decreased only slightly under overcast conditions compared with cloudless sky values over an extensive Arctic snow-field. This decrease was about 15% for measurements made in April.

Haurwitz neglected multiple reflection effects and related global radiation under overcast and cloudless sky conditions to optical air mass using Equations 1.1 and 1.2. The statistically determined coefficients  $a_c$ ,  $a_0$ ,  $b_c$  and  $b_0$  were then used by MacLaren et al. (1979) and Davies (1980) to determine values for the parameters A and B in the transmission expression.

$$t_i = A \exp(-Bm_r) \quad 2.18$$

where  $A = a_c/a_0$

and  $B = b_c - b_0$

Since cloudless sky estimates of global radiation are generally good, transmission has also been calculated semi-empirically from measured irradiances under overcast skies and

theoretical values of cloudless sky irradiance. Schertzer (1974), Davies et al (1975) and Suckling and Hay (1977) have used calculated values for cloudless sky global radiation to compute transmission in layer models. Davies and Hay (1980) showed that cloudless sky global irradiance estimates calculated by the MAC model compared well (within 1%) with those reported by Braslau and Dave (1973) who used detailed radiative transfer calculations.

Atwater and Brown (1974) used the same data as Haurwitz (collected at Blue Hill) to derive transmittance coefficients for a linear expression (Equation 1.3). Results from models using either form have been very similar. Kasten and Czeplak (1980) explain why such similar results occur. The exponential term in Equation 2.18 can be expanded to yield,

$$\exp(-Bm_r) = \left( 1 - Bm_r + \frac{Bm_r^2}{2!} - \frac{Bm_r^3}{3!} + \dots \right) \quad 2.19$$

Since B is small, this expression can be truncated after the second term such that transmittance can be approximated by the linear relation,

$$t_i = A - ABm_r \quad 2.20$$

Working with ten years of data collected at Hamburg, Germany Kasten and Czeplak presented climatic-mean cloud type transmissions. They further suggested cloud transmission is independent of geographical latitude and their values are valid for any location with

a climate similar to that of Hamburg. However, they neglected the effects of multiple reflection in the calculations. Atwater and Ball (1981) included multiple reflection effects in their study and obtained significantly different results from those reported by Kasten and Czeplak. Since multiple reflection was not considered by Kasten and Czeplak, it does not seem justified to suggest that results for Hamburg should apply elsewhere.

It is important to emphasize that layer models which use the Haurwitz cloud transmittances and calculate a separate multiple reflection component are including these secondary effects  $n + 1$  times, where  $n$  is the number of cloud layers. This might be expected to result in consistent irradiance overestimates by the model. However, this is not indicated by previous results from the models. A possible explanation for this is that transmittances are determined from overcast data collected when undetected cloud was present above the lower overcast deck. This would result in transmittances being suppressed. If multiple reflections are not removed from the data before calculating transmittance, they tend to compensate for effects from these unseen cloud layers. The consistently good results from previous tests (MacLaren et al., 1979) of layer model performance suggest that these two effects do compensate.

Atwater and Ball introduce a further complication. They suggest that transmittances determined for an overcast layer of cloud are not necessarily typical of cloud in non-overcast conditions. Clouds of a single type may be thicker in overcast

than in partially cloudy conditions. If this is so, cloud transmittances are underestimated since they were determined under overcast skies.

## CHAPTER THREE

### DETERMINATION OF CLOUD PARAMETERS

#### 3.1 Data

Cloud transmittances were determined using long-term averages of hourly radiation and meteorological data provided by the Atmospheric Environment Service for six Canadian stations. These stations were selected to represent the climatic conditions across the southern, most heavily populated parts of the country. Stations chosen were; Toronto and Montreal (urban), Charlottetown (east coast, maritime), Goose Bay (sub-arctic), Winnipeg (continental) and Vancouver (west coast, maritime).

Nine years of data (1968-1976) were used. In 1977 the Atmospheric Environment Service implemented a new system for recording cloud amount which is not suitable for use in existing layer models. Hence, data after 1976 were not considered in this study.

Records of global and diffuse radiation were available for Toronto, Montreal and Goose Bay. Only global radiation was measured at the other stations for the period 1968-1976. Radiation is measured at all stations with Moll-Goryznski (Kipp) pyranometers. A shadow band is used to occult a second similar sensor to measure



the diffuse flux. The AES corrects measurements to include the diffuse irradiance shaded by the band. Latimer (1972) states that the accuracy of the pyranometer is approximately 4% after correcting for temperature dependence. All necessary data were provided by the AES on magnetic tape in the format described in Appendix C.

Hourly records of overcast sky conditions where one cloud type completely covered the first recorded level of cloud were extracted from the data. Lack of sufficient overcast data for most cumuloform clouds prevented analysis of their transmission. Also, no observations of overcast alto cumulus castellanus (ACC) or cirro cumulus (CC) were recorded. Stratus fractus (SF) was not considered separately from stratus (ST) because of its physical similarity. The following seven cloud types remained: (i) alto cumulus (AC), (ii) alto stratus (AS), (iii) cirro stratus (CS), (iv) cirrus (CI), (v) strato cumulus (SC), (vi) stratus (ST), and fog (FOG). The number of observations for each cloud type is given in Table 3.1.

Global irradiances and air mass values were sorted into fifteen air mass intervals between 1.0 and 5.0. Since irradiances for air masses greater than 5.0 are extremely small, data for zenith angles greater than  $78.5^\circ$  were not considered in the analysis. Radiation and air mass means were calculated for each interval yielding a maximum of fifteen data points. Mid-points of the air mass intervals were 1.1, 1.3, 1.5, 1.75, 2.05, 2.35, 2.65, 2.95, 3.25, 3.55, 3.85, 4.15, 4.45, 4.75, 4.95. This procedure was

TABLE 3.1

## Numbers of Observations with Overcast Conditions

Cloud Type	Goose Bay	Charlottetown	Montreal	Toronto	Winnipeg
AC	52	147	212	191	218
ACC	0	0	0	0	0
AS	81	62	97	92	170
CC	0	0	0	0	0
CS	116	36	102	129	172
CI	97	18	39	92	162
CB	0	4	7	8	7
CU	0	30	3	64	16
CF	0	0	6	14	0
SF	64	1102	235	236	279
TCU	0	0	9	18	0
NS	3	0	39	121	6
SC	756	1273	1069	1094	1545
ST	69	254	141	167	499
FOG	34	287	59	252	69
OTF	605	351	318	209	169

repeated for each station except Vancouver which was excluded to permit testing of the statistically derived transmittance parameters at a completely independent station. Mean values for the five stations considered were also pooled to determine cloud type parameters applicable to Canada in general.

### 3.2 Calculation of Relative Optical Air Mass

The formulation given by Rogers (1967) is used to calculate relative optical air mass,  $m_r$ . This formula was selected over the commonly used secant of the zenith angle because it allows for refraction effects which occur at large zenith angles. This value is corrected for atmospheric pressure by multiplying by  $P/P_0$ . Where  $P$  is station pressure (kPa) and  $P_0$  is sea level pressure (101.3 kPa). Air mass is given by,

$$m_r = [35 / (1224 \mu_0^2 + 1)^{3/2}] P/P_0 \quad 3.1$$

where  $\mu_0$  is the cosine of the zenith angle and is given by

$$\mu_0 = \sin \phi \sin \delta + \cos \phi \cos \delta \cos h \quad 3.2$$

in which  $\phi$  is station latitude,  $\delta$  solar declination and  $h$  the solar hour angle in degrees. Hour angle is calculated from

$$h = 15 | 12 - \text{LAT} | \quad 3.3$$

where LAT is local apparent time calculated from

$$\text{LAT} = \text{LST} + \text{ET}/60 + (\text{LMS} - \text{LS})/15 \quad 3.4$$

where LST is local standard time, ET is the equation of time (in minutes) and LS and LMS are the longitudes of the station and the standard meridian of the appropriate time zone. Values of solar declination  $\delta$ , and the equation of time ET are determined using Spencer's (1971) equations,

$$\begin{aligned} \delta = & 0.006918 - 0.39912 \cos \theta_0 + 0.070257 \sin \theta_0 \\ & - 0.006759 \cos 2 \theta_0 + 0.000907 \sin 2 \theta_0 \\ & - 0.002697 \cos 3 \theta_0 + 0.001480 \sin 3 \theta_0. \end{aligned} \quad 3.5$$

$$\begin{aligned} \text{ET} = & 0.000075 + 0.001868 \cos \theta_0 - 0.032077 \sin \theta_0 \\ & - 0.14615 \cos 2 \theta_0 - 0.040840 \sin 2 \theta_0 \end{aligned} \quad 3.6$$

where  $\theta_0$  is the angle (in radians) defined by the day number,  $d_n$ . Day number ranges from 0 on January 1 to 364 on December 31.

$$\theta_0 = 2\pi d_n / 365 \quad 3.7$$

Also needed for astronomical calculations is the radius vector ( $\bar{R}^*/R^*$ ) which accounts for the elliptical shape of the earth's orbit around the sun. It is also a function of  $\theta_0$  and is given by Spencer,

$$\begin{aligned}
 (R^*/R^*)^2 &= 1.00011 + 0.034221 \cos \theta_0 + 0.00128 \sin \theta_0 \\
 &\quad - 0.000719 \cos 2 \theta_0 + 0.000077 \sin 2 \theta_0
 \end{aligned}
 \tag{3.8}$$

### 3.3 Re-evaluation of Cloud Transmittance Parameters using the Original Haurwitz Method

Parameter values for Equation 1.1 were determined by applying the standard least squares procedure to the logarithmic transformation of Equation 1.1 given by

$$\ln G_c = \ln a_c - \ln m - b_c m \tag{3.9}$$

This method was used by Haurwitz and is referred to as Subroutine EXPFIT.

#### 3.3.1 Results

Values of  $a_c$  and  $b_c$  for individual stations as well as those determined for the pooled data are given in Table 3.2. Also presented are those values of  $a_c$  and  $b_c$  determined by Haurwitz. The parameter values were used to calculate the irradiances plotted in Figures 3.1 - 3.7.

Irradiance curves for Blue Hill and the pooled Canadian data are very similar for alto stratus, cirro stratus, cirrus and strato cumulus.

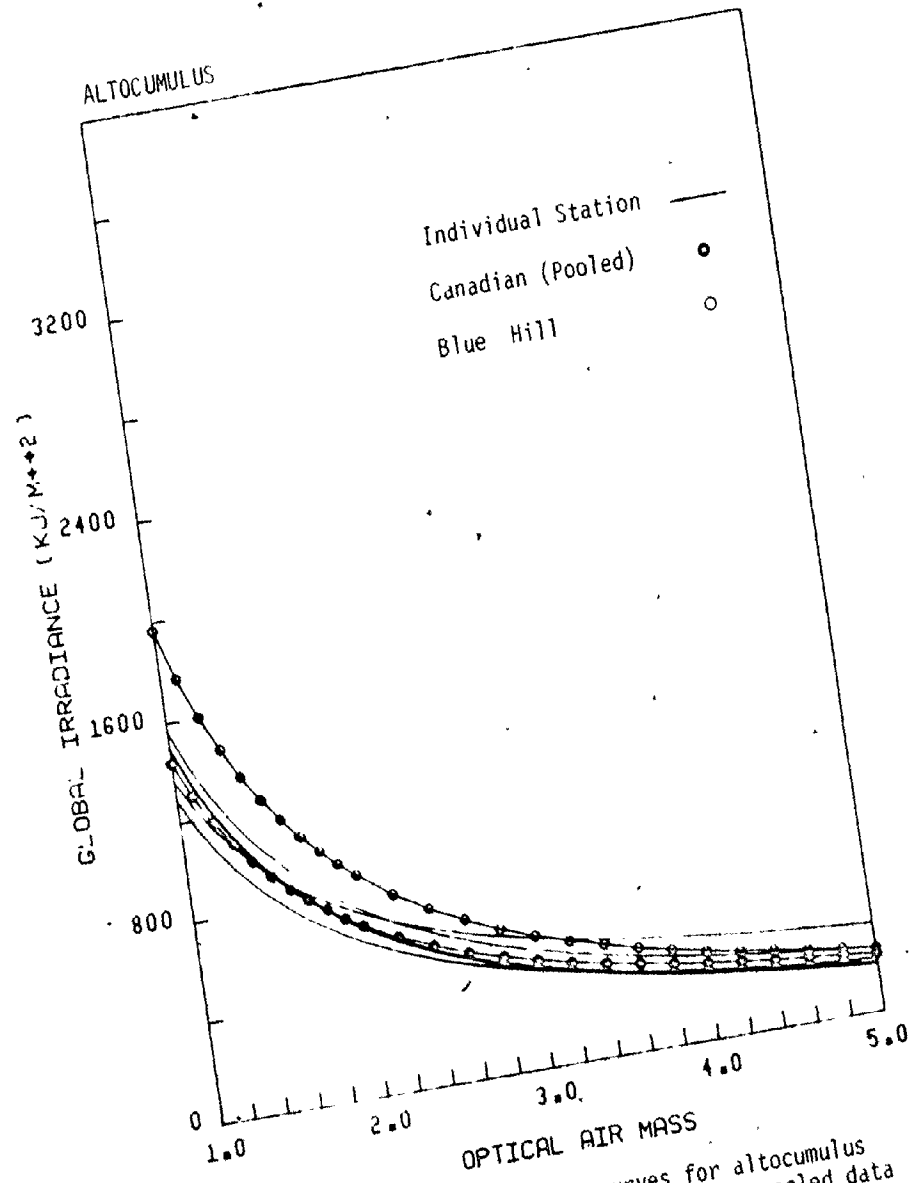


Figure 3.1 Global irradiance curves for altocumulus cloud for individual stations, pooled data and the Haurwitz transmittance parameters.

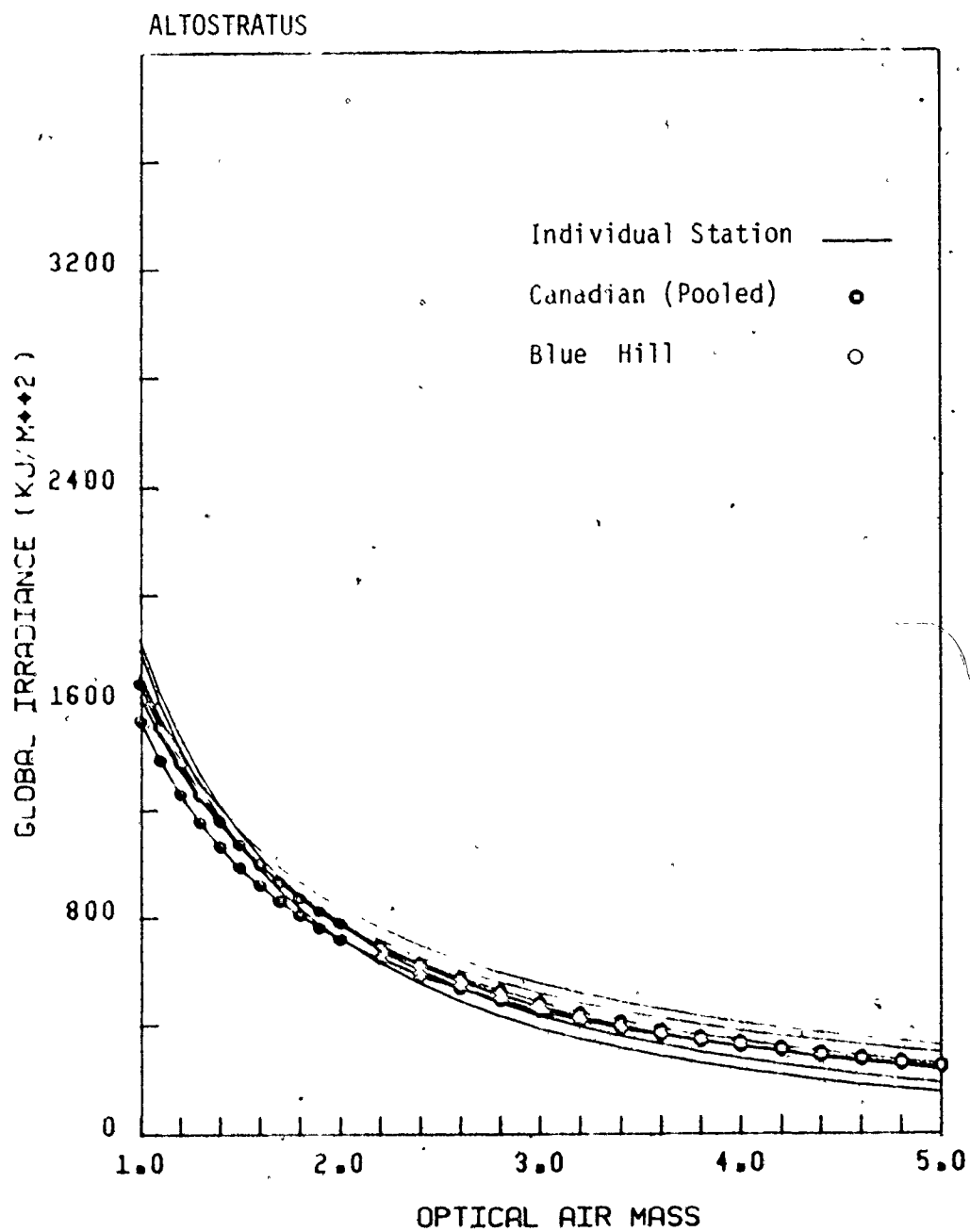


Figure 3.2. Global irradiance curves for altostratus cloud for individual stations, pooled data and the Haurwitz transmittance parameters.

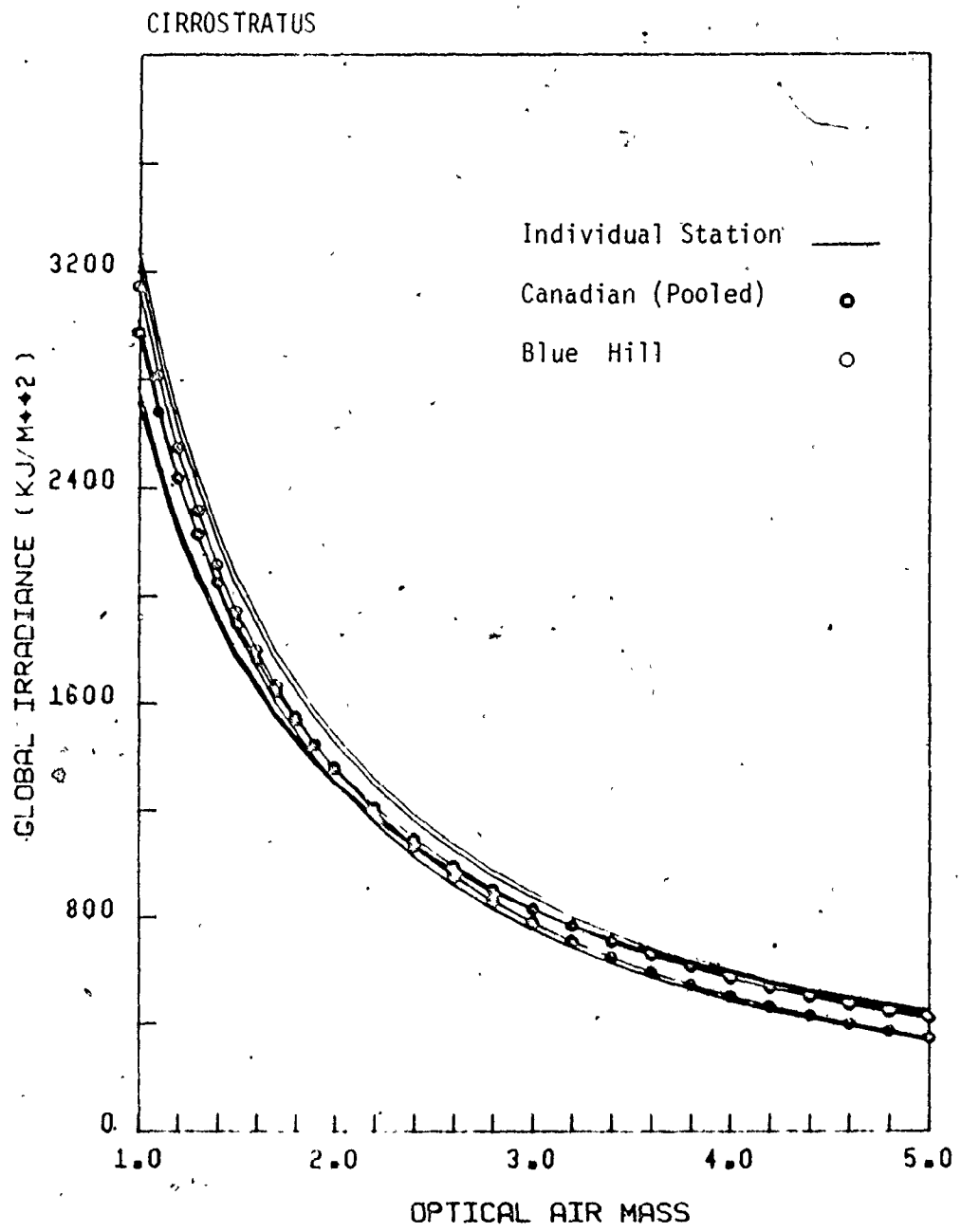


Figure 3.3 Global irradiance curves for cirrostratus cloud for individual stations, pooled data and the Haurwitz transmittance parameters.



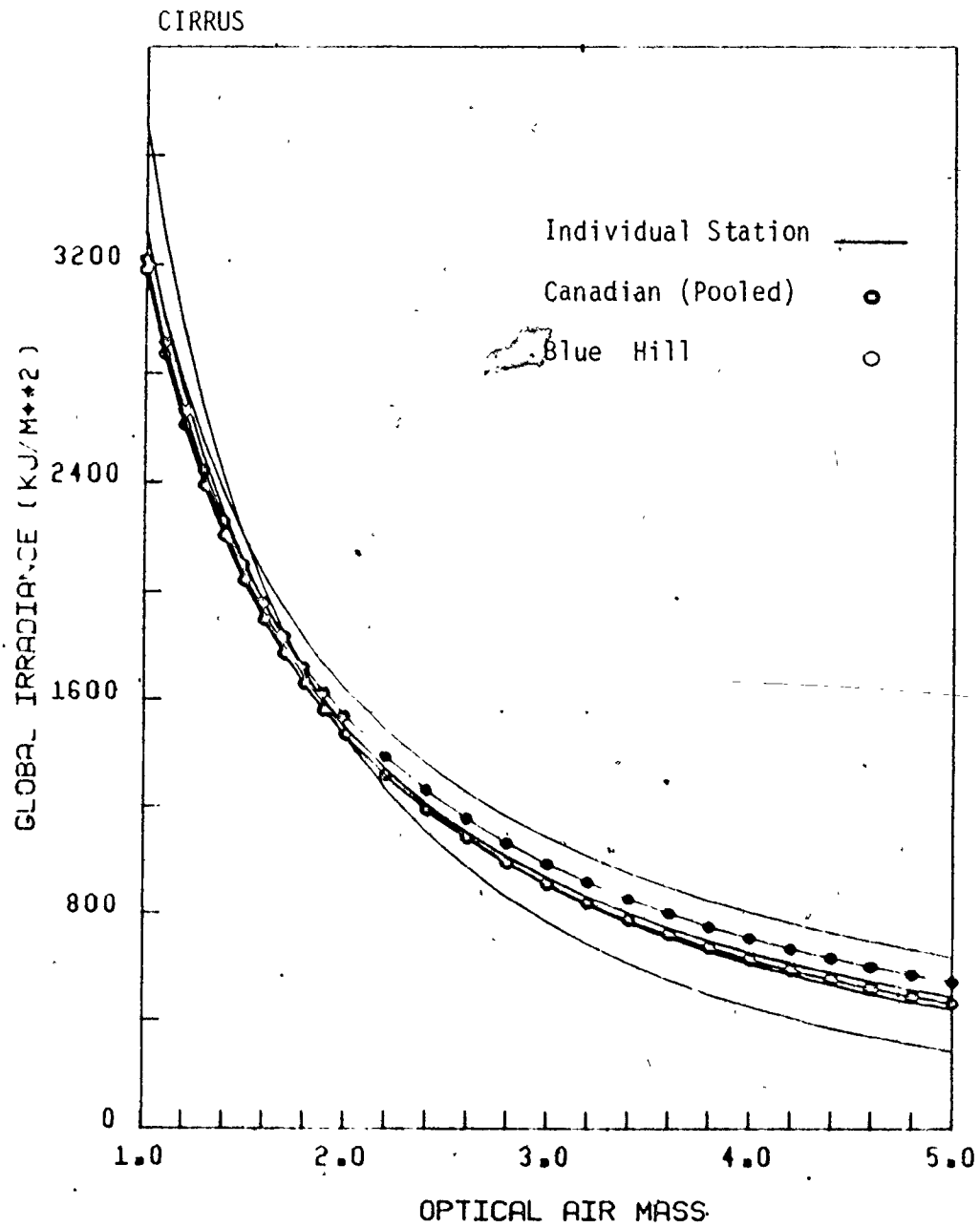


Figure 3.4 Global irradiance curves for cirrus cloud for individual stations, pooled data and the Haurwitz transmittance parameters.

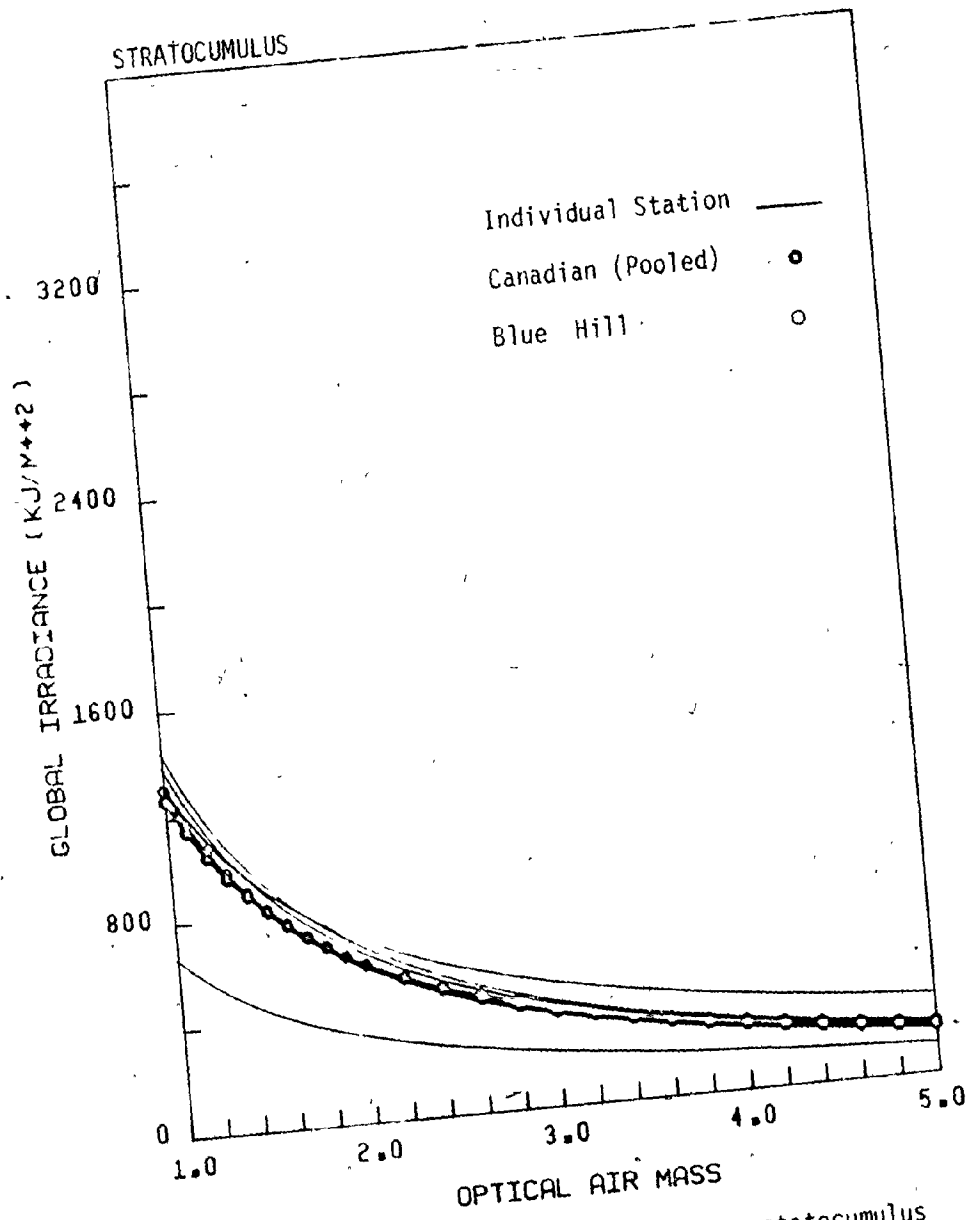


Figure 3.5 Global irradiance curves for stratocumulus cloud for individual stations, pooled data and the Haurwitz transmittance parameters.

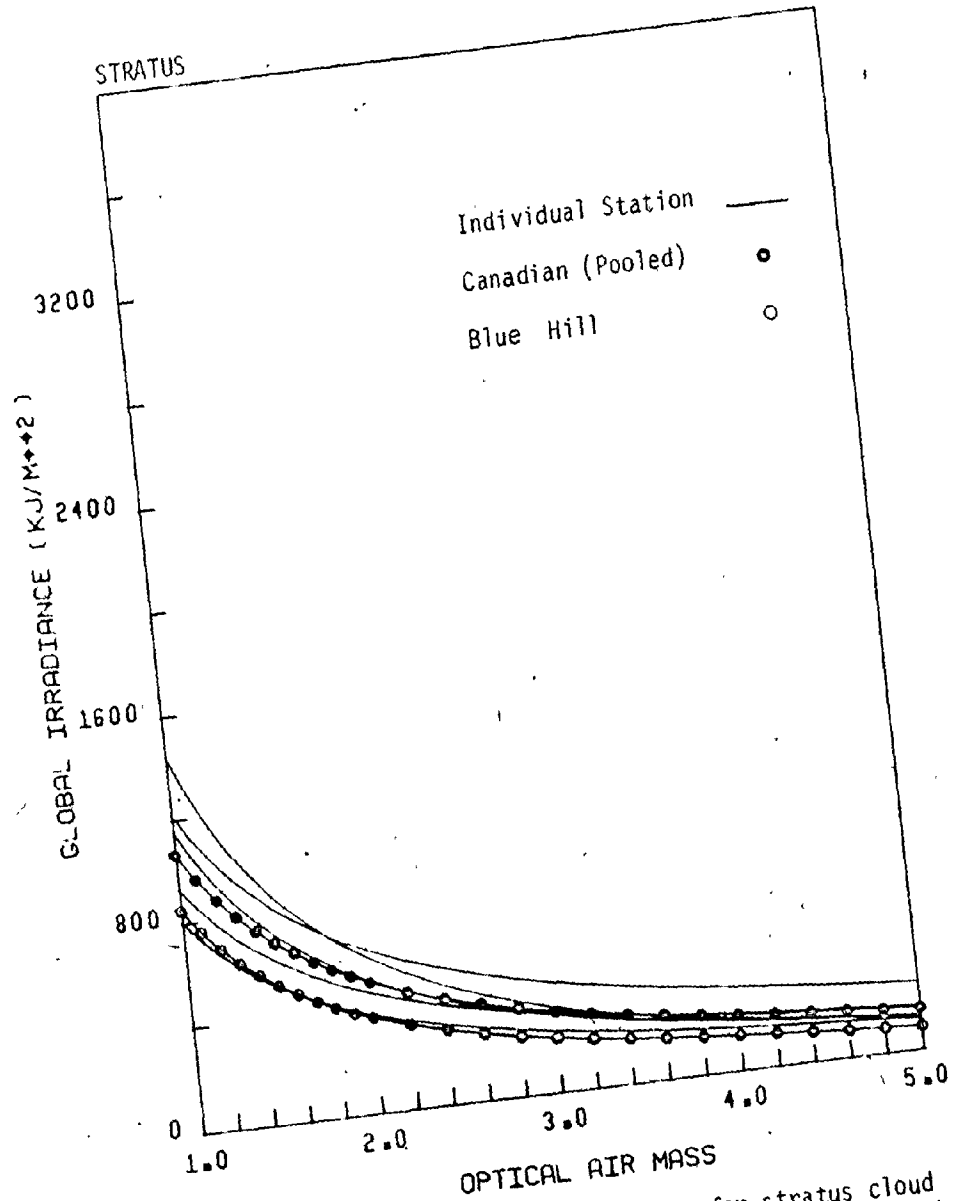


Figure 3.6 Global irradiance curves for stratus cloud for individual stations, pooled data and the Haurwitz transmittance parameters.

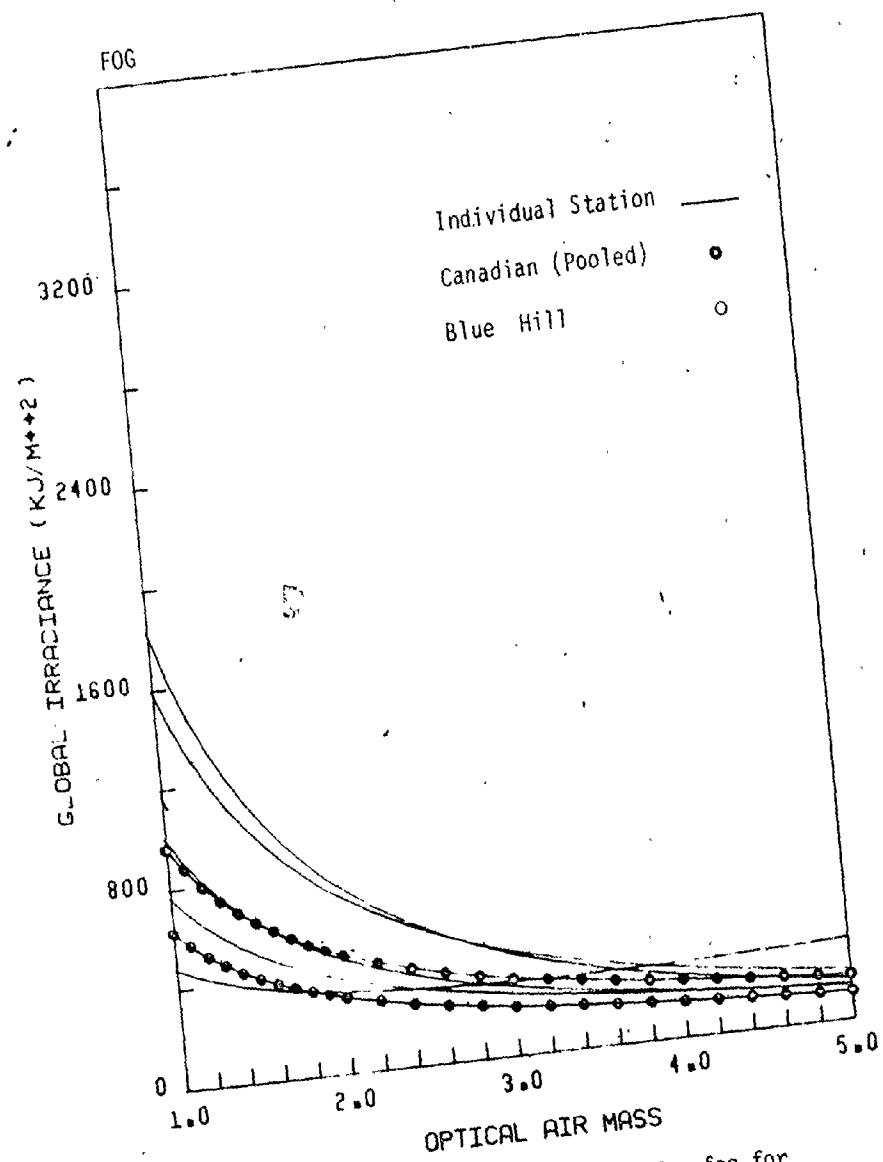


Figure 3.7 Global irradiance curves for fog for individual stations, pooled data and the Haurwitz transmittance parameters.

TABLE 3.2

Parameter Values for Haurwitz's Radiation Model

Cloud Type		Blue Hill	Goose Bay	Charlotte-town	Montreal	Toronto	Winnipeg	Pooled
AC	a	2199	1661	1688	1371	1688	1286	1526
	b	.112	.058	.120	.058	.115	-.060	.059
AS	a	1633	1668	2236	2184	1875	1733	1791
	b	.063	.025	.218	.173	.097	.015	.070
CS	a	3648	3639	2842	2927	3500	3577	3248
	b	.148	.102	.045	.055	.146	.104	.088
CI	a	3443	3365	4760	3714	3423	3444	3361
	b	.079	.012	.243	.105	.067	.070	.043
SC	a	1453	1536	1598	697	1447	1294	1361
	b	.104	.100	.100	.045	.113	-.024	.071
ST	a	997	1770	1325	862	958	1210	1149
	b	.159	.202	.137	.070	.025	-.012	.073
FOG	a	645	354	1105	2245	779	1794	982
	b	.028	-.306	.096	.202	.017	.118	.018

The Blue Hill curves lie within an envelope defined by the set of individual station curves. Curves for strato cumulus, the most common cloud type, are very similar. For stratus and fog the Blue Hill curves define the lower boundary of the group of Canadian irradiance curves.

The largest differences between Canadian and Blue Hill curves are found for alto cumulus. Canadian irradiance values are systematically smaller than those for Blue Hill for air masses up to 3.0. Since this range of air mass (1.0 - 3.0) includes most of the radiation observations throughout the day, this difference will lead to consistently smaller transmittances for alto cumulus. It is difficult to explain why such differences should occur. It will be shown later that seasonal variation may be partially responsible for the differences.

Significant differences between the Blue Hill and Canadian results are confined to alto cumulus. Blue Hill curves for the other cloud types either compare very well with the pooled data curves or lie within the group of curves for the Canadian stations. This suggests that regional variations in the optical characteristics of at least six of the seven cloud types considered are minimal.

#### 3.4 Calculation of Transmittance Parameters after Correcting for Multiple Reflection

Multiple reflection effects are shown schematically in Figure 3.8. Radiation at the surface  $K_{\downarrow}$  is the sum of the trans-

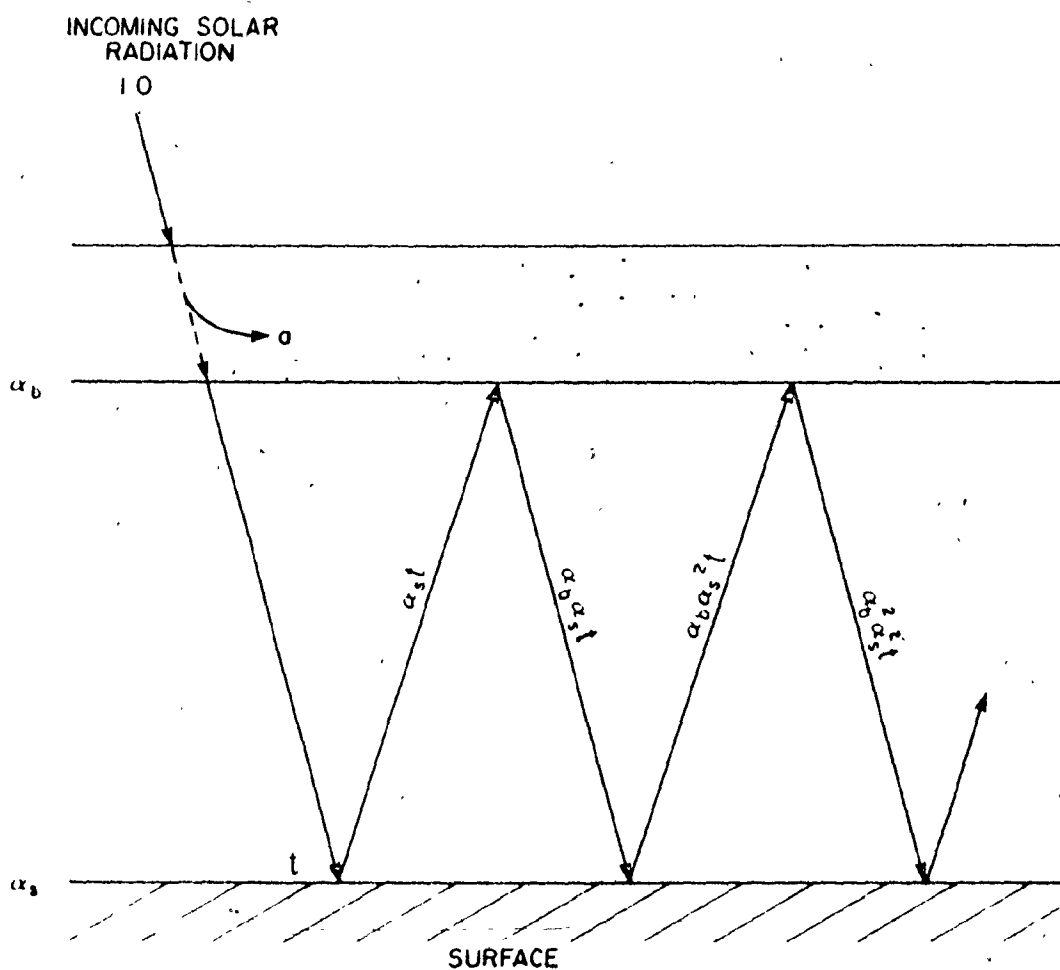


Figure 3.8 Schematic illustration of multiple reflection of transmitted radiation ( $t$ ) between ground surface ( $\alpha_s$ ) and atmosphere ( $\alpha_b$ ).

mitted radiation  $t$ , and numerous secondary diffuse components arising from multiple reflection ( $\alpha_b \alpha_s t + \alpha_b^2 \alpha_s^2 t + \alpha_b^3 \alpha_s^3 t + \dots$ )

$$\begin{aligned} K\downarrow &= t + \alpha_b \alpha_s t + \alpha_b^2 \alpha_s^2 t + \dots \\ &= t / (1 - \alpha_b \alpha_s) \end{aligned} \quad 3.10$$

where  $\alpha_s$  and  $\alpha_b$  are the reflectivities of the surface and atmosphere respectively. Hence the actual transmission before multiple reflection is

$$t = K\downarrow (1 - \alpha_b \alpha_s). \quad 3.11$$

Atmospheric albedo is the sum of individual contributions of Rayleigh ( $\alpha_R$ ) and aerosol scattering ( $\alpha_a$ ) and that of cloud effects ( $\alpha_c$ ). Rayleigh effects are assumed to operate only in the cloudless portion of the sky ( $1 - TCA$ ) and are calculated from

$$\alpha_R = (1 - TCA) 0.0685 \quad 3.12$$

where TCA is the total cloud amount. Under overcast skies  $\alpha_R = 0$ . Aerosol effects are assumed to be limited to the atmosphere below clouds and are given by

$$\alpha_a = (1 + \tau_a') \bar{w}_0 (1 - f') \quad 3.13$$



where  $\tau_a'$  is the aerosol transmission at an optical air mass of 1.66 (Kondrat'yev, 1969) and  $f'$  is the ratio of forward to total scatter by aerosol/also at that air mass. The contribution of cloud to the total atmospheric reflectivity is calculated from

$$\alpha_c = \bar{\alpha}_c TCA \quad 3.14$$

where  $\bar{\alpha}_c$  is the average cloud base albedo set at a constant value of 0.6. Thus atmospheric reflectivity is given by

$$\alpha_b = \alpha_R + \alpha_a + \alpha_c \quad 3.15$$

Surface albedo is calculated as a function of surface temperature  $T_s$  using an algorithm developed for the Maclaren study. Surface albedo is assigned a value ALOW if surface temperature is less than a prescribed TLOW and AHIGH if  $T_s$  exceeds THIGH. Thus,

$$\alpha_s = \begin{cases} \text{ALOW} & \text{when } T_s \leq \text{TLOW} \\ \text{AHIGH} & \text{when } T_s \geq \text{THIGH} \end{cases}$$

If  $T_s$  lies between these two temperatures an intermediate value of surface albedo is calculated as follows:

$$\alpha_s = \text{ALOW} + \frac{\delta\alpha_s}{\delta T_s} \Delta T_s$$

$$\approx \text{ALOW} + (\text{AHIGH} - \text{ALOW}) / (\text{THIGH} - \text{TLOW}) (T_s - \text{TLOW}) \quad 3.16$$

Values assigned for these variables are given in Table 3.3.

Transmittance parameters ( $a_c$  and  $b_c$ ) were determined using Subroutine EXPFIT and also using a non-linear least-squares method. Since Subroutine EXPFIT uses a logarithmic transformation of Equation 1.1, parameter values are determined by minimizing the sum of squares of the differences between the logarithms of the measured and calculated global irradiances. Non-linear least squares methods minimize the sum of squares of actual differences between actual measured and calculated global irradiances. Two non-linear methods were tested. These are referred to as Subroutine GRIDLS (Bevington, 1969) and Subroutine NLLS2 (Marquardt, 1961). Both methods yielded similar results however, Subroutine GRIDLS was selected over NLLS2 because of its simplicity and less computer time requirements.

The Bevington method uses an iterative grid search technique which minimizes the sum of squares of the differences between measured and calculated irradiances to evaluate the transmittance parameters. Using mean values of global radiation for specific air mass intervals permits the "fit" to be weighted according to the standard deviation of the actual measured irradiances around each mean. The unweighted and weighted solutions are referred to as Subroutine GRIDLS (0) and GRIDLS (1) respectively.

### 3.4.1 Results

Estimates of the transmittance parameters for individual

TABLE 3.3

Data for Calculating Surface Albedo

Station	TLOW	ALOW	AHIGH	THIGH
Goose Bay	-3.0	0.6	6.0	0.2
Charlottetown				
Montreal				
Toronto	-6.0	0.6	3.0	0.2
Winnipeg				

stations and for the pooled data are given in Table 3.4. Plots of global irradiances calculated from parameters determined from pooled data after correcting for multiple reflection effects are shown in Figures 3.9-3.15.

Irradiance curves plotted for parameters determined using GRIDLS (0) and EXPFIT are almost identical for all clouds. This is explained by the relatively small range of global irradiances in terms of orders of magnitude. Had global radiation values ranged over numerous orders of magnitude (ie.  $10^2 - 10^{10}$ ), a logarithmic transformation would yield significantly different results because it minimizes the sum of squares of the differences of the logarithms of the measured and calculated irradiances. Over the small range of radiation values measured ( $10^2 - 10^4$ ) however, the transformation has little effect.

For high clouds, weighting the fit resulted in larger irradiance estimates than those from the other methods, whereas estimates for the other cloud types were slightly reduced by weighting. This is a result of less scatter in the distribution of individual measured irradiances for cirriform cloud than for lower cloud types. This can be attributed to the lack of any overlying cloud above an overcast of cirrus. For lower overcasts, overlying cloud may or may not be present. Therefore more uncertainty is introduced which results in a greater scatter in the data and hence larger standard deviations especially at small air masses (Figures 3.16a, b). This causes more significance to be placed on the values of the minimization parameter  $\chi^2$  at larger air masses (where less scatter occurs

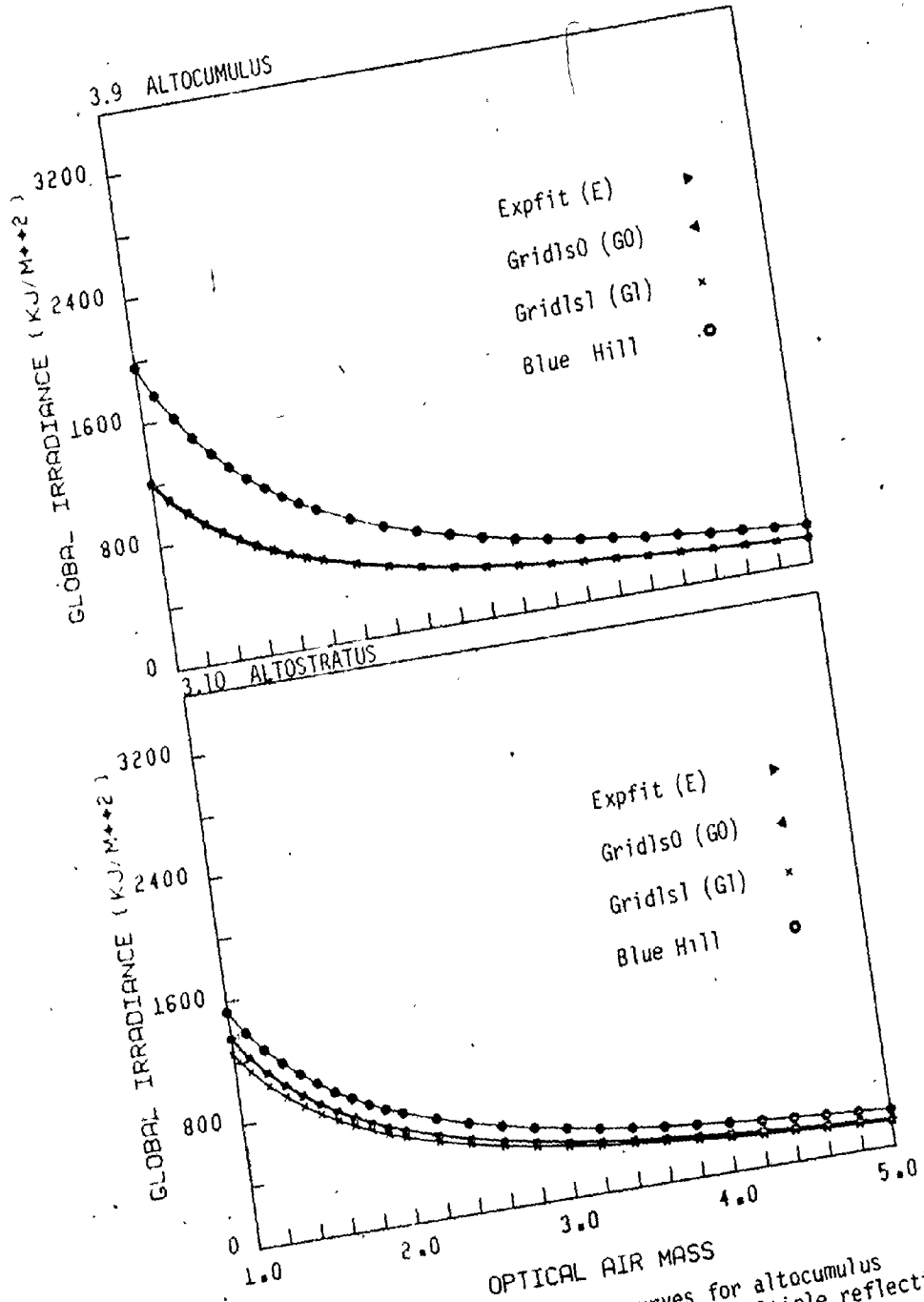


Figure 3.9 Global irradiance curves for altocumulus cloud after correcting for multiple reflection.

Figure 3.10 Global irradiance curves for altostratus cloud after correcting for multiple reflection.

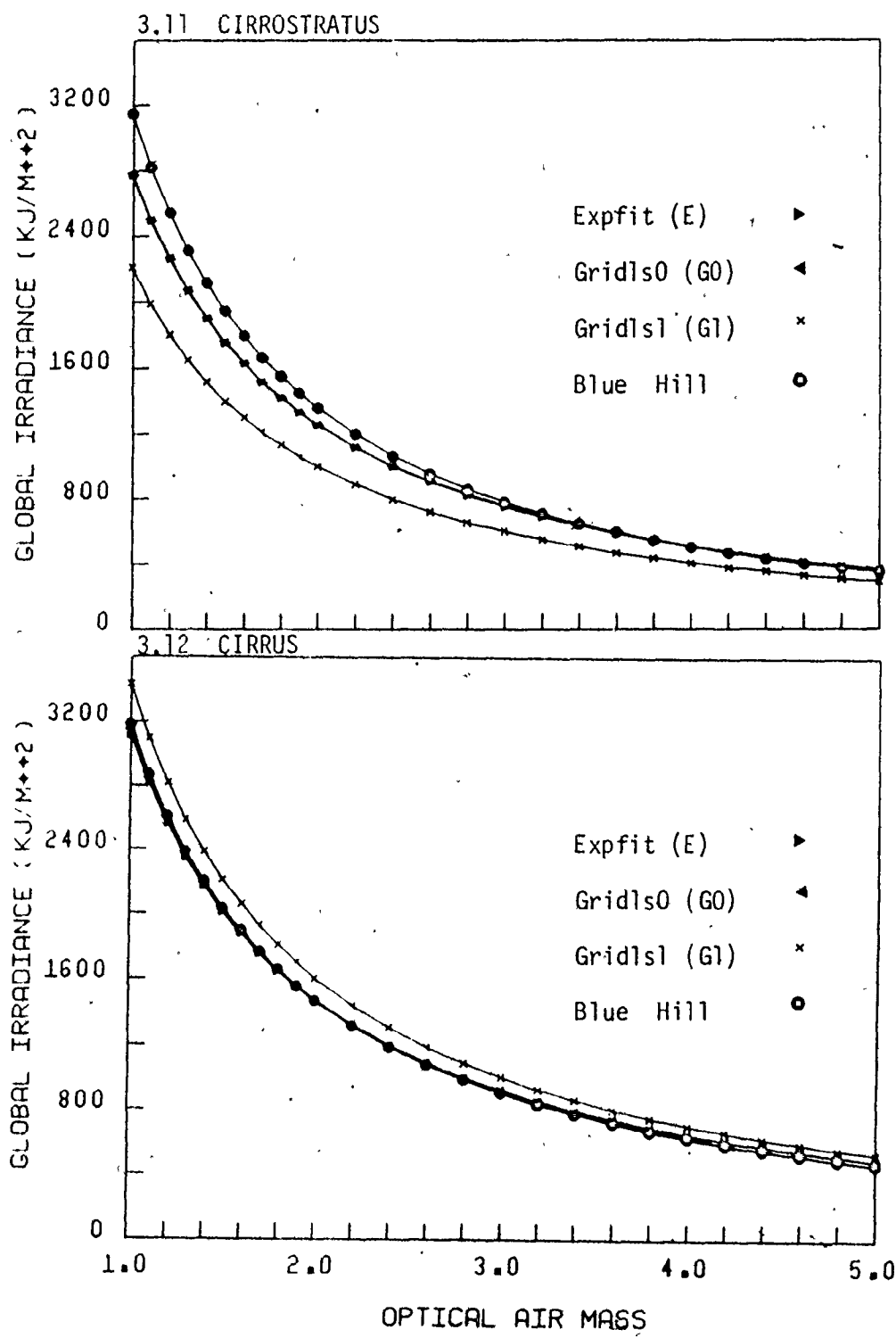


Figure 3.11 Global irradiance curves for cirrostratus cloud after correcting for multiple reflection.

Figure 3.12 Global irradiance curves for cirrus cloud after correcting for multiple reflection.

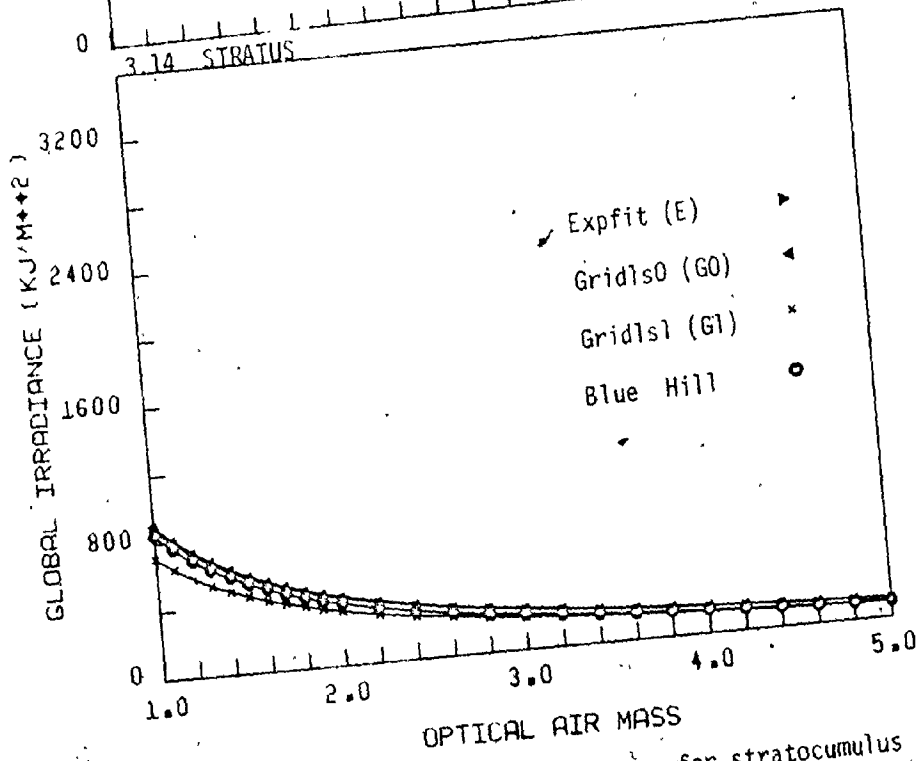
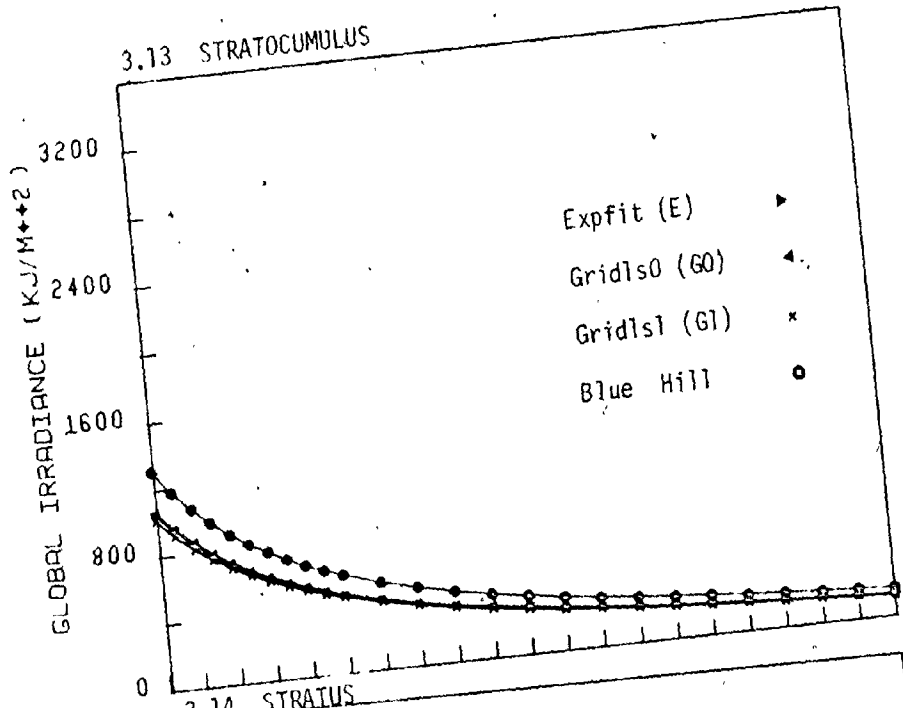


Figure 3.13 Global irradiance curves for stratocumulus cloud after correcting for multiple reflection.

Figure 3.14 Global irradiance curves for stratus cloud after correcting for multiple reflection.

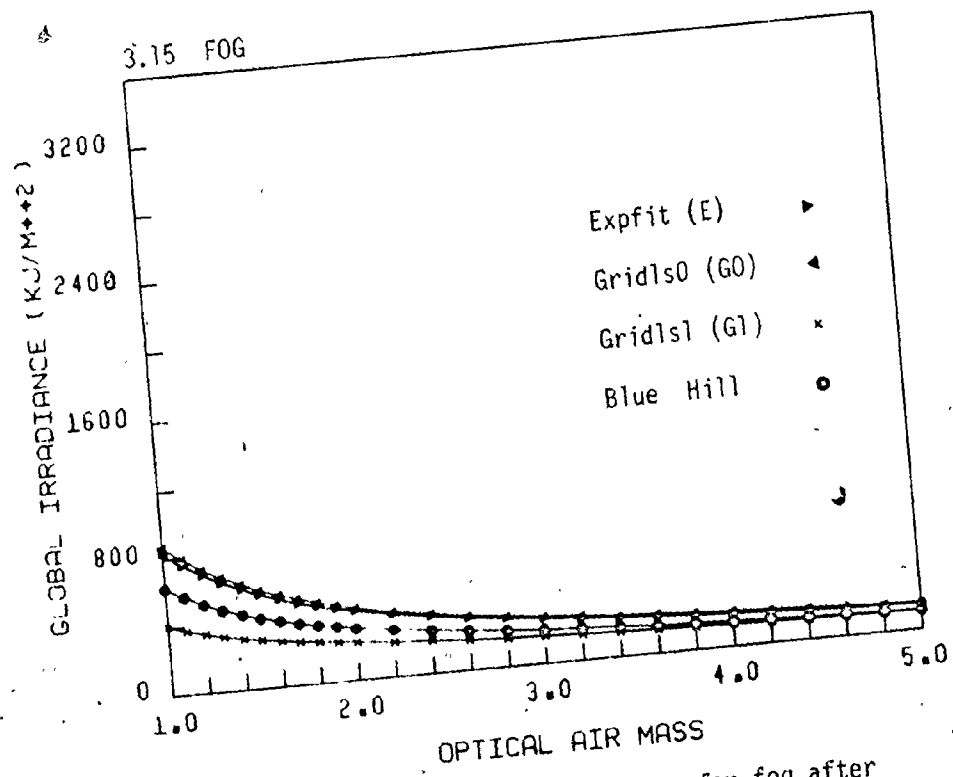


Figure 3.15 Global irradiance curves for fog after correcting for multiple reflection.



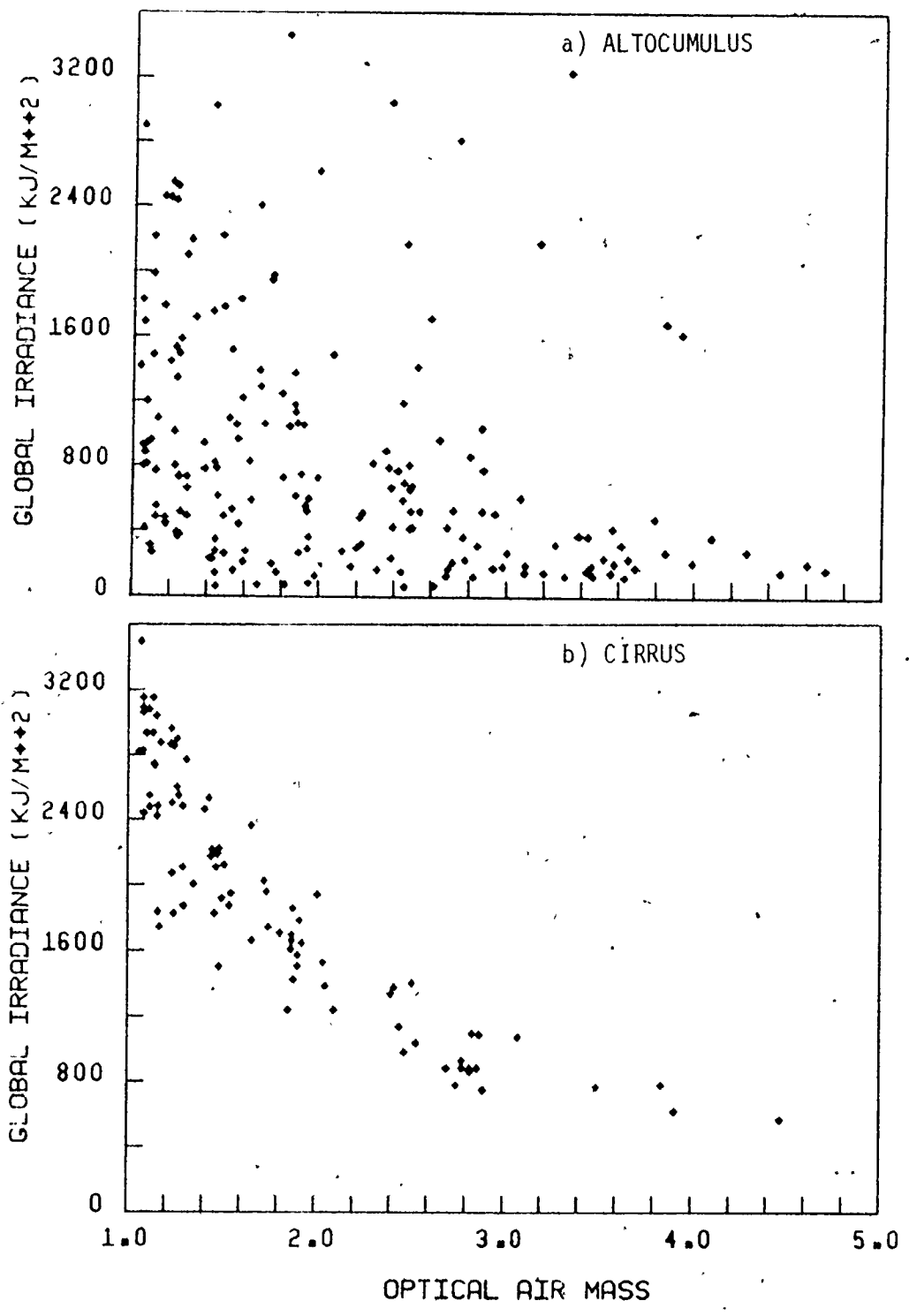


Figure 3.16a, b Distribution of scatter in overcast global irradiance measurements of altocumulus (a) and cirrus (b) clouds.

TABLE 3.4

Parameter values for Haurwitz's radiation model using corrected mean global irradiance data for Canada.

			Goose	Charlotte- town	Montreal	Toronto	Winnipeg	Pooled
AC	E*	a	1461	1510	1213	1505	1106	1345
		b	.098	.163	.093	.150	-.022	.097
	GO*	a	1534	1510	1182	1524	1050	1336
		b	.102	.162	.083	.152	-.050	.089
	G1*	a	1518	1558	1131	1553	1090	1321
		b	.095	.160	.101	.149	-.021	.097
AS	E	a	1361	1726	1866	1614	1534	1522
		b	.066	.224	.211	.136	.076	.114
	GO	a	1345	1608	1915	1583	1511	1523
		b	.060	.194	.214	.126	.070	.108
	G1	a	1366	2064	1622	1519	1476	1412
		b	.072	.224	.222	.135	.075	.114
CS	E	a	3458	2887	2760	3307	3420	3078
		b	.122	.113	.067	.150	.119	.104
	GO	a	3435	2924	2774	3269	3401	3084
		b	.120	.115	.068	.146	.118	.103
	G1	a	3440	3060	2986	2927	3427	2456
		b	.122	.119	.067	.150	.117	.104
CI	E	a	3285	4701	3571	3383	3378	3306
		b	.028	.252	.116	.083	.088	.060
	GO	a	3316	4649	3555	3365	3384	3348
		b	.029	.247	.114	.081	.088	.062
	G1	a	3386	4674	3537	3402	3468	3660
		b	.027	.249	.116	.083	.090	.065
SC	E	a	1338	1369	825	1241	1151	1176
		b	.144	.130	.076	.139	.044	.110
	GO	a	1327	1400	880	1204	1151	1195
		b	.142	.135	.089	.130	.044	.111
	G1	a	1337	1361	778	1227	1154	1157
		b	.144	.129	.081	.140	.044	.111
ST	E	a	1537	1144	769	817	1033	995
		b	.245	.157	.119	.053	.040	.112
	GO	a	1589	1115	804	816	1021	1012
		b	.248	.147	.116	.048	.035	.106
	G1	a	1161	1136	605	800	1034	802
		b	.2468	.153	.101	.052	.040	.114
F	E	a	336	947	1967	677	1562	863
		b	-.266	.097	.0216	.024	.141	.032
	GO	a	352	933	1988	660	1730	897
		b	-.266	.089	.210	-.001	.156	.023
	G1	a	252	880	1716	270	1214	375
		b	-.243	.097	.218	.016	.141	-.078

because of lower radiation levels) where standard deviations are smaller. Hence smaller parameter estimates are obtained.

### 3.5 Analysis of Seasonal Variation

Lack of sufficient data for cirro stratus, cirrus and fog prevented seasonal analysis of their transmittance characteristics. Statistical parameters were calculated for alto cumulus, alto stratus, strato cumulus and stratus. Grouping the data into seasons also precluded the use of radiation means. Actual unmeasured data were used. Table 3.5 lists the numbers of observations for each station and cloud type during the four seasons. Seasons were defined as:

Winter: December, January, February

Spring: March, April, May

Summer: June, July, August

Autumn: September, October, November.

#### 3.5.1 Results

Seasonal parameter estimates for Equation 1.1 were determined using uncorrected and corrected global radiation values for individual stations and the pooled data. Because actual data rather than means were used the fits could not be weighted. Subroutine GRIDLS (0) was used to calculate the parameter values which are

TABLE 3.5

Number of hours of data within each season at each station for each of four cloud types

Cloud	Season	Goose	Charlotte- town	Montreal	Toronto	Winnipeg	Pooled
AC	1	9	34	49	32	58	182
	2	25	42	70	89	69	295
	3	11	51	57	46	46	211
	4	7	20	36	24	45	132
AS	1	20	29	46	45	78	218
	2	44	22	39	34	56	195
	3	13	5	7	8	9	42
	4	4	6	5	5	27	47
SC	1	89	277	318	416	336	1436
	2	385	395	329	295	462	1866
	3	139	267	144	119	258	927
	4	143	334	278	264	489	1508
ST	1	5	44	51	73	172	345
	2	33	119	32	40	146	370
	3	19	53	13	25	32	142
	4	12	38	45	29	149	273

listed in Tables 3.6 and 3.7. Curves for the pooled data parameter estimates are shown in Figures 3.17 - 3.24. Also shown are curves for pooled (all-season) data. It is evident that a seasonal variation exists. Irradiances are greatest in winter for all cloud types and generally lowest in summer. These seasonal differences are reduced when parameters from the corrected data are used to calculate global irradiances. However, again, irradiances are still largest in winter for all-cloud types. These seasonal differences are better illustrated in the next section where cloud transmissions are examined.

TABLE 3.6

Seasonal parameter values for four cloud types using uncorrected global irradiance data.

Cloud	Season*		Goose	Charlotte- town	Montreal	Toronto	Winnipeg	Pooled
AC	1	a	3892	2338	3648	5082	4024	2977
		b	.211	.101	.253	.379	.186	.146
	2	a	2518	1935	1499	1865	1324	1738
		b	.192	.227	.079	.181	-.123	.109
	3	a	1059	1793	1153	1878	1095	1434
		b	.212	.289	.100	.257	.117	.191
	4	a	1676	2592	1222	1123	925	1238
		b	.102	.295	.098	.065	-.101	.039
AS	1	a	6598	1987	2672	4795	2597	2562
		b	.355	.027	.161	.361	.085	.114
	2	a	1327	2455	3222	2417	2599	2278
		b	-.092	.264	.424	.218	.156	.161
	3	a	2020	742	1961	1012	1478	1284
		b	.337	-.354	.296	-.023	.408	.102
	4	a	2233	2281	998	1031	1225	1305
		b	.141	.192	-.068	-.053	-.007	.010
SC	1	a	2693	2234	1381	2006	2403	1762
		b	.149	.133	.115	.137	.068	.065
	2	a	2031	1648	1024	1225	1629	1567
		b	.200	.094	.098	.089	.078	.124
	3	a	1509	1882	1811	1862	1581	1760
		b	.290	.241	.378	.304	.206	.278
	4	a	939	1476	827	1253	852	1017
		b	-.019	.147	.070	.135	-.094	.023
ST	1	a	5221	3680	1055	1240	2132	1483
		b	.309	.347	.063	.063	.090	.031
	2	a	2726	1257	916	1398	1384	1382
		b	.334	.128	.211	.196	.047	.123
	3	a	1812	1364	1387	1273	1116	1151
		b	.385	.212	.106	.405	-.040	.096
	4	a	1475	1558	1226	781	766	868
		b	.167	.298	.227	.100	-.099	-.004

\* 1 Winter  
2 Spring  
3 Summer  
4 Fall

TABLE 3.7

Seasonal parameter values for four cloud types using corrected global irradiance data.

Cloud	Season		Goose	Charlotte- town	Montreal	Toronto	Winnipeg	Pooled
AC	1	a	2871	1614	2513	3819	2858	2130
		b	.235	.096	.248	.392	.193	.153
	2	a	2110	1761	1317	1645	1054	1496
		b	.212	.259	.102	.196	-.116	.129
	3	a	940	1587	1026	1684	971	1276
		b	.213	.288	.101	.259	.115	.192
	4	a	1532	2328	1090	997	857	1135
		b	.109	.303	.105	.070	-.060	.065
AS	1	a	4145	1303	1916	3450	1725	1774
		b	.334	.016	.168	.360	.079	.115
	2	a	1026	1791	2658	2138	2225	1893
		b	-.059	.242	.440	.265	.206	.198
	3	a	1785	657	1743	899	1356	1142
		b	.334	-.354	.293	-.022	.428	.102
	4	a	1653	2181	940	881	1161	1241
		b	.135	.239	-.063	-.071	.035	.051
SC	1	a	1930	1607	1022	1583	1679	1347
		b	.161	.136	.130	.160	.089	.094
	2	a	1703	1415	870	1060	1385	1331
		b	.231	.135	.131	.110	.126	.159
	3	a	1321	1647	1592	1630	1385	1542
		b	.290	.241	.379	.304	.205	.278
	4	a	918	1312	732	1089	826	937
		b	.048	.167	.088	.144	-.013	.069
ST	1	a	3256	2464	770	949	1408	1093
		b	.308	.306	.073	.070	.095	.055
	2	a	2041	1088	719	1160	1114	1153
		b	.333	.151	.226	.210	.070	.151
	3	a	1586	1195	1215	1112	978	1007
		b	.386	.213	.106	.404	-.042	.096
	4	a	1467	1373	1099	695	732	818
		b	.228	.302	.247	.113	-.028	.051

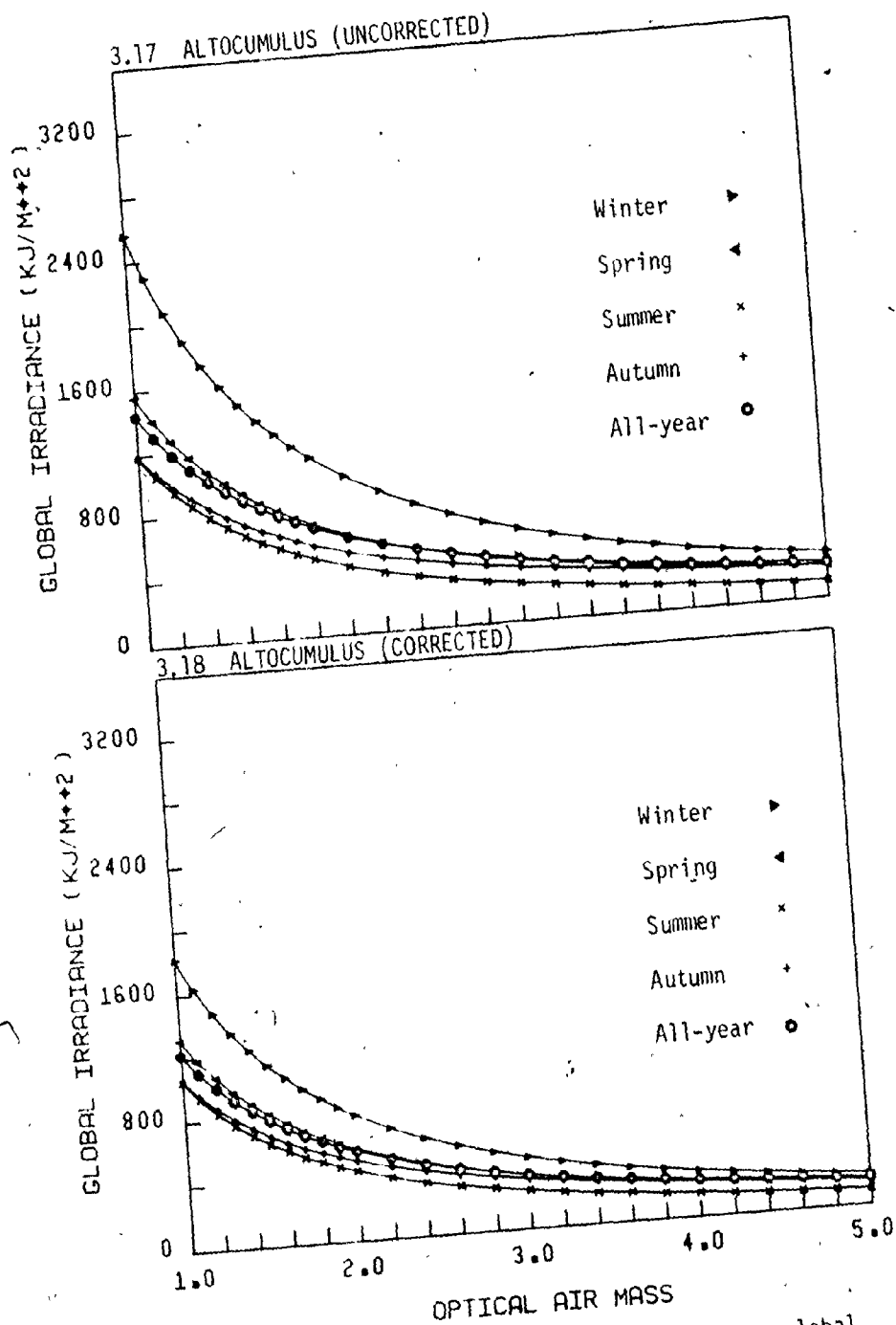


Figure 3.17 Uncorrected seasonal and all-year global irradiance curves for altocumulus cloud.

Figure 3.18 Corrected seasonal and all-year global irradiance curves for altocumulus cloud.



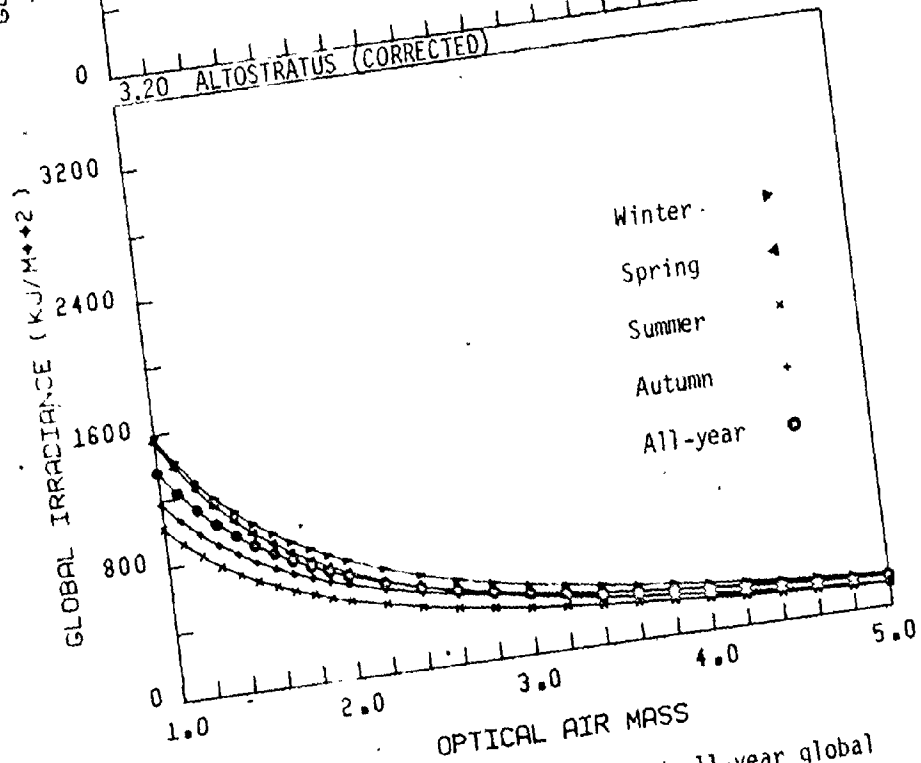
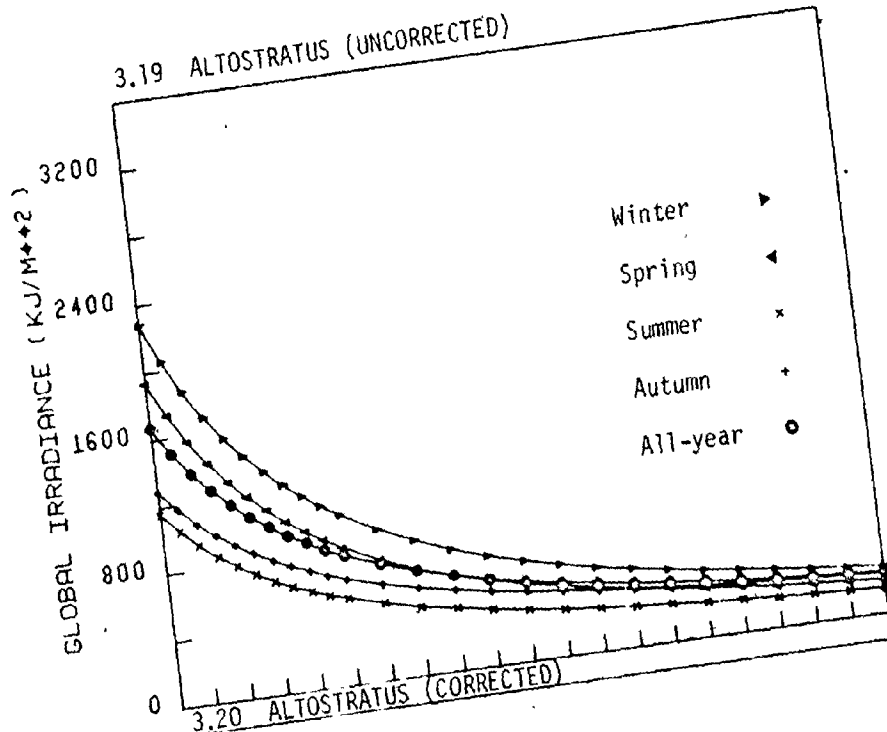


Figure 3.19 Uncorrected seasonal and all-year global irradiance curves for altostratus cloud.

Figure 3.20 Corrected seasonal and all-year global irradiance curves for altostratus cloud.

## 3.21 STRATOCUMULUS (UNCORRECTED)

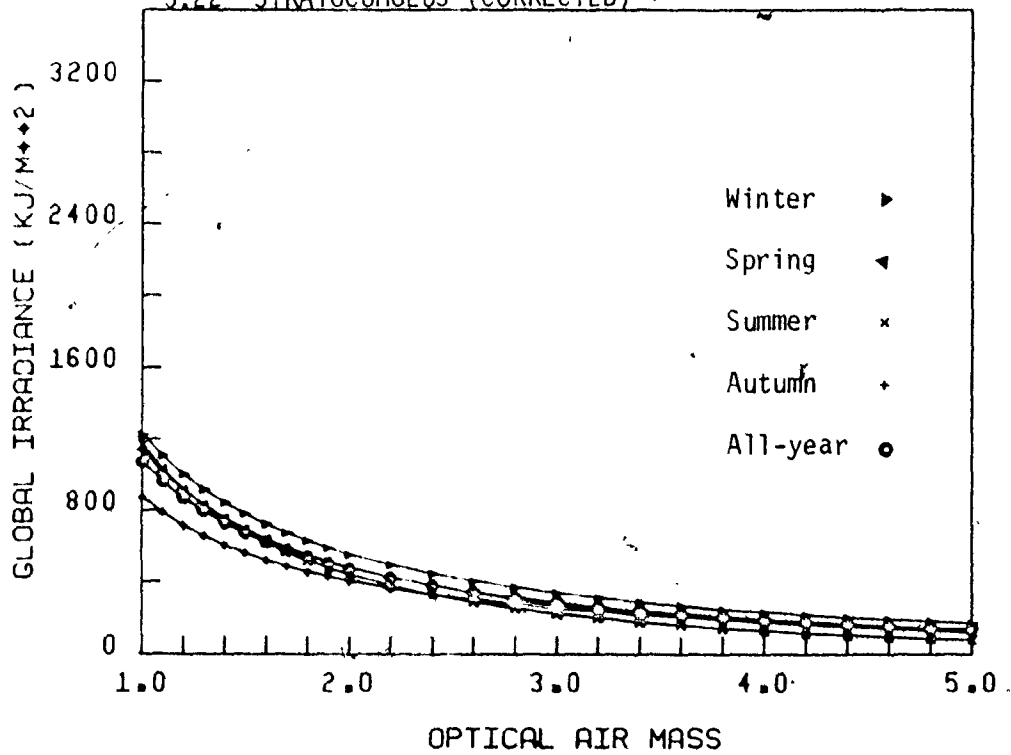
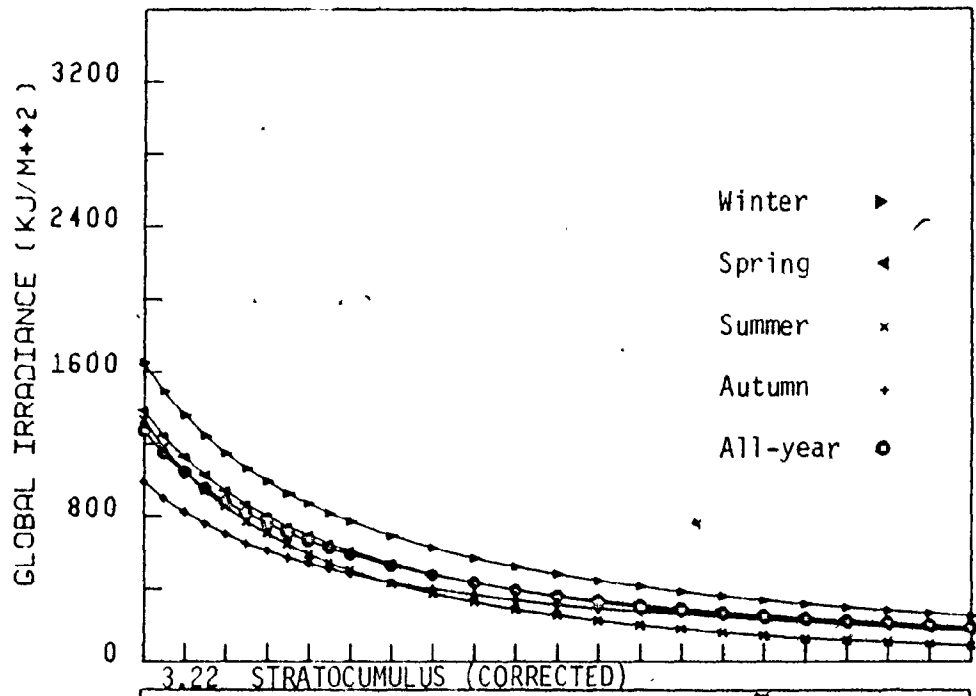


Figure 3.21 Uncorrected seasonal and all-year global irradiance curves for stratocumulus cloud.

Figure 3.22 Corrected seasonal and all-year global irradiance curves for stratocumulus cloud.

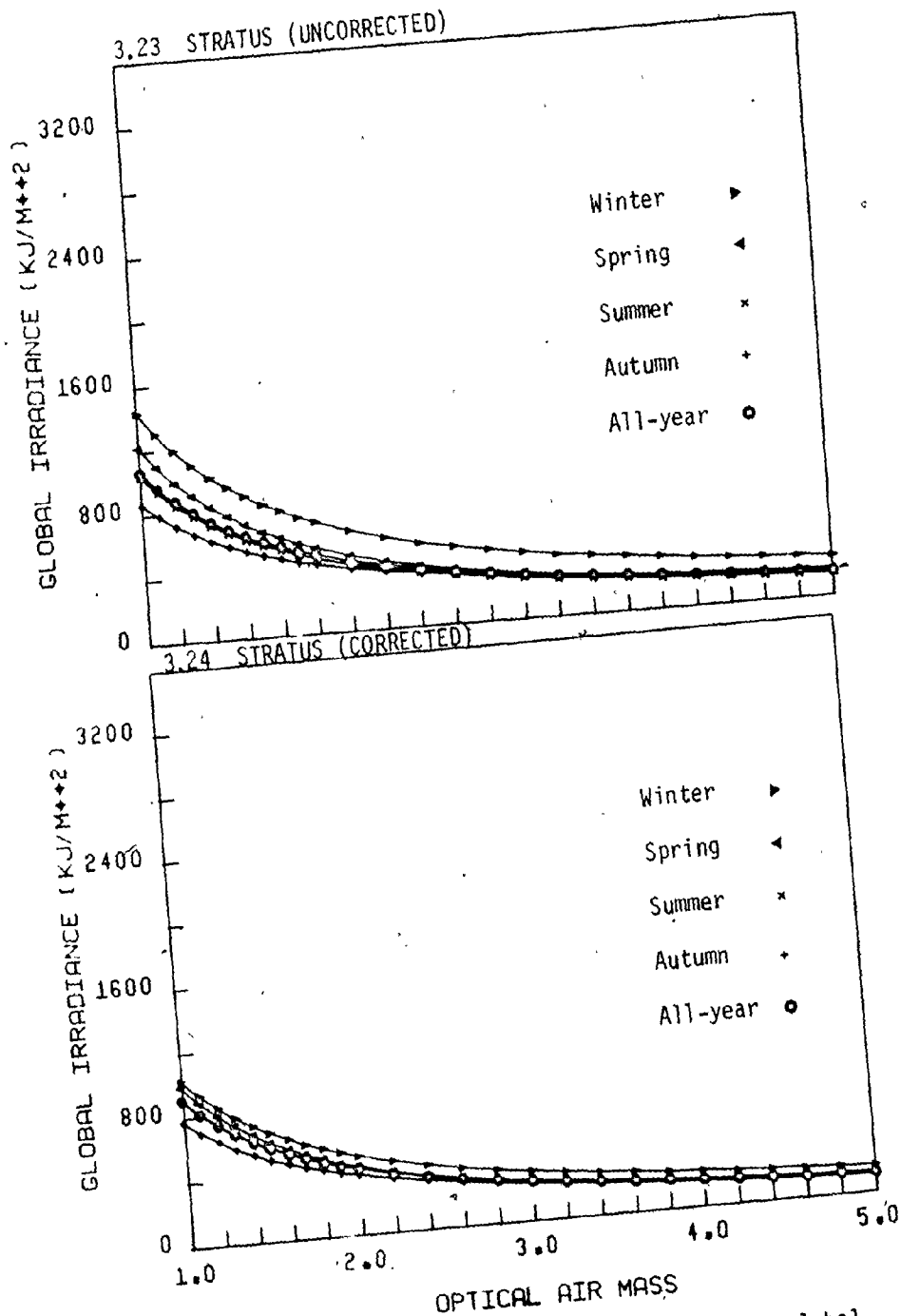


Figure 3.23 Uncorrected seasonal and all-year global irradiance curves for stratus cloud.

Figure 3.24 Corrected seasonal and all-year global irradiance curves for stratus cloud.

## CHAPTER FOUR

### CLOUD TYPE TRANSMITTANCES

#### 4.1 Transmission Calculation

Cloud type transmittances were determined in three ways:  
Method 1 - the ratio of overcast to cloudless global irradiance, both expressed as exponential functions of air mass, empirically determined from measurements. This allows direct comparison of Canadian results with those of Blue Hill.

Method 2 - the ratio of measured overcast to theoretical (MAC model) cloudless sky irradiances.

Method 3 - the ratio of overcast global irradiance, corrected for multiple reflection effects, to theoretical cloudless sky irradiance. This is the procedure used by Atwater and Ball (1980).

#### 4.2 Results

##### 4.2.1 Exponential Transmittance

Parameters for Equation 1.1 are given in Table 3.2.

Analogous parameters ( $a_0$ ,  $b_0$ ) were also determined for cloudless

sky data pooled from the five Canadian stations (Table 4.1). Plots of cloudless sky global irradiances as a function of optical air mass are shown in Figure 4.1.

Cloudless sky irradiances for Canada are slightly larger than those of Blue Hill possibly due to larger aerosol concentrations at Blue Hill which is near Boston. Since the difference between the two curves is systematic transmittances should be consistently larger for Blue Hill than for Canada. Table 4.2 lists values of transmittance parameters A and B of Equation 2.18 for Blue Hill and pooled Canadian data.

Plots of transmittance curves for Blue Hill and Canadian data are shown in Figure 4.2 - 4.8. Blue Hill transmittances are not systematically larger than those for Canada. Alto cumulus transmittance is much larger at Blue Hill than Canada whereas transmittance values for stratus and fog are larger for Canadian data. Very small differences exist between transmittances for the remaining cloud types especially at air masses 1.0 - 3.0. Differences for alto cumulus transmittances are partially due to the larger cloudless sky irradiances for Canada. However this is not large enough to account for all of the difference. Seasonal variation must be responsible for the remainder of the difference. This will be discussed later in this section.

Stratus and fog are low-lying clouds which may be physically and optically thicker at Blue Hill than for Canada. Local topographical features could be responsible for the smaller transmittances at Blue Hill than Canada. This is not unreasonable since

TABLE 4.1  
Parameter Values for Cloudless Sky Global Irradiances

	a [ $W_m^{-2}$ ]	b
Canada	3964	.0465
Blue Hill	3949	.059

TABLE 4.2.  
Cloud-Type Transmittance Parameters

Cloud Type	$A_{CAN}$	$A_{BH}$	$B_{CAN}$	$B_{BH}$
AC	.3850	.556	.0721	.053
AS	.4518	.413	.0237	.004
CS	.8194	.923	.0415	.089
CI	.8479	.871	-.0033	.020
SC	.3433	.368	.0247	.045
ST	.2899	.252	.0264	.100
FOG	.2477	.163	-.0291	-.031

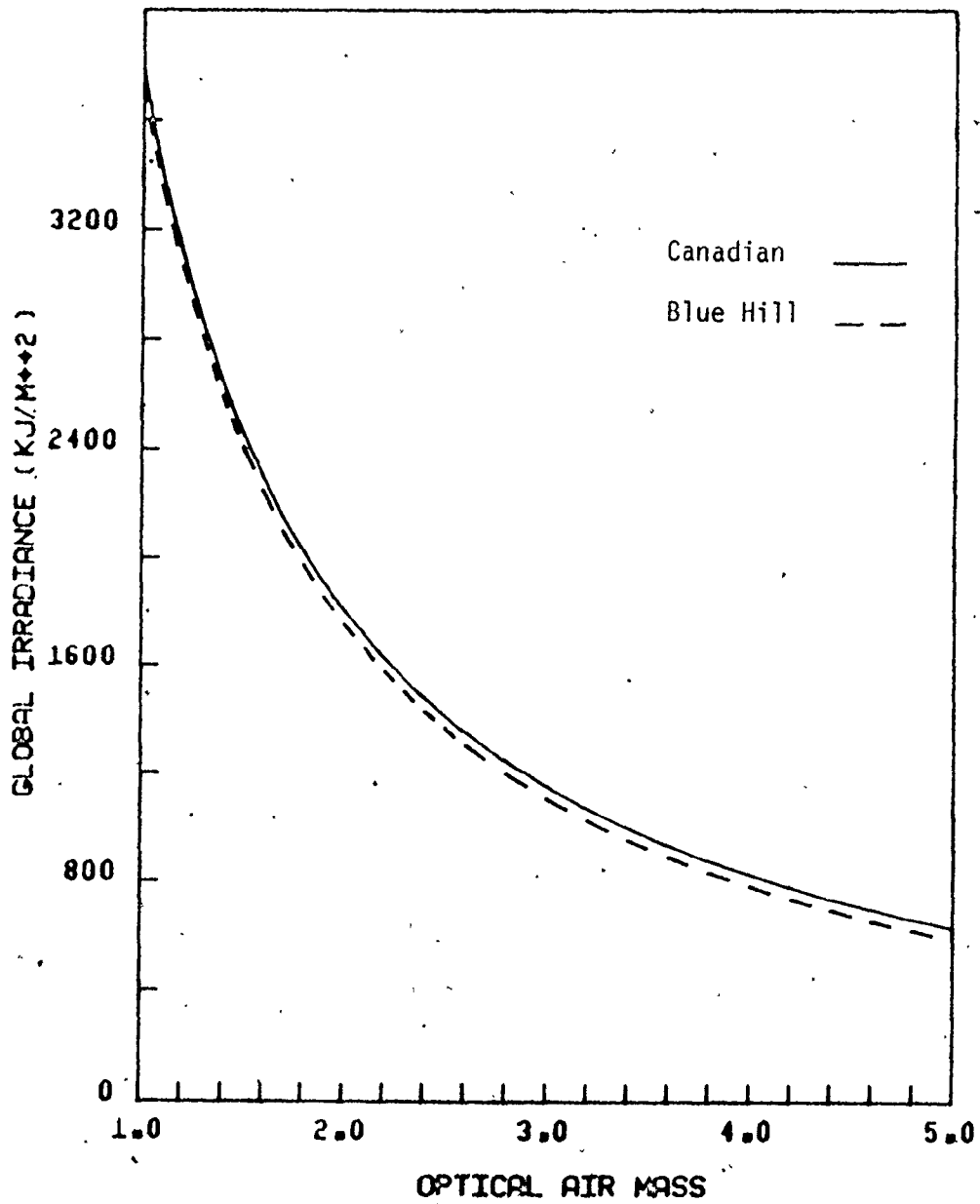
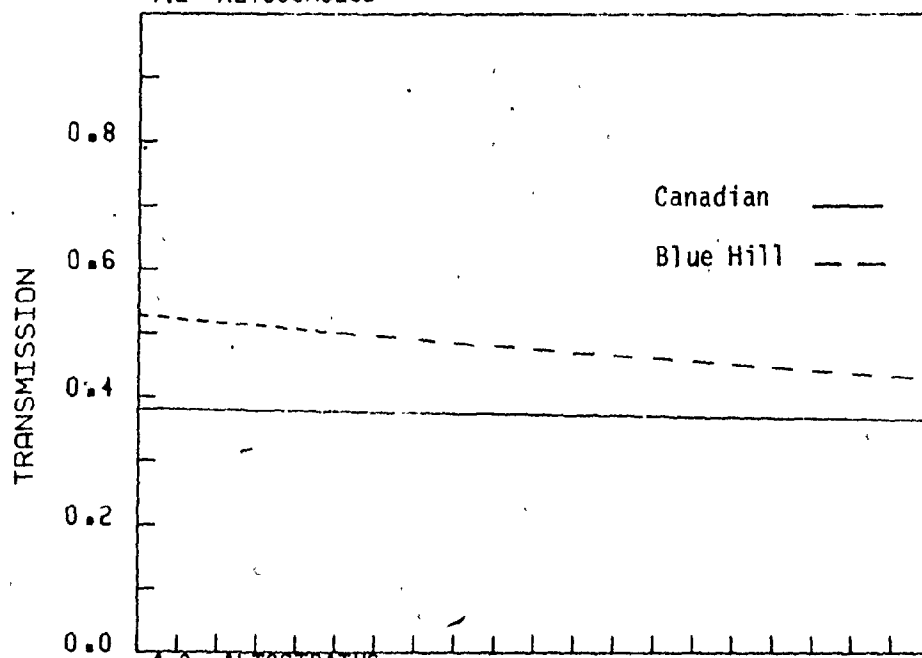


Figure 4.1 Cloudless sky global irradiances of Blue Hill, Massachusetts and pooled data for Canada.

## 4.2 ALTOCUMULUS



## 4.3 ALTOSTRATUS

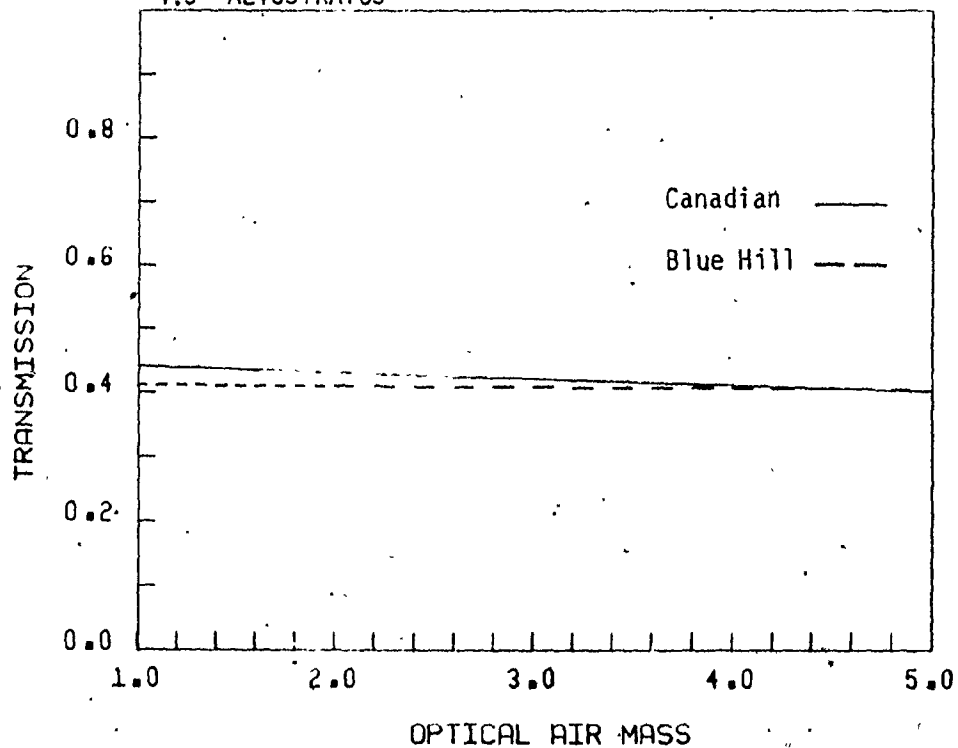
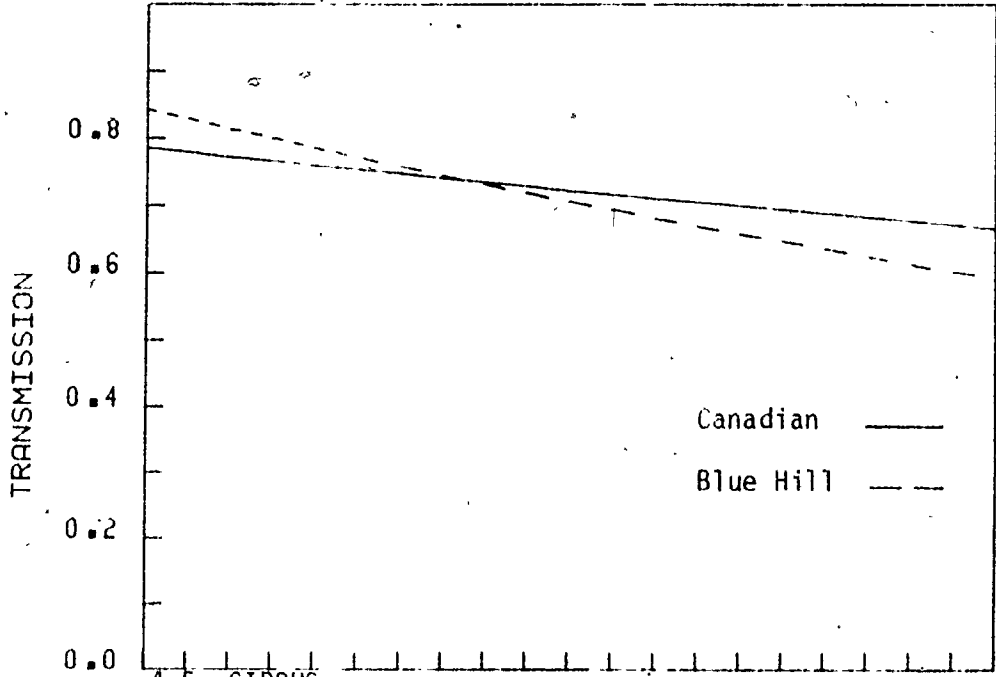


Figure 4.2 Transmittance curves of altocumulus cloud for Blue Hill and pooled Canadian data.

Figure 4.3 Transmittance curves of altostratus cloud for Blue Hill and pooled Canadian data.



4.4 CIRROSTRATUS



4.5 CIRRUS

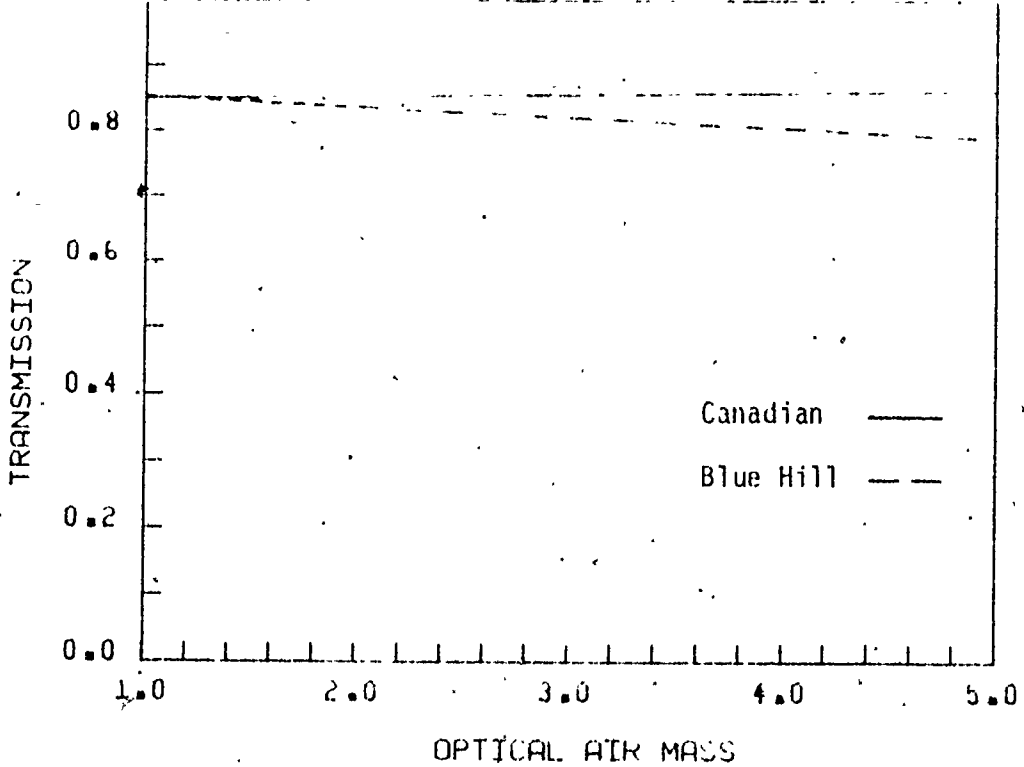


Figure 4.4 Transmittance curves of cirrostratus cloud for Blue Hill and pooled Canadian data.

Figure 4.5 Transmittance curves of cirrus cloud for Blue Hill and pooled Canadian data.

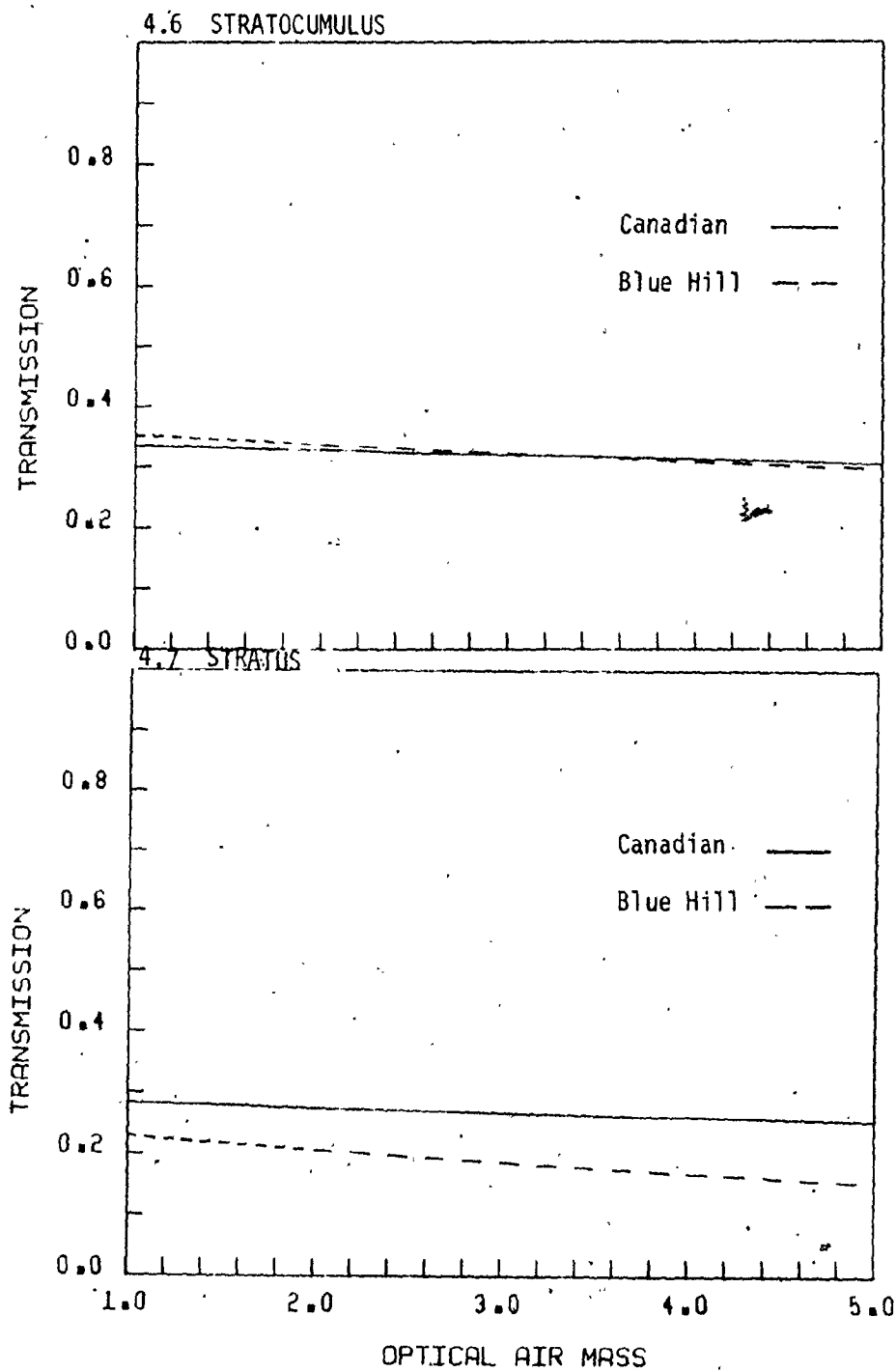


Figure 4.6 Transmittance curves of stratocumulus cloud for Blue Hill and pooled Canadian data.

Figure 4.7 Transmittance curves of stratus cloud for Blue Hill and pooled Canadian data.

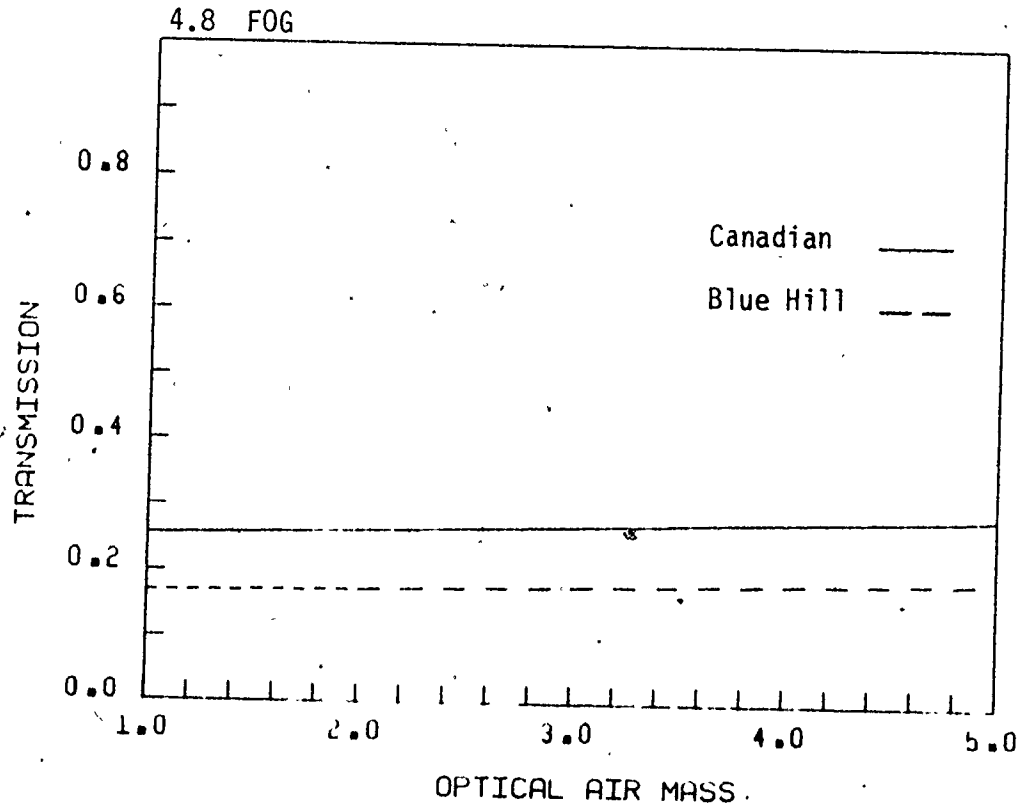


Figure 4.8 Transmittance curves of fog for Blue Hill and pooled Canadian data.

Blue Hill Observatory is located on the east coast on the side of a small mountain.

#### 4.2.2. Linear Transmittance

Transmittance was regressed upon optical air mass to obtain values for  $c_j$  and  $d_j$  in Equation 1.3. Values were calculated for both uncorrected and corrected transmittances. Results for the pooled data are given in Table 4.3. Results for individual stations are listed in Appendix E.

Cloud transmittance is almost independent of air mass. Values of the regression coefficient  $\beta$ , are of order 0.01. This suggests that a constant transmittance may be adequate. This supports the recent work of Atwater and Ball (1981) who replaced their linear transmittance functions in their layer model with constant mean cloud-type transmittances.

#### 4.2.3. Constant Transmittance

Mean cloud-type transmittances were calculated by Methods 2 and 3. Both uncorrected and corrected irradiances were used. Calculated transmittances are listed in Table 4.4 along with those of Kasten and Czeplak (1980) and Atwater and Ball (1981).

Transmittances determined using measured clear sky radiation and those calculated using a theoretical value are very similar. Slightly larger transmittances are obtained by using measured

TABLE 4.3

Cloud transmission results using pooled data for uncorrected and corrected irradiances.  $\bar{T}$  = mean transmittance;  $\sigma T$  = standard deviation;  $\alpha$  and  $\beta$  are the regression constant and coefficient in  $\bar{T} = \alpha + \beta m$ ;  $R$  is the correlation coefficient.

	Cloud	$\bar{T}$	$\sigma T$	$\alpha$	$\beta$	$R$
Uncorrected	AC	.402	.089	.375	.010	.128
	AS	.451	.100	.435	.006	.064
	CS	.763	.072	.787	-.010	-.136
	CI	.891	.081	.835	.023	.288
	SC	.347	.071	.331	.005	.091
	ST	.299	.082	.291	.003	.042
	F	.320	.129	.266	.019	.159
Corrected	AC	.319	.064	.330	-.004	-.071
	AS	.338	.067	.368	-.011	-.177
	SC	.696	.072	.745	.0	-.278
	CI	.841	.074	.825	.007	-.095
	SC	.267	.049	.286	-.007	-.163
	ST	.232	.056	.251	-.007	-.137
	F	.268	.101	.237	.011	.116

TABLE 4.4

Mean transmittance values for Canada calculated

- (1) as the ratio of measured  $G_c$  to measured  $G_o$   
 (2) as the ratio of measured  $G_c$  to theoretical  $G_o$

		Canada		Hamburg (Kasten and Czeplak)	Atwater and Ball
		(1)	(2)		
Uncorrected	AC	.40	.38	.27	
	AS	.45	.42	.27	
	CS	.76	.74	.61	
	CI	.89	.86	.61	
	SC	.35	.33	.25	
	ST	.30	.27	.18	
	F	.32	.27	--	
Corrected	AC	.32			.50
	AS	.34			.40
	CS	.70			.90
	CI	.84			.90
	SC	.27			.25
	ST	.23			.15
	F	.27			

cloudless sky radiation suggesting that calculated values are slightly larger on average than measured values. Using uncorrected global radiation permits comparison with the results of Kasten and Czeplak for Hamburg. The two sets of cloud-type transmittances do not compare well. Values for Hamburg are consistently smaller than those for Canada. These differences indicate that the Hamburg transmittance values are not suitable to North America. Hence, the claim by Kasten and Czeplak that their results have general applicability would seem to be unfounded. Differences are largest for high cloud and smaller for lower cloud. A possible explanation for this disagreement in results may lie in the selection of overcast conditions. This study selected only observations with overcasts for the lowest level. No conditions were placed on the cloud opacity of that layer. As a result, thin clouds with small opacities were included. Kasten and Czeplak however have used a selection technique which may have excluded those observations where opacity was less than ten-tenths. This would result in a data set biased towards optically thicker clouds which would lead to systematically lower transmittance values. Largest effects of this bias in the data would be noticed for cloud types which are often semi-transparent, such as cirrus, and not for thicker clouds such as strato cumulus.

Transmittances determined using corrected global radiation are comparable with those calculated by Atwater and Ball (1981) using GATE data. The GATE transmittances are slightly larger than those for Canada especially for middle and high clouds. Differences

between these results are smaller than those between Hamburg and Canada. There is large disagreement among the resultant mean cloud-type transmittances for the three studies.

#### 4.3 Results of Seasonal Analysis

Mean seasonal transmittances were also calculated. Results for individual stations are listed in Appendix E. Results for uncorrected and corrected transmittances for the pooled data are given in Table 4.5

Transmittances are largest in winter and smallest in summer and fall. Although removal of multiple reflection effects reduces the magnitude of this seasonal variation the same trend remains.

Seasonal transmittance variations are a function of changes in cloud optical characteristics. This has been attributed to differences in convection (Vowinckel and Orvig, 1962). In summer, convective forces are much stronger than in winter. Clouds tend to be physically thicker when convection is strong, which results in greater attenuation of solar radiation. In winter, the reduced convection causes thinner, more stratified clouds which transmit more radiation.

Greatest seasonal variations in transmittances are found in alto cumulus. After removing multiple reflection, winter values are still 0.40 compared to a summer value of 0.26. This suggests alto cumulus formation is extremely sensitive to changes in convection. The larger difference between the Blue Hill and Canadian



TABLE 4.5

## Mean Seasonal Cloud Transmittances

Uncorrected	Season	AC	AS	SC	ST
	Winter	.57	.54	.44	.41
	Spring	.40	.46	.35	.31
	Summer	.30	.31	.32	.29
	Autumn	.34	.39	.29	.27
Corrected	Winter	.40	.37	.30	.28
	Spring	.33	.35	.28	.25
	Summer	.26	.28	.28	.25
	Autumn	.29	.33	.24	.22

alto cumulus transmittances can be partially attributed to seasonal variation. The Blue Hill transmittance is similar to the winter value determined from uncorrected data.

Table 4:5 also shows the magnitude of multiple reflection effects. When these are removed the range of seasonal transmissions is drastically reduced. Strato cumulus shows least seasonal variation of the four types considered. However the range of mean transmission values is reduced from 0.44 - 0.29 for uncorrected estimates to 0.30 - 0.23 for corrected estimates. This trend is present in the four cloud types.

#### 4.4 Variation in Transmittance Among Canadian Stations

Table 4.6 shows the variation of mean cloud-type transmittances among the five stations. Correcting for multiple reflection effects reduces the range of variation in transmittance at all stations. Variation in transmittance between stations for a given cloud type seldom exceeds 5% of the mean transmittance value. Montreal tends to have lower overall transmittances whereas, Winnipeg reports marginally larger values than the other stations for most cloud types. These differences are very small however.

#### 4.5 Comparison of Empirical and Theoretical Cloud Transmissions

Cloud-type transmissions were calculated using a modified two-stream approximation solution of the radiative transfer

TABLE 4.6

## Variation in Mean Transmittance Among Stations

Uncorrected							
	AC	AS	CS	CI	SC	ST	FOG
Goose Bay	.438	.474	.795	.957	.350	.315	.290
Charlottetown	.369	.403	.733	.874	.367	.284	.269
Montreal	.360	.414	.734	.846	.265	.224	.406
Toronto	.380	.443	.730	.877	.327	.274	.246
Winnipeg	.476	.509	.817	.863	.429	.392	.428
Corrected							
	AC	AS	CS	CI	SC	ST	FOG
Goose Bay	.345	.340	.715	.895	.269	.243	.241
Charlottetown	.295	.304	.648	.849	.289	.231	.230
Montreal	.287	.320	.672	.795	.208	.176	.343
Toronto	.309	.345	.683	.836	.260	.216	.210
Winnipeg	.365	.376	.752	.810	.313	.288	.348

equation (Paltridge and Platt, 1976). This method is widely used in numerical models. It requires specification of the single scattering albedo  $\bar{w}_0$ , the asymmetry factor  $g$ , and the optical depth of the cloud,  $\tau$ . The cloud is assumed to consist of water droplets such that the Mie theory for scattering can be applied. Values of  $\bar{w}_0 = 0.995$  and  $g = 0.85$  were chosen. These are comparable with those used in other studies (Joseph, Wiscombe and Weinman, 1976; Shettle and Weinman, 1970). Optical depth  $\tau$ , was calculated from the extinction coefficient  $\beta_{ex}$  and the geometric cloud thickness  $\Delta Z$ . Although the extinction coefficient is a function of wavelength it is fairly constant over most of the visible spectrum of solar radiation. It is far more dependent upon the drop-size distribution within the cloud. Cloud thickness is extremely variable. Singleton and Smith (1960) give geometric thicknesses of stratus cloud which range from 213 - 305 meters to 1975 - 2130 meters. Given that the drop-size distribution for a particular cloud type is quite variable, specification of a single optical depth for one type of cloud is impossible.

#### 4.5.1 Results

Model clouds are proposed which have a range of cloud thicknesses and extinction coefficients used in previous studies. Resulting transmissions are listed in Table 4.7. Also given are theoretical transmissions calculated by Drummond and Hickey (1971), and Liou (1973, 1976) and transmissions measured for clouds over

TABLE 4.7  
Transmission of Solar Radiation Through Clouds

	$\beta_{ex}$ [m]	$\Delta Z$ [m]	$\tau$	T (2-S)	Range of Transmissions	T (Drummond & Hickey, 1971)	T Liou (1976)	T (measured corrected)
AC	$3.9 \times 10^{-2}$	600	23	.19				
	$3.9 \times 10^{-2}$	400	15	.29	.07-.29	.45	.29	.32
	$6.9 \times 10^{-2}$	400	41	.07				
	$6.9 \times 10^{-2}$	600	28	.15				
AS	$3.9 \times 10^{-2}$	600	23	.19	.19-.34	.45	.29	.34
	$3.9 \times 10^{-2}$	300	12	.34				
CS	$1.902 \times 10^{-3}$	1700	3.2	.70	.70	.80	.70	.70
CI						.80	.80	.84
SC	$4.53 \times 10^{-2}$	450	20	.22				
	$4.53 \times 10^{-2}$	400	18	.24				
	$1.00 \times 10^{-1}$	450	45	.06	.06-.24	44-53	24-51	.27
	$1.00 \times 10^{-1}$	400	40	.08				
ST	$1.89 \times 10^{-1}$	450	85	-				
	$1.89 \times 10^{-1}$	400	76	-				
ST	$6.69 \times 10^{-2}$	100	7	.52				
	$6.69 \times 10^{-2}$	200	13	.33				
	$1.00 \times 10^{-1}$	100	10	.40	.09-.52	44-53	24-51	.23
	$1.00 \times 10^{-1}$	200	20	.23				
ST	$1.89 \times 10^{-1}$	100	19	.23				
	$1.89 \times 10^{-1}$	200	38	.09				

Canada.

Measured transmissions generally fall within the range of theoretical values calculated using the two-stream approximation and those reported by other studies. These ranges are large. For stratus, calculated values range from 9 - 52%. It is difficult to draw conclusions about the agreement between measured and theoretical results. Best agreement was obtained for cirriform cloud when both theoretical and empirical transmissions were ~ 70%.

6

## CHAPTER FIVE

### MODEL CALCULATIONS OF SURFACE IRRADIANCE

#### 5.1 Direct Beam Radiation

##### 5.1.1 Expressions for Transmittance

The MAC model calculates direct beam irradiance  $I$  from a theoretical value of the cloudless sky irradiance  $I_0$  and the total cloud opacity TCO:

$$I = I_0(1 - \text{TCO}) \quad 5.1$$

Results from this equation and from eleven other variants (Table 5.1) were compared with nine years (1968-1976) of hourly data for Goose Bay, Montreal and Toronto, the only stations with long records of global and diffuse irradiance from which the direct beam component can be obtained as the difference. For brevity the models are referred to by number.

Model (1) and (2) use "corrected" cloud amount and opacity for each layer,  $i$ . Recorded layer amounts ( $c_i$ ) above the lowest layer are corrected ( $c_i'$ ) for the fraction of the sky obscured from the observer by lower layers of cloud (Davies et al., 1975).

Table 5.1

## Formulation of Direct Beam Transmittance

Model Number	Parameterization
1	$\prod_{i=1}^n (1 - CCA_i)$
2	$\prod_{i=1}^n (1 - CCO_i)$
3	$(1 - TCO)$
4	$(1 - TCA)$
5	$1 - TCO m_r$
6	$1 - TCA m_r$
7	$s$
8	$(s + (1 - TCO))/2$
9	$(s + (1 - TCA))/2$
10	$1 - TCA$
11	$1 - TCO$
12	$\bar{s}$



$$c_1' = c_1$$

$$c_2' = c_2 / (1 - c_1)$$

$$c_3' = c_3 / (1 - c_1 - c_2)$$

$$c_4' = c_4 / (1 - c_1 - c_2 - c_3)$$

Models (3) and (4) estimate the direct beam transmittance in terms of the total cloud cover. Model (4) follows the work of Atwater and Ball (1980).

Models (5) and (6) attempt to account for zenith angle effects on transmittance. If clouds are assumed to be planar surfaces, gaps between clouds decrease with increasing zenith angle (and hence air mass).

Model (7) uses the hourly fractional sunshine duration  $s$ . Although direct beam irradiance is directly related to sunshine duration, previous studies (Davies, 1980; Suckling and Hay, 1977) have shown that it is a poor indicator of direct beam transmittance because sunshine recorders do not respond to weak irradiances at large zenith angles and tend to "overburn" during cloudy bright periods. These effects, especially the latter, lead to large errors in model calculations.

Models (8) and (9), which are based on the cloud-layer-sunshine model of Suckling and Hay (1977), attempt to overcome inadequacies in measures of sunshine duration and cloud cover.

An observer tends to overestimate cloud amount (TCA) thus underestimating transmittance, whereas sunshine duration is known to overestimate transmittance due to overburn at most zeniths (not at large zenith angles). Suckling and Hay (1977) found that these effects are effectively cancelled when the two transmittances are meaned.

Models (10), (11) and (12) attempt to provide a more representative indication of transmittance for an hour. Cloud cover and sunshine data are meaned with that of the preceding hour to obtain a more representative measure for the intervening period.

### 5.1.2 Performance Measures

The root mean square error and mean bias error were used to assess relative model performance. Mean bias error (MBE), which measures the overall tendency for computed irradiance to overestimate or underestimate measured irradiances, was calculated from

$$MBE = \frac{1}{n} \sum_{i=1}^n (F_i' - F_i) / n \quad 5.2$$

where  $F_i'$  and  $F_i$  are the  $i^{\text{th}}$  calculated and measured radiation values respectively, and  $n$  is the total number of observations.

Root mean square error (RMSE) is a measure of the scatter of differences between calculated and measured irradiances. It was calculated from

$$\text{RMSE} = \left[ \sum_{i=1}^n (F_i' - F_i)^2 / n \right]^{1/2} . \quad 5.3$$

For small values of MBE, the square of the RMSE (i.e.  $(\text{RMSE})^2$ ) is approximately the variance of the difference between calculated and measured values since

$$\sigma^2 (F_i' - F_i) = (\text{RMSE})^2 - \text{MBE} . \quad 5.4$$

MBE and RMSE were determined for hourly, daily, monthly and mean hourly irradiances for each month, each year and for the whole period (1968-1976). Both are expressed as percentages of the appropriate mean measured value.

### 5.1.3 Results

Results are listed in Table 5.2. For brevity, models are identified by number.

Clearly, the best MBE values are obtained with the present form of the MAC model (3) and models (11) and (9). Values were less than 4% except for model (9) at Goose Bay (9.9%).

Corrected cloud layer amounts and opacities (1 and 2) systematically underestimated transmittance. Total cloud amount (4) is a poorer measure of cloud cover than opacity due to observer tendency to overestimate amount in partially cloudy

TABLE 5.2

Model performance for direct beam irradiance

		Transmittance Measures												(N)/Mean Irradiance
		1	2	3	4	5	6	7	8	9	10	11	12	
GOOSE	MSE	-20.3	-13.3	1.5	-22.4	-44.9	-61.6	42.3	21.9	9.9	-22.0	1.9	40.7	
MONTREAL	MSE	-36.7	-27.5	-1.1	-21.8	-29.1	-46.9	28.5	13.7	3.4	-21.4	-0.9	26.8	
TORONTO	MSE	-39.0	-32.5	-3.9	-20.4	-30.0	-45.1	28.1	12.1	3.8	-20.2	-3.7	26.6	
		DAILY												
GOOSE	RMSE	77.4	69.6	23.8	45.8	63.8	87.2	65.3	34.1	25.1	45.6	24.5	64.3	(2548)/4.75
MONTREAL	RMSE	65.2	53.4	22.6	38.2	40.8	63.2	48.4	29.8	24.6	37.5	22.5	47.1	(2101)/6.23
TORONTO	RMSE	66.2	57.7	25.9	40.2	43.3	62.1	45.2	28.6	26.2	40.0	26.0	44.2	(2576)/7.04
		HOURLY												
GOOSE	RMSE	137.3	128.3	63.4	87.1	96.4	125.0	101.2	59.8	55.1	86.8	65.7	98.4	(36278)/390
MONTREAL	RMSE	102.9	90.4	50.4	68.8	66.3	93.0	79.2	53.2	50.5	67.4	51.0	76.9	(33073)/549
TORONTO	RMSE	105.7	96.1	52.3	78.4	68.2	91.4	75.9	50.9	50.3	69.3	52.7	76.4	(40613)/598
		MONTHLY MEAN HOURLY												
GOOSE	RMSE	47.1	40.6	18.6	40.9	58.1	81.7	63.8	30.3	18.8	40.3	18.8	63.2	(1408)/369
MONTREAL	RMSE	58.1	45.5	11.9	29.2	41.4	61.7	48.9	25.7	16.6	28.4	12.0	49.0	(1247)/523
TORONTO	RMSE	55.2	47.5	14.9	30.4	36.5	55.1	48.5	28.4	18.4	28.5	22.0	44.2	(1492)/576

conditions. Opacity\* compensates for this tendency since it is often less than cloud amount. Thus for observations where amount exceeds opacity, model (3) increases transmittance.

Models (5) and (6) further augment the problem of overestimation since scaling total cloud cover by the air mass ( $m_r > 1$ ) can only decrease transmittance further.

Sunshine duration (7) gives large positive MBE values. This is attributed to the sunshine recorder's propensity to overburn alternating cloud and bright conditions. It is often difficult to distinguish between sunny and cloudy periods on the recorder card when periods are short. Sunshine duration therefore is overestimated and so is direct beam transmittance. Overestimation due to overburn clearly has a greater effect on direct beam transmittances than failure of the recorder to respond to weak irradiances which causes underestimates to occur.

Models (8) and (9) use the average of sunshine duration and cloudiness (opacity and amount respectively). Because opacity is a better indicator of cloudiness than amount, it does not compensate as well for overestimation of cloud-bright conditions by sunshine measurements. Hence better results are obtained for model (9) than model (8).

---

\*Cloud opacity is defined as that portion of the whole sky that is observed to be concealed (i.e. hidden, or rendered invisible) by the cloud; Manual of Surface Weather Observation; Seventh Edition, 1977. Environment Canada. Hence thin translucent clouds have opacities less than amount because they do not render the whole clouded portion invisible.

The use of mean values for an hour and the preceding hour (10, 11, and 12) produced essentially the same results as the use of actual hourly values (3, 4 and 7). Nothing was gained by averaging adjacent hourly values.

Root mean square error values follow the mean bias error results. Overall, smallest values were obtained with models (3) and (9) on daily, hourly and mean hourly bases. Hourly root mean square error values are always greater than 50% but monthly mean hourly values are much smaller for models (3), (9) and (11) (generally less than 20%).

These results confirm that cloud opacity is the most suitable observed variable for determining direct beam transmittance.

## 5.2 Global Radiation

### 5.2.1 MAC Model Transmittance Formulation

Transmittance parameters determined in Chapters (3) and (4) were used to estimate global and diffuse irradiances. Cloud effects are incorporated into the model using a scheme devised by Manabe and Strickler (1964). The cloud field within each layer is considered to consist of one cloud type, uniformly distributed over the sky. Surface-based cloud observations made on the hour were assumed to be representative of the time period between observations.

Transmission of global radiation  $\tau_{c_i}$ , through the  $i^{\text{th}}$  layer is the sum of contributions from the cloudy and cloudless

portions of the sky:

$$\tau_{c_i} = (1 - c_i) + t_i c_i \quad 5.4$$

where  $c_i$  is the fractional cloud cover and  $t_i$ , the climatic-mean transmittance for the particular cloud type. Total transmission through all layers of the atmosphere  $T$  is the product of individual layer transmissions.

$$T = \prod_{i=1}^n [1 - c_i(1 - t_i)] \quad 5.5$$

Cloud data are usually recorded for a maximum of four layers in Canada. The global irradiance at the surface under  $n$  layers of cloud (not corrected for multiple reflection)  $G_c$  is given by

$$G_c = G_0 \prod_{i=1}^n [1 - c_i(1 - t_i)] \quad 5.6$$

where  $G_0$  is the cloudless sky global irradiance. Introducing the effects of multiple reflection

$$G_c = G_0 \prod_{i=1}^n [1 - c_i(1 - t_i)] / (1 - \alpha_s \alpha_b) \quad 5.7$$

The albedo calculations have been described in Chapter Three. However, atmospheric reflectivity was modified slightly in this study to allow for changes in cloud opacity. Cloud base albedo  $\alpha_c'$  is given by

$$\alpha_c' = \sum \alpha_{c_i} \text{co}_i / \text{TCO}$$

5.8

where  $\alpha_{c_i}$  is layer cloud type albedo as given in Table 5.3

Diffuse radiation  $D$  is the difference between the global and direct beam irradiances.

### 5.2.2 Results

Four cloud transmittance formulations (Table 5.4) were evaluated using coefficients calculated from uncorrected and corrected overcast irradiances.

Transmittance parameters obtained from corrected and uncorrected irradiances are used in MACB, MACC and MACD. The model variants are given in Table 5.5

Global irradiances were calculated for the five stations used to determine cloud transmittance parameters, and for Vancouver, for which data were available from a previous study. Since transmittances were not determined for some observed cloud types because of insufficient data, these were assigned the parameter values of physically similar cloud types (Table 5.6). Table 5.7 gives the parameter values used in each model variant.

Error statistics were calculated for global and diffuse irradiance for the same time periods as direct beam radiation.

Global irradiance results are listed in Table 5.8. With the exception of the present form of the model (1) all variants underestimate irradiance. This could imply that cloud trans-



TABLE 5.3

## Cloud Type Albedo

Number	Cloud Type	Symbol	Albedo
1	Alto cumulus	AC	.55
2	Alto cumulus Castellanus	ACC	.55
3	Alto stratus	AS	.55
4	Cirro stratus	CS	.35
5	Cirrocumulus	CC	.35
6	Cirrus	CI	.35
7	Cumulonimbus	CB	.60
8	Cumulus	CU	.60
9	Cumulus Fractus	CF	.60
10	Stratus Fractus	SF	.60
11	Towering Cumulus	TCU	.60
12	Nimbostratus	NS	.60
13	Stratocumulus	SC	.60
14	Stratus	ST	.60
15	Fog	FOG	.60
16	Obstruction	OTF	.60

TABLE 5.4

## Cloud Transmittance Functions

Model	Form of Transmittance Function
MACA	$t = A \exp(-Bm)$
MACB	$t = a/m \exp(-bm_p)$
MACC	$t = c + dm$
MACD	$t = \bar{T}$

TABLE 5.5  
Model Variants

Model	Number	Method	Data Source	Irradiances
MACA	1	Expfit	Blue Hill	uncorrected
MACA	2	Expfit	Canadian(Pooled)	uncorrected
MACB	3	Expfit	Blue Hill	uncorrected
MACB	4	Expfit	Canadian(Pooled)	uncorrected
MACB	5	Gridls(0)	Canadian(Pooled)	corrected
MACB	6	Gridls(1)	Canadian(Pooled)	corrected
MACC	7	Correg	Canadian(Pooled)	uncorrected
MACC	8	Correg	Canadian(Pooled)	corrected
MACD	9	Constant	Canadian(Pooled)	uncorrected
MACD	10	Constant	Canadian(Pooled)	corrected

TABLE 5.6  
Cloud-Type Groups

AC	AS	CS	CI	SC	ST	FOG
ACC		CC		CB	SF	OTF
				*CU	NS	
				CF		
				TCU		

TABLE 5.7

## Parameter Values used in Model Variants

Model A ( $t_i = A_i \exp(-B_i m)$ )

Cloud Type Code	Blue Hill		Cánada	
	$A_i$	$B_i$	$A_i$	$B_i$
1	0.556	0.053	0.385	0.013
2	0.556	0.053	0.385	0.013
3	0.413	0.004	0.452	0.024
4	0.923	0.089	0.819	0.042
5	0.923	0.020	0.819	0.042
6	0.871	-0.226	0.848	-0.004
7	0.119	0.045	0.343	0.025
8	0.368	0.045	0.343	0.025
9	0.368	0.045	0.343	0.025
10	0.252	0.100	0.290	0.027
11	0.368	0.045	0.343	0.025
12	0.119	-0.226	0.290	0.027
13	0.368	0.045	0.343	0.025
14	0.252	0.100	0.290	0.027
15	0.163	-0.031	0.248	-0.029
16	0.163	-0.031	0.248	-0.029

TABLE 5.7  
(continued)

$$\text{Model B } t_i = (a_i/m) \exp(-b_i m)/G_0$$

Cloud Type Code	PARAMETERS FROM UNCORRECTED IRRADIANCES				PARAMETERS FROM CORRECTED IRRADIANCES			
	Blue Hill		Canada		GRIDLS0		GRIDLS1	
	$a_c$	$b_c$	$a_c$	$b_c$	$a_c$	$b_c$	$a_c$	$b_c$
1	2199	.112	1526	.059	1336	0.089	1321	0.097
2	2199	.112	1526	.059	1336	0.089	1321	0.097
3	1633	.063	1791	.070	1523	0.108	1412	0.114
4	3648	.148	3248	.088	3084	0.103	2456	0.104
5	3648	.148	3248	.088	3084	0.103	2456	0.104
6	3443	.079	3361	.043	3348	0.062	3660	0.065
7	1453	.104	1361	.071	1195	0.111	1137	0.111
8	1453	.104	1361	.071	1195	0.111	1137	0.111
9	1453	.104	1361	.071	1195	0.111	1137	0.111
10	997	.159	1149	.073	1012	0.106	802	0.114
11	1453	.104	1361	.071	1195	0.111	1137	0.111
12	469	.167	1149	.073	1012	0.106	802	0.114
13	1453	.104	1361	.071	1195	0.111	1137	0.111
14	997	.159	1149	.073	1012	0.106	802	0.114
15	645	.028	982	.018	897	0.023	375	-0.078
16	645	.028	982	.018	897	0.023	375	-0.078

TABLE 5.7  
(continued)

Model C ( $t_i = \alpha_i + \beta_i m$ )

Cloud Type Code	FROM UNCORRECTED IRRADIANCES		FROM CORRECTED IRRADIANCES	
	$\alpha_i$	$\beta_i$	$\alpha_i$	$\beta_i$
1	0.375	0.010	0.330	-0.004
2	0.375	0.010	0.330	-0.004
3	0.435	0.006	0.368	-0.011
4	0.787	-0.010	0.745	-0.020
5	0.787	-0.010	0.745	-0.020
6	0.835	0.023	0.825	0.007
7	0.331	0.005	0.286	-0.007
8	0.331	0.005	0.286	-0.007
9	0.331	0.005	0.251	-0.007
10	0.291	0.003	0.286	-0.007
11	0.331	0.005	0.286	-0.007
12	0.291	0.003	0.251	-0.007
13	0.331	0.005	0.286	-0.007
14	0.291	0.003	0.251	-0.007
15	0.266	0.019	0.237	0.011
16	0.266	0.019	0.237	0.011

TABLE 5.7  
(continued)

Model D ( $t_i = \bar{T}_i$ )

Cloud Type Code	FROM UNCORRECTED IRRADIANCES	FROM CORRECTED IRRADIANCES
	$t_i$	$t_i$
1	0.402	0.319
2	0.402	0.319
3	0.451	0.338
4	0.763	0.696
5	0.763	0.696
6	0.891	0.841
7	0.347	0.267
8	0.347	0.267
9	0.347	0.267
10	0.299	0.232
11	0.347	0.267
12	0.299	0.232
13	0.347	0.267
14	0.299	0.232
15	0.320	0.268
16	0.320	0.268

mittances used in models 2 - 10 are too small. Model 3 uses Blue Hill overcast irradiance estimates and a theoretical value of cloudless sky radiation. All other model transmittances (model 2, 4 - 10) were derived from pooled Canadian data. Several reasons can be suggested for this consistent underestimation.

Firstly, cloud transmittances were determined using overcast data. The optical characteristics of a cloud in overcast conditions may not be representative of partially cloudy conditions. Atwater and Ball (1981) have suggested that clouds become optically thicker as cloud amount increases. They proposed a cloud transmittance  $\bar{t}_i$ , which was a function of cloud amount  $c_i$ .

$$\bar{t}_i = t_i^{c_i/c_x} \quad 5.9$$

The value of  $c_x$  was determined empirically from data collected during GATE and found to be 0.85. Ball (1981) found that a value of 0.75 was more representative for the United States.

Secondly, observed values of cloud amount may be poor measures of actual cloudiness. Under partially cloudy conditions, upper layers can be obscured.

Thirdly, the contribution of multiple reflection effects may be underestimated in the model. This could be due to underestimates of cloud base reflectivity and surface albedo.

Fourthly, the effects of aerosol uncertainty are large. Values for the aerosol transmission that were assigned to individual stations could be incorrect and produce systematic errors. Uncertainties due to aerosol effects are better seen by comparing the

first four models. Models 1 and 3 use Blue Hill derived transmittance parameters whereas models 2 and 4 use Canadian derived values. Differences between mean bias errors of models 1 and 3 (and those of 2 and 4) result from differences in cloudless sky transmittances only, since the same cloud-type parameters were used in 1 and 3 and in 2 and 4. Differences between the values of mean bias errors for 1 and 3 (Blue Hill) at non-urban stations are much larger than the differences for urban stations.

		$\Delta$ MBE (%)
non-urban	Goose Bay	-6.7
	Charlottetown	-3.7
	Winnipeg	-4.8
urban	Toronto	-0.6
	Montreal	-0.7

Cloudless sky irradiances at Blue Hill are in better agreement with those recorded (1) or calculated (3) for Toronto and Montreal than with those of the relatively cleaner sites. Since cloudless conditions are usually associated with anticyclonic activity, they are also associated with greatest concentration of and maximum attenuation by aerosol. Northeastern United States is heavily populated and the dominating westerly winds could transport pollutants east to the Boston area.

The transmittance parameters used for testing the layer model were derived from pooled data which included stations with relatively clean air as well as Toronto and Montreal. If Blue Hill



TABLE 5.8

Model performance for global irradiance

	A			B			C			D			N	F
	BH	C	BH	G	C	GRIDLS	GRIDLS	G	Linear	G	Constant	G		
MBE	1	2	3	4	5	6	7	8	9	10				
GOOSE BAY	0.2	-2.0	-6.5	-6.7	-14.6	-19.3	-2.5	-12.6	-2.1	-12.3				
CHARLOTTETOWN	0.2	-0.5	-3.5	-2.8	-9.2	-13.3	0.2	-7.6	0.8	-6.6				
MONTREAL	1.0	-1.5	-0.4	-0.8	-7.1	-10.3	-2.2	-9.6	-1.6	-9.4				
TORONTO	-3.3	-5.3	-2.6	-3.5	-9.5	-14.7	-5.5	-12.3	-4.9	-12.3				
WINNIPEG	1.1	-0.4	-3.7	-3.8	-9.4	-12.2	-1.8	-9.1	-1.4	-8.7				
VANCOUVER	-0.8	-3.6	-4.7	-5.9	-11.8	-13.9	-2.9	-10.5	-2.5	-10.2				
<u>RMSE</u>														
(a) DAILY														
GOOSE BAY	15.1	15.9	16.1	16.8	22.4	28.1	15.2	21.2	14.8	21.3	2949	10.621		
CHARLOTTETOWN	12.7	13.0	12.6	12.9	16.2	20.5	12.8	15.6	12.7	15.8	1989	12.471		
MONTREAL	11.1	11.9	10.9	11.2	13.5	16.7	11.7	15.4	11.5	15.4	2913	12.154		
TORONTO	11.0	12.1	11.4	11.7	14.8	20.0	12.5	17.1	12.1	17.0	3081	13.372		
WINNIPEG	11.3	11.3	11.7	11.5	14.9	18.7	10.9	14.8	10.7	14.7	3130	13.290		
VANCOUVER	12.9	14.5	13.7	15.3	19.9	22.3	14.2	19.1	13.8	19.1	3189	11.776		
(b) HOURLY														
GOOSE BAY	34.1	34.5	33.8	36.5	38.0	44.1	33.7	37.1	33.1	37.4	36472	872		
CHARLOTTETOWN	28.9	29.5	28.5	29.2	31.6	36.5	29.2	31.2	29.0	31.6	24625	1034		
MONTREAL	29.1	29.5	28.7	29.1	30.2	33.4	29.2	30.9	29.0	31.1	35397	1011		
TORONTO	27.0	27.5	26.9	27.3	29.1	35.2	27.5	30.3	27.2	30.4	38049	1102		
WINNIPEG	25.2	25.3	25.0	25.0	27.3	32.2	24.6	27.1	24.2	27.2	38212	1098		
VANCOUVER	28.8	30.0	29.0	30.6	33.6	36.3	29.9	33.0	29.4	33.2	38935	977		
(c) MONTHLY MEAN														
HOURLY														
GOOSE BAY	10.4	12.6	14.0	15.4	22.4	28.8	13.5	21.0	12.0	21.4	1334	823		
CHARLOTTETOWN	7.6	8.6	9.7	10.1	15.0	20.0	9.5	14.1	8.7	14.5	872	981		
MONTREAL	7.2	7.8	6.8	7.2	11.2	14.9	8.1	13.4	7.4	13.5	1292	960		
TORONTO	7.2	8.7	7.8	8.3	13.5	19.8	9.6	15.9	8.7	16.2	1340	1060		
WINNIPEG	6.6	7.5	8.8	9.3	14.1	18.1	8.6	14.1	7.7	14.1	1350	1045		
VANCOUVER	9.0	11.3	10.8	13.4	18.7	21.4	12.1	17.9	11.0	18.1	1376	927		

cloudless conditions are similar to those of Toronto and Montreal (i.e. relatively high aerosol concentration) cloudless sky irradiances measured at Blue Hill would be slightly smaller than those of the pooled Canadian data. This would reduce cloud-type transmittances over Canada and hence result in consistently lower estimates from model 2 than model 1.

Values of root mean square errors for global irradiance estimates on a daily basis range from 11 - 16% for models 1 and 2 at all stations. Using corrected transmittances resulted in larger root mean square errors. Hourly error values are much larger but show the same trend as daily statistics. Monthly mean hourly statistics range from 7 - 10% for model 1 at all stations and are generally less than 12% for all models which used uncorrected transmittances.

It should also be emphasized that model 8 which used a constant cloud-type transmittance value (uncorrected) performed very well. This would represent a significant simplification to the layer model calculations.

### 5.3 Diffuse Radiation

#### 5.3.1 Results

Since diffuse radiation records were available only for Goose Bay, Montreal and Toronto, model estimates could not be compared for other stations. Results of diffuse irradiance error statistics are given in Table 5.9. Because diffuse radiation is

TABLE 5.9

Model performance for diffuse irradiance

	1	2	3	4	5	6	7	8	9	10	N	F
<u>MBE</u>												
GOOSE BAY	-0.5	-4.6	-12.5	-13.0	-28.1	-37.0	-5.2	-24.5	-4.4	-25.9		
MONTREAL	3.2	-2.0	2.1	-0.4	-14.0	-20.9	-3.4	-19.0	-2.1	-16.4		
TORONTO	-2.8	-7.3	-1.1	-3.2	-16.1	-27.2	-7.7	-22.1	-6.3	-22.0		
<u>RMSE</u>												
(a) DAILY												
GOOSE BAY	27.1	29.1	30.1	31.5	42.0	51.8	28.2	39.4	27.7	39.6	2806	5.6
MONTREAL	25.7	28.1	24.1	25.9	31.0	37.0	27.7	35.3	27.2	35.4	2975	5.6
TORONTO	24.3	26.3	23.6	24.5	30.0	40.2	26.2	34.6	25.5	34.8	2917	6.3
(b) HOURLY												
GOOSE BAY	57.2	58.5	57.0	63.1	64.9	74.5	57.2	63.1	56.6	63.7	35533	465
MONTREAL	55.8	57.2	54.0	55.6	58.3	64.6	56.2	60.2	56.0	60.6	36883	474
TORONTO	51.0	52.0	49.9	51.0	54.3	66.3	51.2	56.6	51.1	57.2	36046	518
(c) MONTHLY MEAN												
HOURLY												
GOOSE BAY	15.2	17.1	22.5	23.3	36.6	47.6	18.4	33.5	16.4	34.0	1332	436
MONTREAL	15.3	16.6	13.0	14.5	22.2	29.7	16.8	27.2	15.5	27.4	1348	447
TORONTO	12.2	14.9	11.6	13.1	22.4	35.2	16.0	28.1	14.4	28.6	1315	500

determined as a residual, estimates will depend upon errors in the calculation of global and direct beam radiation. All models tend to underestimate measured values. At Goose Bay mean bias errors are much smaller for 1 and 2 than for 3 and 4. This trend is not present for Toronto or Montreal. Since mean bias errors of models 3 and 4 are more negative than those of 1 and 2, cloudless sky global radiation estimates must be too large. This could result from inaccurate estimation of multiple reflection effects. Goose Bay is colder for longer periods of the year than Toronto or Montreal. The temperature based algorithm used to compute multiple reflection assumes a constant snow cover once temperature falls below  $-6.0^{\circ}\text{C}$ . and then assigns an albedo value applicable for snow. The surface may in fact not be snow-covered. Hence the model will overestimate the cloudless sky irradiance.

Although RMSE values for diffuse radiation exceed those for global radiation it should be noted that they are calculated as a percentage of the mean measured flux. Since the diffuse flux is approximately half the global flux, absolute RMSE values are very similar. Modes (1-4) and model (8) perform well. Hourly statistics are much poorer but monthly mean hourly values are relatively good.

#### 5.4 Discussion of Results

These results provide insight into the problems of estimating climatic-mean cloud-type transmittances. The use of transmittances corrected for multiple reflection resulted in lower irradiance

estimates than those obtained using uncorrected transmittances. In Chapter 3 multiple reflection effects were shown to be very significant to the surface irradiance. Hence using uncorrected transmittances should result in overestimation of the surface flux. This enhancement is compensated by the presence of overlying cloud. Transmittances were determined from overcast data of a single cloud type. Therefore it was impossible to specify whether or not overlying cloud existed. Figure 3.16 a, indicates the distribution of scatter in the data for alto cumulus. Irradiances at small air masses have a wide range of values. The lower irradiances at smaller air masses infer the presence of overlying cloud. These observations bias the sample such that transmittance is underestimated. Considering the consistently better results using uncorrected rather than corrected transmittances, underestimation due to overlying clouds compensates overestimation due to multiple reflection effects quite well.

It should also be noted that the model estimates are sensitive to errors in the calculation of various cloudless sky parameters.

#### 5.4.1 Solar Constant

In this study a value of  $1353 \text{ Wm}^{-2}$  was used. However, recently Ramanathan(1981) used a value of  $1370 \text{ Wm}^{-2}$ . Any change in the value of the solar constant will result in change in the surface irradiances of the same relative magnitude. Hence an increase in the value of the solar constant from  $1353 \text{ Wm}^{-2}$  to  $1370 \text{ Wm}^{-2}$  would

increase the surface flux and MBE by 1.26%. The relative performance of models is changed. MBE values for models (2), (4) and (9) would then be smaller than that for model (1).

#### 5.4.2 Aerosol Parameterization

As mentioned earlier, a value for the aerosol extinction coefficient  $k$  was assigned to each station, based on expected local aerosol conditions. Values were 0.91 for Toronto and Montreal, and 1.0 for Charlottetown, Winnipeg, Vancouver and Goose Bay.

In a previous study (Davies, 1980) the model was tested using  $k$  values  $< 1.0$  as well as using  $k = 1.0$  (i.e. no aerosol attenuation).

The results can be used to show the sensitivity of the model to the value of  $k$ . Table 5.10 lists the MBE values for  $k = 1.0$  and for the values of  $k$  assigned to each station. The sensitivity of the MBE to  $k$  was calculated from

$$\frac{dMBE}{dk} \approx \frac{MBE(1) - MBE(2)}{k(1) - k(2)}$$

where (1) refers to the values of MBE and  $k$  for results of the study where  $k = 1.0$  and (2) refers to those of the study where  $k$  was assigned a value.

MBE values will change by 0.70 to 0.93% with a 0.01 change in  $k$ . This means that an error of 0.01 in the specification of  $k$  leads, on average, to ~ 0.82% change in the MBE value. The limit of accuracy for specifying  $k$  is ~ 0.05 at best. Therefore,

TABLE 5.10

Mean Bias Errors for  $k = 1.0$  and  $k < 1.0$ 

	Goose Bay	Charlotte- town	Montreal	Toronto	Winnipeg	Vancouver
k	0.97	0.95	0.91	0.91	0.95	0.95
MBE	-2.2	3.8	0.8	-3.5	-3.6	-5.1
k	1.0	1.0	1.0	1.0	1.0	1.0
MBE	-0.1	0.3	9.2	4.1	0.7	-0.9
$\frac{\Delta\text{MBE}}{\Delta k}$	0.70	0.70	0.93	0.84	0.86	0.84

TABLE 5.11

Errors In Precipitable Water Estimates

$T_d$ [°C]	$\Delta G/G$ [mm <sup>-1</sup> ]	$a_w$	$da_w/dU_w$ [mm <sup>-1</sup> ]	$U_w$ [mm]	$\Delta U_w$ [mm]	
-20	-0.00828	0.06978	0.007057	3.21	~ 1.2	(37%)
-10	-0.00553	0.08296	0.004638	5.54	~ 1.8	(32%)
0	-0.00367	0.09786	0.003027	9.56	~ 2.7	(28%)
10	-0.00242	0.11455	0.001956	16.49	~ 4.5	(27%)
20	-0.00158	0.13304	0.001248	28.45	~ 7.0	(25%)
30	-0.00102	0.15324	0.000785	49.08	~ 10.0	(20%)

the MBE has an uncertainty of ~ 4%.

Considering Toronto results, model (4) performs best when only the aerosol uncertainty is accounted for whereas if the solar constant and aerosol uncertainty are included model (2) has an MBE  $\approx 0.0$ . Model 9 also greatly improves.

#### 5.4.3 Water Vapour Absorption

Uncertainties in the calculation of water vapour absorption arise mainly from errors involved in specifying precipitable water  $U_w$  using Won's (1977) empirical formula,

$$U_w = \exp(2.2572 + 0.05454 T_d)(P/P_0)^{3/4}(T^0/T_s)^{1/2} \quad 5.1$$

where  $T_d$  is dew point temperature ( $^{\circ}\text{C}$ ), and  $T_s$  and  $T^0$  the surface temperature and standard surface temperature 273K respectively. Ignoring aerosol effects and setting transmittances after ozone and Rayleigh depletion to 0.97 and 0.9 respectively, the relative error in global irradiance estimates due to errors in the specification of precipitable water is given by,

$$\frac{\Delta G}{G} = \frac{.1}{a_w - 0.9215} \frac{da_w}{dU_w} \Delta U_w \quad 5.1$$

Selecting a range of dew point temperatures from  $-20^{\circ}\text{C}$  to  $30^{\circ}\text{C}$ , the error in the precipitable water estimate needed to produce a 1% change in the global flux can be calculated (Table 5.11). In



general, a 1% change in the global flux results from a 25 - 35% error in  $U_w$ . Choosing a mean value of  $a_w = 0.1$  and a range of values for  $da_w/dU_w$ , the relative error in the estimated irradiance is,

$$\frac{\Delta G}{G} = \begin{array}{l} -0.002 \Delta U_w \text{ in summer} \\ -0.006 \Delta U_w \text{ in winter} . \end{array}$$

Since a relatively large error (25-35%) is needed in the calculation of precipitable water to produce a 1% error in the surface flux, it is unlikely that uncertainties in the resulting calculated irradiances are due to inaccuracies in the specification of water vapour absorption.

#### 5.4.4 Surface Albedo

In Chapter Three multiple reflection between surface and atmosphere was shown to have a pronounced effect on the surface irradiance. Hence errors in the calculation of surface albedo will also have a large effect. Relative error of model estimates to errors in surface albedo can be calculated from

$$\frac{\Delta G}{G} = \alpha_b \Delta \alpha_s / (1 - \alpha_b \alpha_s)$$

Using Vancouver, where  $k = 1$ , errors in surface albedo are easily calculated. Since temperature seldom falls below  $0^\circ\text{C}$ , surface albedo would be assigned a value  $\alpha_s = 0.2$ . Assuming a mean cloud

amount of 50% with an average cloud base albedo of 0.6, the relative error in the global irradiance due to a change in surface albedo can be estimated by

$$\frac{\Delta G}{G} = 0.3729 \Delta \alpha_s$$

Therefore, a change of 0.05 in surface albedo from 0.20 to 0.25 would result in an increase in the global surface flux by ~ 1.9%. Since aerosol effects can not be increased at Vancouver ( $k = 1.0$ ), surface albedo errors may be partly responsible for the large MBE value for Vancouver. Considering the marked difference in the reflectivity of snow compared to vegetation, accurate specification of surface albedo is very important, especially at stations where  $k = 1.0$ .

#### 5.4.5 Atmospheric Backscatter

The relative error in the global flux resulting from error in atmospheric backscatter is

$$\frac{\Delta G}{G} = \alpha_s \Delta \alpha_b / (1 - \alpha_b \alpha_s)$$

Assuming a mean cloud amount of 50% with a cloud base albedo of 0.6 yields a value of 0.347 for  $\alpha_b$ . However the major part of atmospheric backscatter is due to cloud reflectivity (.30 of .347). Setting surface albedo at 0.2 for summer and 0.8 for winter con-

ditions, the relative error in the global flux resulting from a 10% error in  $\alpha_b$  can be shown.

$$\frac{\Delta G}{G} = \begin{array}{l} .022\% \text{ in summer} \\ .110\% \text{ in winter} \end{array}$$

Hence, errors in the specification of atmospheric backscatter are relatively small and are mainly a result of errors in cloud cover factors.

## CHAPTER SIX

### SUMMARY AND CONCLUSIONS

#### 6.1 Summary

The objectives of this study were to:

- (i) develop climatic-mean transmittance properties of clouds and
- (ii) improve upon the method of estimating direct beam transmittance through a cloudy atmosphere.

Cloud transmittance parameters were calculated using Canadian radiation and meteorological data employing the same method as Haurwitz (1948). Parameters were evaluated for individual stations and for Canada using pooled data from the five stations. Transmittances for Canada were similar but smaller than those of Haurwitz, with the exception of alto cumulus.

Transmittance parameters were also evaluated using global radiation data which had been corrected for multiple reflection between the surface and atmosphere. This resulted in lower estimates of the transmittance parameters. Because the transmittance function was exponential, a non-linear least-squares method was employed in statistically fitting the irradiance curve, as well as the logarithmic transformation used by Haurwitz. Results of both the linear and non-linear statistical routines were very similar. The non-linear method

was also weighted by the standard deviation. This did not improve parameter estimates.

Cloud-type transmissions were calculated using three expressions; (i) exponential  $t = A \exp(-Bm)$

(ii) linear  $t = c + dm$

(iii) constant  $t = \bar{T}$

Transmissions were evaluated using uncorrected and corrected global radiation data for individual stations and for the pooled data.

Effects of multiple reflection were found to be significant. Mean transmission values for corrected radiation were larger than those for uncorrected radiation. Multiple reflection enhancement of the surface flux ranged from ~ 8% for cirrus to ~ 25 - 30% for stratiform clouds.

Transmittance parameters and cloud-type transmissions were evaluated seasonally. Results showed transmittance to be greatest in winter and smallest in summer. This trend was present in both uncorrected and corrected transmissions. Seasonal differences were attributed to seasonal variation in convection. Physically and optically thicker clouds are formed when convective forces are stronger in summer. Variation in cloud transmissions across Canada was found to be minimal. However comparison of Canadian results with those obtained for Hamburg (Kasten and Czeplak, 1980) and GATE data (Atwater and Ball, 1980) showed large differences. Canadian transmissions were consistently larger than those for Hamburg whereas better agreement was obtained between Canadian and GATE results. It is suggested that the data samples from

which the cloud transmittances were determined are not totally compatible.

Empirical results of this study were compared with theoretically calculated transmission values determined using the modified two-stream approximation method (Paltridge and Platt, 1976).

Results are difficult to compare because of the wide range of physical shapes and sizes of clouds which occur in nature.

Direct beam transmittances were calculated using a number of clear sky indicators in the MAC layer model. The present form which uses total cloud opacity as a measure of cloudiness gave best results overall.

The revised cloud transmittance parameters as well as those of Haurwitz which are presently used were tested in the MAC layer model for estimating global and diffuse irradiances. Use of the present transmittances yielded best results. Correcting the transmittances for multiple reflection effects led to lower model estimates and larger root mean square errors. The use of mean cloud-type transmittance values gave similar results to those obtained using a transmittance function. This could be a significant simplification to layer model calculations.

## 6.2 Conclusions

Use of cloud transmittances determined empirically from Canadian global radiation data led to larger errors in the overall performance of the layer model. These errors however were well

within the range of errors expected from the relative sensitivities of clear sky parameters. Since the layer model calculates a secondary diffuse term due to multiple reflection, this component should be removed prior to cloud transmittance evaluation. However this led to larger errors. Mean bias errors showed calculated model values underestimated measured global irradiances. This suggests cloud transmittances are too low. However when the revised value of the solar constant was used model estimates using Canadian transmittance parameters increased by 1.26%. Blue Hill parameters then overestimated irradiances and Canadian parameters performed better.

Transmittances were determined from overcast global radiation data. In overcast conditions it is impossible to specify any overlying cloud above the overcast deck. Transmittance will be reduced if overlying cloud exists. Hence, long-term average transmittances will be underestimated.

It has also been suggested by Atwater and Ball that clouds become proportionately thicker as their amount increases. Using overcast conditions to determine mean-climatic transmittances then is not representative for partially cloudy conditions.

Multiple reflection has been shown to be an important aspect of the radiation balance. For highly reflective snow-covered surfaces in winter this enhancement may be as much as ~ 30 - 40% of the global irradiance at the surface. Better results were obtained using transmittances that were not corrected for this enhancement. Multiple reflection compensates for the underestimated cloud-type transmittances. In view of the good results using uncorrected

transmittances, these two factors must compensate each other effectively.

Aerosols were not considered in this study. In the study by Davies (1980), it was shown that aerosols could affect mean bias errors by as much as 8% of the mean flux. Considering the differences in mean bias errors of models 1 - 4 for global radiation estimates, all differences can be explained by uncertainty in aerosol parameterization.

### 6.3 Recommendations for Future Study

If layer model estimates are to improve from their present state, a better indication of cloud cover must be used. Surface-based observations are not adequate to describe the condition of cloud in the atmosphere. A possible improvement would include the use of satellite data which would permit a view of the atmosphere from above. However many problems of resolution still exist with this method.

The Atmospheric Environment service adopted a new system of recording cloud cover in 1977. Amount is no longer recorded, rather the sky is considered to be clear or cloudy. If cloudy, conditions are recorded as scattered, broken or overcast cloud. Modifying the MAC layer model to this new cloud cover system may prove worthwhile.

Much of the uncertainty in the results of this study has been attributed to multiple reflection. The present model assigns a value for reflectivity of the surface based upon the temperature. As was shown for Goose Bay, this may not be a good indicator of



surface albedo. An indicator of snow cover is the only way to consider the large differences associated with snow-covered and snow-free surface reflectivity. In Canada, the multiple reflection component is especially significant because the largest gaps in the measurement network occur in the north where snow-cover exists for much of the year.

## REFERENCES

- Atwater, M.A. and J.T. Ball, 1976: Comparison of radiation computation using observed and estimated precipitable water. J. Appl. Meteorol., 15, 1319-1320.
- Atwater, M.A. and J.T. Ball, 1978a: A numerical solar radiation model based on standard meteorological observations. Solar Energy, 21, 163-170.
- Atwater, M.A. and J.T. Ball, 1978b: Intraregional variations of solar radiation in the eastern United States. J. Appl. Meteorol., 17, 1116-1125.
- Atwater, M.A. and J.T. Ball, 1980: A surface solar radiation model for cloudy atmospheres. Mon. Wea. Rev.
- Atwater, M.A. and J.T. Ball, 1981: Effects of clouds on insolation models. Solar Energy, 27, 37-44.
- Atwater, M.A. and P.S. Brown, Jr., 1974: Numerical computation of the latitudinal variations of solar radiation for an atmosphere of varying opacity. J. Appl. Meteorol., 13, 289-297.
- Ball, J.T., S.J. Thoren, M.A. Atwater, 1980a: Cloud coverage characteristics during Phase III of GATE as derived from satellite and ship data. Mon. Wea. Rev., 108, (in press).
- Ball, J.T., M.A. Atwater, S.J. Thoren, 1980b: Sensitivity of computed incoming solar radiation to cloud analyses (submitted for publication).
- Bevington, P.R., 1969: Data Reduction and Error Analysis for the Physical Sciences. McGraw-Hill, New York, 336.
- Braslau, N. and J.V. Dave, 1973: Effects of aerosols on the transfer of solar energy through realistic model atmospheres. Part I: Nonabsorbing aerosols. J. Appl. Meteorol., 21, 601-615.
- Carrier, L.W., G.A. Cato, and K.J. von Essen, 1967: The backscattering and extinction of visible and infra-red radiation by selected major cloud models. Appl. Optics, 7, 1209-1216.
- Coulson, K.L., 1975: Solar and Terrestrial Radiation. Academic Press, New York, 322 p.

- Danielson, R.E., D.R. Moore and H.C. Van de Hulst, 1969: The transfer of visible radiation through clouds. J. Atmos. Sci., 26, 1078-1087.
- Davies, J.A., 1980: Models for estimating incoming solar irradiance. Report to the Atmospheric Environment Service, DSS Contract No. OSU79-00163, 100.
- Davies, J.A. and J.E. Hay, 1978: Calculation of Solar Radiation Data. Proceedings of the Canadian Solar Radiation Workshop, April 17-19, 1978 (in press).
- Davies, J.A. and J.E. Hay, 1980: Calculation of the solar radiation incident on a horizontal surface. Proceedings of the First Solar Radiation Data Workshop, edited by T. Wan and J.E. Hay, 32-58.
- Davies, J.A. and Idso, S.B., 1978: Estimating the surface radiation balance and its components. In Gerberm J.F. and B.J. Banfield (editors), Modification of the aerial environment of Plants, ASAE Monograph (in press).
- Davies, J.A. and D.C. McKay, 1981a: Evaluation of methods for estimating solar irradiance in Canada. Fourth Conference on Atmospheric Radiation, American Meteorological Society, 43-47.
- Davies, J.A. and D.C. McKay, 1981b: Estimating solar irradiance and compartments. Solar Energy (in press).
- Davies, J.A., W. Schertzer and M. Nunez, 1975: Estimating global solar radiation. Boundary Layer Meteorol., 9, 33-52.
- Davies, J.A. and Uboegbulam, T.C., 1979: Parameterization of surface incoming radiation in tropical cloudy conditions, Atmosphere, (in press).
- Deirmendjian, D., 1969: Electromagnetic Scattering on Spherical Polydispersions. Elsevier, New York, 290.
- Driedger, H.L. and A.J.W. Catchpole, 1970: Estimation of solar radiation receipt from sunshine duration at Winnipeg, Meteorol. Magazine 99, 285-291.
- Drummond, A.J. and J.R. Hickey, 1971: Large-scale reflection and absorption of solar radiation by clouds as influencing earth radiative budgets. New Aircraft Measurements. Preprint, Intern. Conf. Weather Modification, Canberra, Australia, Amer. Meteorol. Soc., 267-276.
- Duffie and Beckman, 1974: Solar energy thermal processes, Wiley, Toronto, 386.

- Gibbons, J.D., 1976: Non-parametric Methods for Quantitative Analysis, New York, Holt, Rinehardt and Winston, 463.
- Hardyck, C.D. and L.F. Petrinovich, 1969: Introduction to Statistics for the Behavioural Sciences. Philadelphia, W.B. Saunders Co., 302.
- Haurwitz, B., 1945: Insolation in relation to cloudiness and cloud density. J. of Meteorol. 2, 154-166.
- Haurwitz, B., 1946: Insolation in relation to cloud type. J. Meteorol., 3, 123-124.
- Haurwitz, B., 1948: Insolation in relation to cloud type. J. Meteorol., 5, 110-113.
- Hay, J.E., 1970: Precipitable water over Canada. I. Computation, Atmosphere, 8, 128-143.
- Holmgren, B. and G. Weller, 1973: Studies of the solar and terrestrial radiation fluxes over Arctic pack ice. Geophysical Institute, Univ. of Alaska, ARPA Order No. 1783, 23.
- Hottel, H.C., 1976: A simple model for estimating the transmittance of direct solar radiation through clear atmospheres. Solar Energy, 18, 129-134.
- Houghton, H.G., 1954: On the heat balance of the Northern Hemisphere. J. Meteorol., 11, 1-9.
- Hoyt, D.V., 1977: A redetermination of the Rayleigh optical depth and its application to selected solar radiation problems. J. Appl. Meteorol., 16, 432-436.
- Hoyt, D.V., 1978: A model for the calculation of solar global insolation. Solar Energy, 21, 27-35.
- Idso, S.B., 1969: Atmospheric attenuation of solar radiation. J. Atmospheric Sci., 26, 1088-1095.
- Idso, S.B., 1970: The transmittance of the atmosphere for solar radiation on individual clear days. J. Appl. Meteorol., 9, 239-241.
- Irvine, W.M., 1968: Multiple scattering by large particles. II. Optically thick layers. Astrophys. J., 152, 823-834.
- Joseph, J.H., W.J. Wiscombe and J.A. Weinman, 1976: The Delta-Eddington approximation for radiative flux transfer. J. Atmos. Sci., 33, 2452-2459.
- Kasten, F., 1966: A new table and approximation formula for the

- relative optical air mass. Archiv. for Meteorol., Geophys. und Bioklim, B 14, 206-223.
- Kasten, F. and G. Czeplak, 1980: Solar and terrestrial radiation dependence on the amount and type of cloud. Solar Energy, 34, 177-190.
- Kimura, K. and D.G. Stephenson, 1969: Solar radiation on cloudy days. Research Paper No. 418, Division of Building Research, National Research Council, Ottawa, 9.
- King, L.J., 1969: Statistical Analysis in Geography. Englewood Cliffs, N.J., Prentice-Hall Inc., 288.
- King, R. and R.O. Buckius, 1979: Direct solar transmittance for a clear sky. Solar Energy, 22, 297-301.
- Kondrat'yev, K. Ya., 1969: Radiation in the atmosphere, Academic Press, New York, 912.
- Lacis, A.A. and J.E. Hansen, 1974: A parameterization for the absorption of solar radiation in the earth's atmosphere. J. Atmos. Sci., 31, 118-133.
- Latimer, J.R., 1972: Radiation Measurement. Int. Field Year for the Great Lakes. Tech. Manual Ser., 2, 53.
- Lettau, H. and K. Lettau, 1969: Short-wave radiation climatology. Tellus, 21, 208-222.
- Liou, K.N., 1973: Transfer of solar irradiance through cirrus cloud layers. J. Geophys. Res., 78, No. 9, 1409-1418.
- Liou, K., 1976: On the absorption, reflection and transmission of solar radiation in cloudy atmospheres. J. Atmos. Sci., 33, 798-805.
- Liu, B.Y.H. and R.C. Jordan, 1960: The interrelationship and characteristic distribution of direct, diffuse and total solar radiation. Solar Energy, 4 (3), 1-19.
- Lumb, F.E., 1964: The influence of cloud on hourly amounts of total solar radiation at the sea surface. Quart. J. Roy. Met. Soc., 90, 43-56.
- MacLaren, J.F. Ltd., Hooper and Angus Assoc. Ltd., J.E. Hay and J.A. Davies, 1976: Define, develop and establish a merged solar and meteorological computer data base. Report to the Atmospheric Environment Service.
- Manabe, S. and R.F. Strickler, 1964: Thermal equilibrium of an atmosphere with a convective adjustment. J. Atmos. Sci.,

21, 361-385.

- Mateer, C.L., 1955: Average insolation in Canada during cloudless days. Canadian J. of Technology, 33, 12-32.
- McCartney, E.J., 1976: Optics of the Atmosphere. John Wiley and Sons Inc., New York, 408.
- McClatchey, R.A., J.E. Selby, J.S. Garing, R.W. Fenn and F.E. Voltz, 1971: Optical properties of the atmosphere. Air Force Cambridge Research Laboratories, Environmental Research Papers No. 354, 85.
- McDonald, J.E., 1960: Direct absorption of solar radiation by atmospheric water vapor. J. Meteorol., 17, 319-328.
- Monteith, J.L., 1962: Attenuation of solar radiation: a climatological study. Quart. J. Roy. Meteorol. Soc., 88, 508-521.
- Norris, D.J., 1968: Correlation of solar radiation with clouds. Solar Energy, 12, 107-112.
- Orgill, J.F. and K.G.T. Hollands, 1977: Correlation equation for hourly diffuse radiation on a horizontal surface. Solar Energy, 19, 357-359.
- Paltridge, G.W., 1973: Direct measurement of water vapor absorption of solar radiation in the free atmosphere. J. Atmos. Sci., 30, 156-160.
- Paltridge, G.W. and C.M.R. Platt, 1976: Radiative Processes in Meteorology and Climatology. Developments in Atmospheric Science, 5, Elsevier, New York, 318.
- Parker, D.E., 1971: The effect of cloud on solar radiation receipt at the tropical ocean surface. Meteorol. Mag., 100, 231-240.
- Powell, G.L., 1980: A comparative evaluation of hourly solar global irradiation models. Ph.D. thesis, Arizona State University, 240.
- Powell, G.L., 1981: The comparative performance of related solar global models. Fourth Conference on Atmospheric Radiation, American Meteorological Society.
- Reynolds, D.W., T.H. Vonder Haar and S.K. Cox, 1975: The Effect of Solar Radiation Absorption in the Tropical Atmosphere. J. Appl. Meteorol., 14, 433-444.
- Rietveld, H.R., 1978: A new method to estimate the regression coefficients in the formula relating radiation to sunshine. Agric. Meteorol., 19, 243-252.

- Rogers, C.D., 1967: The radiative heat budget of the troposphere and lower stratosphere. Rep. No. A2, Planetary Circulation Project, Dept. of Meteorology, M.I.T., 99.
- Ruth, D.W. and R.E. Chant, 1976: The relationship of diffuse radiation to total radiation in Canada. Solar Energy, 18, 153-154.
- Schertzer, W., 1975: A model for calculating daily rates of global solar radiation in cloudless and cloudy sky conditions. M.Sc. thesis, McMaster University, Hamilton, 143.
- Schneider, S.H. and R.E. Dickenson, 1976: Parameterization of fractional cloud amounts in climatic models: the importance of modeling multiple reflection. J. Appl. Meteorol., 15, 1050-1056.
- Shettle, E.P. and J.A. Weinman, 1970: The transfer of solar irradiance through in homogenous turbid atmospheres evaluated by Eddington's approximation. J. Atmos. Sci., 27, 1048-1055.
- Singleton, F. and D. Smith, 1960: Some observations of drop size distribution in low layer clouds. Quart. J. Roy. Meteorol. Soc., 86, 454-457.
- Spencer, J.W., 1971: Fourier series representation of the position of the sun. Search, 2, 1972.
- Suckling, P.W. and J.E. Hay, 1976: Modelling direct, diffuse and total solar radiation for cloudless days. Atmosphere, 14, 298-308.
- Suckling, P.W. and J.E. Hay, 1977: A cloud layer-sunshine for estimating direct, diffuse and solar radiation. Atmosphere, 15, 194-207.
- Vowinckel, E. and S. Orvig, 1962: Relations between solar radiation and cloud type in the Arctic. J. Appl. Meteorol. 1, 552-559.
- Won, T., 1977: The simulation of hourly global radiation from hourly reported meteorological parameters - Canadian Prairie area. Paper presented at the 3rd Conference, Canadian Solar Energy Society Inc., Edmonton, Alberta, 23.
- Yamamoto, G., 1962: Direct absorption of solar radiation by atmospheric water vapour, carbon dioxide and molecular oxygen. J. Atmos. Sci., 19, 182-188.

## Appendix A

## List of Symbols

A, B	Parameters for cloud transmittance function
ALOW, AHIGH	Albedo values corresponding to the lower and upper temperature limits in the surface albedo algorithm
$C_{ex}$	Optical cross-section of cloud droplet
CA	Cloud layer amount
CCA	Corrected cloud layer amount
CCO	Corrected cloud layer opacity
CO	Cloud layer opacity
D	Diffuse irradiance
$D_A$	Diffuse irradiance due to aerosol scattering
$D_C$	Diffuse irradiance for cloudy skies
$D_R$	Diffuse irradiance due to Rayleigh scattering
$D_S$	Diffuse irradiance due to multiple reflection
ET	Equation of time
F	Measured irradiance
F'	Calculated irradiance
G	Global irradiance
$G_O$	Global irradiance for cloudless skies
$G_C$	Global irradiance for cloudy skies
$G_x$	Geometric cross-section of cloud droplet
I	Direct beam irradiance



$I(0)$	Solar constant ( $1353 \text{ Wm}^{-2}$ )
$I_0$	Direct beam irradiance for cloudless skies
$I_c$	Direct beam irradiance for cloudy skies
$K\downarrow$	Incident solar radiation at the surface
LAT	Local apparent time
LMS	Longitude of standard meridian
LS	Longitude of a station
LST	Local standard time
MBE	Mean bias error
P	Station pressure
$P_0$	Standard sea level pressure (101.3 kPa)
$P_f$	Phase function
$Q_{ab}$	Mie Efficiency factor of water droplet for absorption
$Q_{ex}$	Mie Efficiency factor of water droplet for extinction
$Q_{sc}$	Mie Efficiency factor of water droplet for scattering
RMSE	Root mean square error
$R^*$	Actual Sun-Earth distance
$\bar{R}^*$	Mean Sun-Earth distance
T	Transmittance of cloudy atmosphere
$T_r$	Theoretical cloud transmittance
$T_s$	Surface temperature
$T^0$	Standard surface temperature
TCA	Total cloud amount
$\bar{TCA}$	Mean total cloud amount (of present and preceding hour)
$\bar{TCO}$	Total cloud opacity
$\bar{TCO}$	Mean total cloud opacity (of present and preceding hour)

THIGH, TLOW	Upper and Lower temperature limits for surface albedo algorithm
X	Mie size parameter
$a_j, b_j$	Cloud transmissivity parameters (exponential)
$a_0, b_0$	Cloudless sky transmissivity parameters
$a_o$	Absorptivity of ozone
$a_w$	Absorptivity of water vapour
bf	Backward to forward scattering ratio
$c_i$	Cloud layer amount
$c_i'$	Corrected cloud layer amount
$c_x$	Prescribed cloud layer amount (0.85)
$c_j, d_j$	Cloud transmissivity parameters (linear)
$d_n$	Day number
f	Ratio of forward to total scatter
f'	f at $m_r = 1.66$
g	Assymetry factor
h	Hour angle of sun
i	Individual layer
k	Aerosol transmission parameter
$m_r$	Relative optical air mass (
$m_{IR}$	Refractive index
$m_{IMAG}$	Imaginary fraction of refractive index
$m_{REAL}$	Real fraction of refractive index
n	Number of layers
$n(r)$	Number density of a particle size distribution
r	Radius of particle
s	Hourly fraction of bright sunshine

$\bar{s}$	Mean hourly fraction of bright sunshine (of preceding and present hour)
$t_i$	Cloud transmittance
$\bar{t}_i$	Modified cloud transmittance
$u$	Effective water vapour amount in the vertical depth of the layer
$\bar{w}_0$	Single scattering albedo
$\alpha_a$	Atmospheric albedo due to aerosol scattering
$\alpha_b$	Albedo of the atmosphere for surface reflected radiation
$\alpha_c$	Cloud type albedo
$\bar{\alpha}_c$	Cloud base albedo
$\alpha_R$	Atmospheric albedo due to Rayleigh scattering
$\alpha_s$	Surface reflectivity
$\beta_{ab}$	Spectrally averaged absorption coefficient for cloud droplet
$\beta_{ex}$	Spectrally averaged scattering coefficient for cloud droplet
$\delta$	Solar declination
$\gamma$	Angle between impinging and scattered beam
$\phi$	Station latitude
$\theta$	Zenith angle
$\theta_0$	$2\pi dn/365$
$\lambda$	Wavelength
$\mu_0$	Cosine of zenith angle
$\sigma^2$	Standard deviation
$\tau$	Optical depth
$\tau_a$	Transmissivity after aerosol extinction
$\tau_{c_i}$	Transmissivity of $i^{\text{th}}$ cloud layer

$\tau_o$	Transmissivity after ozone absorption
$\tau_R$	Transmissivity after depletion by Rayleigh scattering
$\tau_w$	Transmissivity after water vapour absorption
$\tau_{eff}$	Effective optical depth
$\chi^2$	Chi square

## Appendix B

## Formulation of the MAC Layer Model

Global radiation at the surface under cloudless skies is the sum of transmitted direct beam and diffuse radiation. The spectrally integrated direct beam component,  $I$ , is given by

$$I_0 = I(0) \cos \theta [\tau_0(\mu_0 m_r) \tau_R(m_r) - \tau_w(\mu_w m_r)] \tau_a \quad \text{B.1}$$

where  $\tau_0$ ,  $\tau_R$ ,  $\tau_w$  and  $\tau_a$  are the transmissions after:

- (i) absorption by ozone  $\tau_0$ ,
- (ii) absorption by water vapour  $\tau_w$ ,
- (iii) attenuation by Rayleigh scattering  $\tau_R$ , and
- (iv) absorption and scattering by aerosol  $\tau_a$ .

The extraterrestrial flux is given by  $I_0 \cos \theta$  and  $\mu_0$  and  $\mu_w$  are the vertical depths of ozone and water vapour respectively. The downward component of scattered radiation is recorded as the diffuse flux. It is calculated as the sum of three components which result from,

- (i) Rayleigh scatter  $D_R$ ;
- (ii) aerosol scatter  $D_A$ , and

(iii) multiple reflections between the surface and atmosphere

Rayleigh scattering is isotropic such that half of the scattered radiation is in the forward direction. The Rayleigh and aerosol components are given by,

$$D_R = I(0) \cos \theta \tau_0(\mu_0 m_r) [1 - \tau_R(m_r)] \tau_a(m) / 2 \quad B.2$$

$$D_A = I(0) \cos \theta [\tau_0(\mu_0 m_r) \tau_R(m_r) - a_w(\mu_w m_r)] [1 - \tau_a(m)] w_0 \beta_a \quad B.3$$

where  $\bar{w}_0$  is the single scattering albedo and  $\beta_a$  is the ratio of forward to total scattering by aerosol. The multiple reflection term  $D_S$  is given by

$$D_S = \alpha_s \alpha_b (I_0 + D_R + D_A) / (1 - \alpha_b \alpha_s) \quad B.4$$

The total cloudless sky irradiance at the surface  $G_0$ , is the sum of the form contributing components.

$$G_0 = I_0 + D_R + D_A + D_S \quad B.5$$

Under cloudy skies the global and direct beam irradiances are calculated from

$$G_c = (I + D_R + D_A) \prod_{i=1}^n [(1 - C_i) + t_i C_i] / (1 - \alpha_s \alpha_b) \quad B.6$$

$$I_c = I_0 (1 - \text{TCO}) \quad B.7$$

$$D_c = G_c - I_c \quad \text{B.8}$$

Parameterizations:

(i) transmissivity after ozone absorption (Lacis and Hansen, 1974)

$$\tau_o = 1 - a_o \quad \text{B.9}$$

$$a_o = \frac{0.1082X_1}{(1 + 13.86X_1)^{0.805}} + \frac{0.00658X_1}{1 + (10.36X_1)^3} + \frac{0.002118X_1}{1 + 0.0042X_1 + 0.0000323X_1^2} \quad \text{B.10}$$

where  $X_1 = \mu_o m$

$$\mu_o = 3.5 \text{ mm (McClatchey et al., 1971)}$$

(ii) transmissivity after water vapour absorption

$$\tau_w = 0.29X_2 / [(1 + 14.15X_2)^{0.635} + 0.5925X_2] \quad \text{B.11}$$

where

$$X_2 = \mu_w m$$

$$U_w = U_w' (P/P_o)^{3/4} (T_o/T)^{1/2} \quad \text{Paltridge and Platt (1976) B.12}$$

and

$$U_w' = \exp(2.2572 + 0.05454T_d) \quad \text{Won (1977)}$$

B.13

(iii) transmissivity after Rayleigh scattering (Elterman, 1968; Thekaekara and Drummond, 1971)

Spectrally integrated values of  $\tau_R$  are given in Table B.1 (Davies, 1980)

TABLE B.1

## Transmissivity after Rayleigh scattering

Relative Optical Air Mass ( $m_r$ )	Transmissivity
0.5	0.9385
1.0	0.8973
1.2	0.8830
1.4	0.8696
1.6	0.8572
1.8	0.8455
2.0	0.8344
2.5	0.8094
3.0	0.7872
3.5	0.7673
4.0	0.7493
4.5	0.7328
5.0	0.7177
6.0	0.7037
10.0	0.6108
30.0	0.4364

(iv) transmissivity after aerosol extinction

$$\tau_a = \exp(-k m_r)$$

$$= k^{m_r}$$

B.14



Values for  $k$  assigned to specific stations are listed in Table B.2. Also given are values of single scattering albedo  $\bar{w}_0$  and the backward to forward scattering ratio,  $f$ . Aerosol extinction coefficient ( $k$ ) values were determined by Davies et al. (1975) and Suckling and Hay (1977). Robinson's (1962) empirical values of backward to forward scattering ratio are used. These are a function of air mass (and hence zenith angle).

TABLE B.2  
Aerosol Parameter Values

Station	$\bar{w}_0$	$k$
Toronto	0.70	0.91
Montreal	0.70	0.91
Charlottetown	0.75	1.00
Winnipeg	0.75	1.00
Vancouver	0.75	1.00
Goose Bay	0.90	1.00

Zenith Angle	Air Mass	$f$
0	1.0	0.92
25.8	1.11	0.91
36.9	1.25	0.89
45.6	1.43	0.86
53.1	1.66	0.83
60.0	2.00	0.78
66.4	2.50	0.71
72.5	3.33	0.67
78.5	5.02	0.60
90.0	0	0.60

## Appendix C

## Description of Data

## C.1 Data Base

All data used in this study were provided by the Atmospheric Environment Service on labelled 9 track, 1600 bpi magnetic tapes. Each tape contained nine years of hourly data (1968-1976) for an individual station, hence a total of six tapes were used. Data are recorded for each station in ascending order of element number within the data.

## C.2 Record Format Specification

Data are stored on the tapes as described in Table C.1

TABLE C.1

## Record Format Specification

Column	Field	Data Type
1-7	Station Identification	alphanumeric
8-10	Year (i.e. 976 = 1976)	numeric
11-12	Month (i.e. 01 = JAN.)	numeric
13-14	Day (i.e. 01 - 31 as appropriate)	numeric
15-17	Element Number (i.e. 061, 062 etc.)	numeric
18	Sign "-" = negative "0" = positive	alphanumeric
19-23	Data Value	numeric
24	Flag (e.g. "E" denotes "estimated")	alphanumeric

## C.3 Required Data

Data required in this study are listed in Table C.2. Also given are the element numbers and the units in which the data are recorded.

TABLE C.2

## Data Used

Element Number	Description of Data	Units	Sym- bol
061	Global Radiation	X.001 megajoules m <sup>-2</sup>	G
062	Diffuse Radiation	X.001 megajoules m <sup>-2</sup>	D
068	Direct Beam Radiation	X.001 megajoules m <sup>-2</sup>	S
074	Dew Point Temperature	0.1 C	DPT
077	Station Pressure	0.01kPa	STP
078	Dry Bulb Temperature	0.1 C	DBT
081	Total Cloud Opacity	tenths	TCO
082	Total Cloud Amount	tenths	TCA
107,111,115,119	Cloud Layer Opacity	tenths	CO
108,112,116,120	Cloud Layer Amount	tenths	CA
109,113,117,121	Cloud Layer Type	0-16 types	CT
133	Sunshine Duration	0.1 hrs.	S

All radiation data are recorded in local apparent time (LAT).

All meteorological data are recorded in local standard time (LST).

Appendix D

Listings of Computer Programs

```

SUBROUTINE EXPFIT (N,G,M,A,B)
C
C SUBROUTINE EXPFIT TRANSFORMS THE EXPONENTIAL EQUATION INTO A
C LINEAR FUNCTION BY TAKING THE NATURAL LOGARITHMS OF BOTH SIDES.
C
C DIMENSION G(N),M(N)
C REAL M
C
C SM=SG=SLM=SGM=NN=SMLM=SMSQ=SGSQ=0
C
C DO 1 J=1,N
C IF (G(J).EQ.-999.0) GO TO 10
C Y=ALOG(G(J))
C X=ALOG(M(J))
C SM=SM+M(J)
C SG=SG+Y
C SLM=SLM+X
C SGM=SGM+Y*M(J)
C SMLM=SMLM+M(J)*X
C SMSQ=SMSQ+M(J)*M(J)
C SGSQ=SGSQ+G(J)*G(J)
C GO TO 1
10 NN=NN+1
1 CONTINUE
C
C XN=N-NN
C B=((SM/XN)*(SG+SLM)-SGM-SMLM)/(SMSQ-SM*SM/XN)
C ZETA=SG/XN+SLM/XN+B*SM/XN
C A=(X**ZETA)
C RETURN
C END

```

```

SUBROUTINE CORREG (N,X,Y,A,B,R,R2,SY)
C
C SUBROUTINE CORREG DETERMINES THE PARAMETER VALUES USING LINEAR
C LEAST-SQUARES.
C
C DIMENSION X(N),Y(N)
C SUMX=0.0
C SUMY=0.0
C SUMXY=0.0
C SUMXSQ=0.0
C SUMYSQ=0.0
C
C Z=N
C DO 3 J=1,N
C SUMX=SUMX+X(J)
C SUMY=SUMY+Y(J)
C SUMXY=SUMXY+X(J)*Y(J)
C SUMXSQ=SUMXSQ+X(J)**2
C SUMYSQ=SUMYSQ+Y(J)**2
3 CONTINUE
C
C XBAR=SUMX/Z
C YBAR=SUMY/Z
C SIGX=SQRT(SUMXSQ/Z-XBAR**2)
C SIGY=SQRT(SUMYSQ/Z-YBAR**2)
C R=((SUMXY/Z)-(XBAR)*YBAR)/(SIGX*SIGY)
C R2=R*R
C B=R*SIGY/SIGX
C A=YBAR-(B*XBAR)
C SY=SIGY*(SQRT(1.0-(R**2)))
C
C RETURN
C END

```

SUBROUTINE GRIDL (X,Y,SIGMAY,NPTS,NTERMS,MODE,A,DELTA, SIGMAA, YFIT, CHISQR, AG, BG)

C SUBROUTINE GRIDL MAKES A GRID-SEARCH LEAST SQUARES FIT TO WITH  
C A SPECIFIED FUNCTION WHICH IS NOT LINEAR IN COEFFICIENTS.

C X - ARRAY OF DATA POINTS FOR INDEPENDENT VARIABLE  
C Y - ARRAY OF DATA POINTS FOR DEPENDENT VARIABLE  
C SIGMAY - ARRAY OF STANDARD DEVIATIONS FOR Y DATA POINTS  
C NPTS - NUMBER OF PAIRS OF DATA POINTS  
C NTERMS - NUMBER OF PARAMETERS  
C MODE - DETERMINES METHOD OF WEIGHTING LEAST-SQUARES FIT  
C +1 (INSTRUMENTAL) WEIGHT(I)=1./SIGMAY(I)\*\*2  
C 0 (NO WEIGHTING) WEIGHT(I)=1.  
C -1 (STATISTICAL) WEIGHTING=1./Y(I)  
C A - ARRAY OF PARAMETERS  
C DELTAA - ARRAY OF INCREMENTS FOR PARAMETERS A  
C SIGMAA - ARRAY OF STANDARD DEVIATIONS FOR PARAMETERS A  
C YFIT - ARRAY OF CALCULATED VALUES OF Y  
C CHISQR - REDUCED CHI SQUARE FIT

C DIMENSION X(1),Y(1),SIGMAY(1),A(1),DELTA(1),SIGMAA(1),  
C YFIT(1)  
C 11 NFREE=NPTS-NTERMS  
C FREL=NFREE  
C CHISQR=0.  
C IF (NFREE) 100,100,20  
C 20 DO 90 J=1,NTERMS

C EVALUATE CHI SQUARE AT FIRST TWO POINTS.

C 21 DO 22 I=1,NPTS  
C 22 YFIT(I)=FUNCTN (X,I,A)  
C 23 CHISQ1=FCHISQ (Y,SIGMAY,NPTS,NFREE,MODE,YFIT)  
C FN=0.  
C DELTA=DELTA(J)  
C 41 A(J)=A(J)+DELTA  
C DO 43 I=1,NPTS  
C 43 YFIT(I)=FUNCTN (X,I,A)  
C 44 CHISQ2=FCHISQ (Y,SIGMAY,NPTS,NFREE,MODE,YFIT)  
C 45 IF (CHISQ1-CHISQ2) 51,41,61

C REVERSE DIRECTION OF SEARCH IF CHI SQUARE IS INCREASING.

C 51 DELTA=-DELTA  
C A(J)=A(J)+DELTA  
C DO 54 I=1,NPTS  
C 54 YFIT(I)=FUNCTN (X,I,A)  
C SAVE=CHISQ1  
C CHISQ1=CHISQ2  
C 57 CHISQ2=SAVE

C INCREMENT A(J) UNTIL CHI SQUARE INCREASES

C 61 FN=FN+1.  
C A(J)=A(J)+DELTA  
C DO 64 I=1,NPTS  
C 64 YFIT(I)=FUNCTN (X,I,A)  
C CHISQ3=FCHISQ (Y,SIGMAY,NPTS,NFREE,MODE,YFIT)  
C 66 IF (CHISQ3-CHISQ2) 71,81,81  
C 71 CHISQ1=CHISQ2  
C CHISQ2=CHISQ3.  
C GO TO 61

C FIND MINIMUM OF PARABOLA DEFINED BY LAST THREE POINTS.

C 81 DELTA=DELTA\*(1./(1+(CHISQ1-CHISQ2)/(CHISQ3-CHISQ2))+0.5)  
C 82 A(J)=A(J)-DELTA  
C 83 SIGMAA(J)=DELTA(J)\*SQRT(2./(FREL\*(CHISQ3-2.\*CHISQ2+CHISQ1)))  
C 84 DELTAA(J)=DELTA(J)\*FN/3.  
C 90 CONTINUE

C EVALUATE FIT AT CHI SQUARE FOR FINAL INTERVAL.

C 91 DO 92 I=1,NPTS  
C 92 YFIT(I)=FUNCTN (X,I,A)  
C 93 CHISQR=FCHISQ (Y,SIGMAY,NPTS,NFREE,MODE,YFIT)  
C AG=A(1)  
C BG=A(2)

```

      FUNCTION FUNCTN (X,I,A)
C
C  EVALUATES TERMS OF FUNCTION FOR NON-LINEAR LEAST-SQUARES SEARCH.
C  FUNCTION HAS THE FORM  $Y = A/X * EXP(-BX)$ 
C
      DIMENSION X(1),A(1)
      X1=X(I)
      FUNCTN=(A(1)/X1)*EXP(-A(2)*X1)
      RETURN
      END

```

```

      FUNCTION FCHISQ (Y,SIGMAY,NPTS,NFREE,MODE,YFIT)
C
C  EVALUATES REDUCED CHI SQUARE FOR FIT TO DATA.
C  FCHISQ=SUM((Y-YFIT)**2/SIGMA**2/NFREE)
C
      DIMENSION X(1),Y(1),SIGMAY(1),A(1),DELTA(1),SIGMAA(1),
      1YFIT(1)
      11 CHISQ=0.
      12 IF (NFREE) 13,13,20
      13 FCHISQ=0.
      GO TO 40
C
C  ACCUMULATE CHI SQUARE
C
      20 DO 30 I=1,NPTS
      21 IF (MODE) 22,27,29
      22 IF (Y(I)) 25,27,23
      23 WEIGHT=1./Y(I)
      GO TO 30
      25 WEIGHT=1./(-Y(I))
      GO TO 30
      27 WEIGHT=1.
      GO TO 30
      29 WEIGHT=1./SIGMAY(I)**2
      30 CHISQ=CHISQ+WEIGHT*(Y(I)-YFIT(I))**2
C
C  DIVIDE BY NUMBER OF DEGREES OF FREEDOM.
C
      31 FREE=NFREE
      32 FCHISQ=CHISQ/FREE
      40 RETURN
      END

```

PROGRAM TST(TAPE1-/185,TAPE9,OUTPUT)  
 DIMENSION V(24),F(24)  
 DIMENSION TA(24),C7(24),P(24),RF8(24)  
 DIMENSION XAM(20),RST(20)

DIMENSION S1(24),D1(24),K1(24)  
 DIMENSION S2(24),D2(24),K2(24)  
 DIMENSION S3(24),D3(24),K3(24)  
 DIMENSION S4(24),D4(24),K4(24)  
 DIMENSION S5(24),D5(24),K5(24)  
 DIMENSION S6(24),D6(24),K6(24)  
 DIMENSION S7(24),D7(24),K7(24)  
 DIMENSION S8(24),D8(24),K8(24)  
 DIMENSION S9(24),D9(24),K9(24)  
 DIMENSION S10(24),D10(24),K10(24)  
 DIMENSION A1(16),A2(16),A3(16),A4(16),A5(16),A6(16),  
 A7(16),A8(16)  
 DIMENSION B1(16),B2(16),B3(16),B4(16),B5(16),B6(16),  
 B7(16),B8(16)  
 DIMENSION TBARM(16),TBARP(16)

REAL MLONG,JULIAN,K1,K2,K3,K4,K5,K6,K7,K8,K9,K10

COMMON BLOCK DATA CONTAINS HOURLY WEATHER DATA USED IN TST AND  
 IN SUBROUTINE WEATHER.  
 COMMON/DATA/HR(24),DPT(24),STP(24),DHT(24),TPO(24),TCA(24),  
 ICO(24,4),CA(24,4),ST(24),RF1(24),RF2(24),SH(24),  
 ISLONG,MLONG,DAY,MON,JULIAN,DEC,RSQ,ET,YR

COMMON BLOCK LAYER CONTAINS DATA FOR CLOUD LAYER MODELS.  
 COMMON/LAYER/CT(24,4),Z(24),PW(24),AMC(24),XK,EXTRA(24),  
 ICCA(24,4),AS(24),ZLN(9),BAA(9),TORAW(24),TOTR(24),JS,JF,  
 ICCO(24,4),FT(24)

COMMON/ALBEDO/TLOW,ALOW,THIGH,AHIGH.

COMMON/STADAY/STA,DAYS

#### RAYLEIGH SCATTERING TABLE

DATA XAM/0.5,1.,1.2,1.4,1.6,1.8,2.,2.5,3.,3.5,4.,  
 14.5,5.,5.5,6.,10.,30.,0.,0.,0./  
 DATA RST/.9385,.8973,.883,.8696,.8572,.8455,.8344,  
 1.8094,.7872,.7673,.7443,.7328,.7177,.7037,.6907,.6108,  
 1.4364,.0.,0.,0./

#### ROBINSON'S TABLE OF RATIO OF FORWARD TO TOTAL SCATTER BY AEROSOL.

DATA ZEN/0.,25.8,36.9,45.6,53.1,60.,66.4,72.5,78.5/  
 DATA BAA/0.92,0.91,0.89,0.86,0.83,0.78,0.71,0.67,0.67

DATA STATEMENT CONTAINS VALUES REQUIRED FOR COMPUTATION OF ALBEDO.  
 DATA TLOW,ALOW,THIGH,AHIGH/-6.0,0.6,3.0,0.2/

\*\*\* DENOTES VARIABLES WHICH ARE SPECIFIC TO INDIVIDUAL STATION.  
 \*\*\* DATA SLAT,SLONG,MLONG/43.80,79.55,75.00/

DATA STATEMENTS CONTAIN CLOUD PARAMETERS FOR TRANSMISSION  
 FUNCTIONS.

DATA A1/.556,.556,.413,.923,.923,.871,.119,.368,.368,  
 1.252,.368,.119,.368,.252,.163,.163/  
 DATA B1/.053,.053,.004,.004,.089,.020,-.226,.045,  
 1.045,.100,.045,-.226,.045,.100,-.031,-.031/

DATA A2/.385,.385,.452,.813,.819,.848,.343,.343,.343,  
 1.290,.343,.290,.343,.290,.248,.248/  
 DATA B2/.013,.013,.024,.042,.042,-.004,.025,.025,.025,  
 1.027,.025,.027,.025,.027,-.029,-.029/

DATA A3/2199.,2199.,1633.,3648.,3648.,3443.,1453.,  
 11453.,1453.,997.,1453.,469.,1453.,997.,645.,645./  
 DATA B3/.112,.112,.063,.148,.148,.079,.104,.104,  
 1.104,.159,.104,-.167,.104,.159,.028,.028/



```

C   DATA A4/1526.,1526.,1791.,3248.,3248.,3361.,1361.,
11361.,1361.,1149.,1361.,1149.,1361.,1149.,987.,987./
C   DATA B4/.059.,.059.,.070.,.088.,.088.,.043.,.071.,.071.,
1.073.,.071.,.073.,.071.,.073.,.018.,.018/
C   DATA A5/1336.,1336.,1523.,3084.,3084.,3348.,1195.,
11195.,1195.,1012.,1195.,1012.,1195.,1012.,837.,897./
C   DATA B5/.089.,.089.,.108.,.103.,.103.,.062.,.111.,.111.,.111.,
1.106.,.111.,.106.,.111.,.106.,.023.,.023/
C   DATA A6/1321.,1321.,1412.,2456.,2456.,3600.,1137.,1137.,
11137.,802.,1137.,802.,1137.,802.,375.,375./
C   DATA B6/.097.,.097.,.114.,.104.,.104.,.065.,.111.,.111.,.111.,
1.114.,.111.,.114.,.111.,.114.,-.078.,-.078/
C   DATA A7/.375.,.375.,.435.,.787.,.787.,.835.,.331.,.331.,.331.,
1.291.,.331.,.291.,.231.,.291.,.266.,.266/
C   DATA B7/.010.,.010.,.006.,-.010.,-.010.,.023.,.005.,.005.,.005.,
1.003.,.005.,.003.,.005.,.003.,.019.,.019/
C   DATA A8/.330.,.330.,.368.,.745.,.745.,.825.,.286.,.286.,.286.,
1.251.,.286.,.251.,.286.,.251.,.237.,.237/
C   DATA B8/-.004.,-.004.,-.011.,-.020.,-.020.,-.007.,-.007.,-.007.,
1-.007.,-.007.,-.007.,-.007.,-.007.,.011.,.011/
C   DATA TBARM/.402.,.402.,.451.,.763.,.763.,.891.,.347.,.347.,.347.,
1.249.,.347.,.299.,.347.,.299.,.320.,.320/
C   DATA TBARP/.319.,.319.,.338.,.696.,.696.,.841.,.267.,.267.,.267.,
1.232.,.267.,.232.,.267.,.232.,.268.,.268/
C
C   CONV=4.0*ATAN(1.0)/180.
C   SLAT=SLAT*CONV
C   NRAY=17
C   NHAA=9
C   OZ=3.5
***  XK=0.91
***  W=0.98

**
**
***  READ 53321, TLOW,ALOW,THIGH,ANIGH
C   READ 53321, SLAT,SLONG,MLONG
C   INPUT# NOT IN PROGRAM STATEMENT
C   READ 53321, XK,W
C   53321 FORMAT(4F10.0)
**
**
*
*
*
C   READ(1,510) STA,YR,MON,DAY,E,(V(J),F(J),J=1,74)
C   510 FORMAT(A7,F5.0,I2,F4.0,I3,24(F7.0,A1))
C   RECORD LENGTH EXCEEDS 137 COLUMNS -- MAY EXCEED I/O DEVICE
C   BACKSPACE 1
*
*
C
C   K=1
C   11 CONTINUE
C   READ HOURLY WEATHER DATA
C   CALL WEATHER
C   IIDAYS=DAYS
C
C   CALCULATE SOLAR ZENITH ANGLE, OPTICAL AIR MASS AND
C   EXTRATERRESTRIAL RADIATION (KJ/M**2/HR).
C   AA=SIN(DEC)*SIN(SLAT)
C   BB=COS(DEC)*COS(SLAT)
C

```

```

DO 30 J=1,24
IF (STP(J).LT.-999.) STP(J)=101.3
HA=ABS(12.-ST(J))*15.*CONV
CZ(J)=AA+BB*COS(HA)
Z(J)=ACOS(CZ(J))/CONV
TA(J)=DBT(J)+273.
IF (DBT(J).LT.-999.) TA(J)=273.
PW(J)=EXP(2.2572+0.05454*DBT(J))
PW(J)=PW(J)*(STP(J)/101.3)**0.75*(273./TA(J))**0.5
AM=35./((SQRT(1224.*CZ(J)*CZ(J)+1.))
IF (AM.GT.30) AM=30.
AMC(J)=AM*STP(J)/101.3
EXTRA(J)=1353.*R5Q*CZ(J)*3.6
IF (Z(J).GE.90.) EXTRA(J)=0.0
P(J)=STP(J)/101.3
CALL ALBTO (DBT(J),AS(J))
30 CONTINUE
C
C DEFINE LIMITS FOR THE DAYLIGHT PERIOD.
C
DO 20 J=1,24
IF (EXTRA(J).EQ.0.) GO TO 21
IF (EXTRA(J-1).EQ.0.) JS=J
GO TO 20
21 IF (J.EQ.1) GO TO 20
IF (EXTRA(J-1).GT.0.) JE=J-1
20 CONTINUE
WRITE(19,500) JS,JE
500 FORMAT(2I5)
C
C -----
C
C CALCULATE TRANSMISSIONS FOR CLOUDLESS SKIES.
C
DO 10 J=JS,JE
C
C OZONE TRANSMISSION
C
X=OZ*AMC(J)
AA=0.002118*X/(1.+0.0042*X+0.00000323*X*X)
BB=0.1082*X/(1.+11.86*X)**0.805
C=0.00658*X/(1.+(10.36*X)**3)
AO3=AA+BB+C
TOZ=1.-AO3
C
C ABSORPTION BY WATER VAPOUR.
C
X=PW(J)*AMC(J)
AW=0.29*X/((1.+14.15*X)**0.635+0.5925*X)
C
C INTERPOLATE TRANSMITTANCE DUE TO RAYLEIGH SCATTERING AS A FUNCTION
C OF AIR MASS.
C
AAMC=AMC(J)
CALL INTERP (XAM,RST,AAMC,TR,NRAY)
C
C INTERPOLATE RATIO OF FORWARD TO TOTAL SCATTER FOR AEROSOL AS A
C FUNCTION OF ZENITH ANGLE (DATA FROM ROBINSO).
C
Z7=Z(J)
IF (Z7.GT.78.5) GO TO 99
CALL INTERP (ZEN,UAA,Z7,BA,NBAA)
GO TO 199
99 BA=0.6
199 CONTINUE
FT(J)=BA
TORAW(J)=TOZ*TR-AW
TOTR(J)=TOZ*(1.-TR)
C
C 10 CONTINUE
C

```



```

SUBROUTINE WEATHER
DIMENSION HR(24),ST(24),STP(24),DPT(24),V(24),F(24),DBT(24),
1 TCO(24),TCA(24),CO(24,4),CA(24,4),RF1(24),RF2(24),SH(24),
1 CT(24,4),KM(24),DM(24),SN(24),CCA(24,4),SUMCA(4)
DIMENSION Z(24),PW(24),AMC(24),EXTRA(24),AS(24)
DIMENSION TORAW(24),TOTR(24),FT(24)

C
COMMON/LAYER/CT,7,PW,AMC,XK,EXTRA,CCA,AS,ZEN,BAA,TORAW,
1 TOTR,JS,JE,CCO,FT

COMMON/LAYER/CT,7,PW,AMC,EXTRA,AS,CCA,JS,JE,TORAW,TOTR,FT

COMMON/DATA/HR,DPT,STP,DBT,TCO,TCA,CO,CA,ST,RF1,RF2,SH,
1 SLONG,MLONG,DAY,MON,JULIAN,DEC,RSQ,ET,YR

COMMON/DATA/HR,DPT,STP,DBT,TCO,CO,ST,RF1,RF2,SH,SLONG,
1 MLONG,DAY,MON,JULIAN,DEC,RSQ,ET,YR

C
REAL LAT,MLONG,KM
INTEGER E

DATA MONSV,DAYSV/1,1/
DATA KKHECK/1/
DATA NEED/1/
IF(NEED.GT.1) GO TO 2

DAYSV=DAY
MONSV=MON
2 CONTINUE

C
C INITIALIZE ALL DATA ARRAYS WITH -99999
DO 14 J=1,24
DPT(J)=STP(J)=DBT(J)=TCO(J)=TCA(J)=RF1(J)=RF2(J)=SH(J)=-99999.
DM(J)=KM(J)=-99999.
DO 14 L=1,4
CO(J,L)=CA(J,L)=CT(J,L)=-99999.
14 CONTINUE

C
C READ DATA FROM TAPES SUPPLIED BY AES.
16 READ(1,1)STA,YR,MON,DAY,E,(V(J),F(J),J=1,24)

IF(E.OF(1).NE.0.0) STOP 1
IF(DAY.NE.DAYSV.OR.MON.NE.MONSV) GO TO 13

1 FORMAT (A7,F5.0,I2,F4.0,I3,24(F7.0,A1))
RECORD LENGTH EXCEEDS 137 COLUMNS -- MAY EXCEED I/O DEVICE
IF(KKHECK.NE.1) GO TO 6

C
C CALCULATE HR,LAT,AND ST. SUBROUTINE ASTRO CALCULATES ASTRONOMICAL
C QUANTITIES.
DO 10 J=1,24
JJ=J-1
HR(J)=JJ
IF(HR(J).EQ.0) GO TO 3
GO TO 4
3 CALL ASTRO(DAY,MON,JULIAN,DEC,RSQ,ET,YR)
LAT=HR(J)+(ET/60.)+(MLONG-SLONG)/15.
4 CONTINUE
IF(HR(J).EQ.0) GO TO 5
ST(J)=ST(J-1)+1.
IF(ST(J).GT.24)ST(J)=ST(J)-24.
GO TO 10
5 CONTINUE
C CORRECT NEGATIVE LAT AND LAT G.E. 24
IF(LAT.LT.0)LAT=2J.+(1.-ABS(LAT))
IF(LAT.GE.24)LAT=LAT-24.

```

```

C ADJUST LAT.
  ILAT=INT(LAT)
  XLAT=ILAT
  ST1=XLAT+0.5
  IF(ST1.GE.24)ST1=-24.
  ST(J)=ST1
  10 CONTINUE
  6 CONTINUE
C IDENTIFY HOURLY VARIABLES FROM THE AES TAPE. APPLY APPROPRIATE
C CALIBRATION FACTORS. NO CALIBRATION FACTORS ARE APPLIED TO -99999
C WHICH DESIGNATES MISSING DATA. LAYER CLOUD AMOUNTS WITH VALUES
C OF -99999 ARE SET EQUAL TO ZERO SINCE THEY ONLY INDICATE THAT
C THE SKY IS COMPLETELY COVERED BY LOWER LAYERS. ELEMENT 156
C INDICATES THE END OF DATA FOR DAY.
  DO 15 J=1,24
  IF(L.EQ.61.AND.F(J).NE.1HM)KH(J)=V(J)
  IF(L.EQ.62.AND.F(J).NE.1HM)DM(J)=V(J)
  IF(L.EQ.74.AND.F(J).NE.1HM)OPT(J)=V(J)/10.
  IF(L.EQ.77.AND.F(J).NE.1HM)STP(J)=V(J)/100.
  IF(L.EQ.78.AND.F(J).NE.1HM)DBT(J)=V(J)/10.
  IF(L.EQ.81.AND.F(J).NE.1HM)TCO(J)=V(J)/10.
  IF(L.EQ.82.AND.F(J).NE.1HM)TCA(J)=V(J)/10.
  IF(L.EQ.107.AND.F(J).NE.1HM)CO(J,1)=V(J)/10.
  IF(L.EQ.108.AND.F(J).NE.1HM)CA(J,1)=V(J)/10.
  IF(L.EQ.109.AND.F(J).NE.1HM)CT(J,1)=V(J)
  IF(L.EQ.111.AND.F(J).NE.1HM)CO(J,2)=V(J)/10.
  IF(L.EQ.112.AND.F(J).NE.1HM)CA(J,2)=V(J)/10.
  IF(L.EQ.113.AND.F(J).NE.1HM)CT(J,2)=V(J)
  IF(L.EQ.115.AND.F(J).NE.1HM)CO(J,3)=V(J)/10.
  IF(L.EQ.116.AND.F(J).NE.1HM)CA(J,3)=V(J)/10.
  IF(L.EQ.117.AND.F(J).NE.1HM)CT(J,3)=V(J)
  IF(L.EQ.119.AND.F(J).NE.1HM)CO(J,4)=V(J)/10.
  IF(L.EQ.120.AND.F(J).NE.1HM)CA(J,4)=V(J)/10.
  IF(L.EQ.121.AND.F(J).NE.1HM)CT(J,4)=V(J)
  IF(L.EQ.133.AND.F(J).NE.1HM)SN(J)=V(J)/10.
  15 CONTINUE
  KKHECK=9
  GO TO 16
  17 CONTINUE
  NLEO=4
  KKHECK=1
  DAYSV=DAY
  MONSV=MON
  BACKSPACE 1

  DO 20 J=1,24
  DO 20 L=1,4
  IF(CA(J,L).LT.0)CA(J,L)=0.
  IF(CT(J,L).LT.0)CT(J,L)=0.
  20 CONTINUE
C CLOUD AMOUNTS FOR EACH LAYER ARE CORRECTED FOR OBSTRUCTION
C BY LOWER LAYERS.
  SUMCA(1)=0.
  DO 18 J=1,24
  CCA(J,1)=CA(J,1)
  DO 18 L=2,4
  SUMCA(L)=SUMCA(L-1)+CA(J,L-1)
  IF(SUMCA(L).GE.1) GO TO 19
  CCA(J,L)=CA(J,L)/(1.-SUMCA(L))
  IF(CCA(J,L).GT.1)CCA(J,L)=1.
  GO TO 18
  19 CCA(J,L)=CA(J,L)
  18 CONTINUE
C SHIFT RADIATION AND SUNSHINE ARRAYS TO CORRESPOND WITH LAT
C OF HOURLY OBSERVATIONS.
  RADT1=0.5
  IF(ST1.GT.20)ST1=ST1-24.
  DIFF=RADT1-ST1
  IF(DIFF.GT.0)DIFF=1.
  IF(DIFF.LT.0)DIFF=-1.
  DO 9 J=1,24
  IF(DIFF)8,17,7
  7 CONTINUE

```

```

      IF (J.EQ.1) GO TO 12
      RF1(J)=KM(J-1)
      RF2(J)=DM(J-1)
      SH(J)=SN(J-1)
      GO TO 9
8     CONTINUE
      IF (J.EQ.24) GO TO 11
      RF1(J)=KM(J+1)
      RF2(J)=DM(J+1)
      SH(J)=SN(J+1)
      GO TO 9
11    RF1(24)=KM(23)
      RF2(24)=DM(23)
      SH(24)=SN(23)
      GO TO 9
17    RF1(J)=KM(J)
      RF2(J)=DM(J)
      SH(J)=SN(J)
      GO TO 9
12    RF1(1)=KM(1)
      RF2(1)=DM(1)
      SH(1)=SN(1)
9     CONTINUE
      RETURN
      END

```

```

      SUBROUTINE ASTRO (DAY, MON, JJDA, DEC, RSQ, ET, YR)
C     CALCULATES JULIAN DAY, RADIUS VECTOR, DECLINATION AND THE EQUATION
C     OF TIME.
C     COMMON/STADAY/STA, DAYS
C     DIMENSION DAYN(12)
C     REAL JJDA
C     JULIAN DAY FROM MONTH AND DAY.
      DATA (DAYN(I), I=1, 12) / 31., 28., 31., 30., 31., 30., 2*31., 30.,
      131., 30., 31./
      PY=3.14159
C     IF A LEAP YEAR ADJUST DAYN(2)
      XYR=YR/4.
      IYR=INT(XYR)
      XIYR=IYR
      IF (XIYR.EQ.XYR) DAYN(2)=29.
      DAYS=365.
      IF (DAYN(2).EQ.29) DAYS=366.
      M=MON-1
      SUM=0.
      DO 1 I=1, M
1     SUM=SUM+DAYN(I)
      JJDA=SUM+DAY
C     DECLINATION, RADIUS VECTOR SQUARED AND THE EQUATION OF TIME.
      DNUM=JJDA-1.
      THETA=2.*PY*DNUM/DAYS
      CA=COS(THETA)
      SA=SIN(THETA)
      THET2=2.*THETA
      C2A=COS(THET2)
      S2A=SIN(THET2)
      THET3=3.*THETA
      C3A=COS(THET3)
      S3A=SIN(THET3)
      DEC=0.006918-0.349912*CA+0.070257*SA-0.006759*C2A+
      10.000907*S2A-0.002697*C3A+0.001480*S3A
      LT=0.000075+0.001868*CA-0.032077*SA-0.014615*C2A-
      10.040849*S2A
C     CONVERT ET TO MINUTES.
      ET=LT*180.*4./PY
      RSQ=1.000110+0.034221*CA+0.001280*SA+0.000719*C2A+
      10.000077*S2A
      RETURN
      END

```

SUBROUTINE MACA (S,D,K,W,A,B)

MACA USES AN EXPONENTIAL TRANSMISSION FUNCTION IN THE 1980 FORM OF THE LAYER MODEL.

T=A\*EXP(-BM)

DIMENSION K(24),D(24),S(24),A(16),B(16),CTAN(4),TLAY(4),ALFA(16)  
 REAL K1,K  
 COMMON/DATA/HR(24),DPT(24),STP(24),DBT(24),TCO(24),TCA(24),  
 1CO(24,4),CA(24,4),ST(24),RF1(24),RF2(24),SH(24),  
 1SLONG,MLONG,DAY,MON,JULIAN,DEC,RSQ,ET,YR,DDAYY,MMONH  
 COMMON/LAYER/CT(24,4),Z(24),PW(24),AMC(24),XK,EXTRA(24),  
 1CCA(24,4),AS(24),ZLN(9),BAA(9),TORAW(24),TOTR(24),JS,JE,  
 1CCO(24,4),FT(24)

DATA STATEMENT CONTAINS CLOUD ALBEDO VALUES.

DATA ALFA/3\*.55,3\*.35,10\*.60/

BSR=0.0685

HAD=0.83

TAD=XK\*\*1.66

DO 10 J=JS,JE

C AEROSOL TRANSMISSION

TAS=XK\*\*AMC(J)

C CLOUDLESS SKY IRRADIANCES.

DB1=EXTRA(J)\*TORAW(J)\*TAS

SR=EXTRA(J)\*TOTR(J)\*TAD/2.

SA=EXTRA(J)\*TORAW(J)\*(1.-TAS)\*W\*FT(J)

D1=SR+SA

K1=DB1+SR+SA

S(J)=DB1

D(J)=D1

K(J)=K1

C CLOUD LAYER TRANSMISSIONS.

TFUN=1.0

DO 5 L=1,4

IF (CCA(J,L).EQ.0) GO TO 4

IF (CT(J,L).EQ.0) GO TO 4

ITYP=CT(J,L)

CTAN(L)=A(ITYP)\*EXP(-B(ITYP)\*AMC(J))

TLAY(L)=1.-CCA(J,L)+CTAN(L)\*CCA(J,L)

GO TO 3

4 CTAN(L)=TLAY(L)=1.

3 CONTINUE

TFUN=TFUN\*TLAY(L)

5 CONTINUE

TFUN1=1.-TCO(J)

C COMPUTE EFFECT OF MULTIPLE REFLECTION BETWEEN GROUND AND

C ATMOSPHERE.

SUMAC=0.0

DO 400 L=1,4

IF (CO(J,L).EQ.0.) GO TO 400

IF (CT(J,L).EQ.0.) GO TO 400

ITYP=CT(J,L)

XALF=ALFA(ITYP)\*CO(J,L)

SUMAC=SUMAC+XALF

400 CONTINUE

ALFAC=SUMAC/TCO(J)

C

IF (TCO(J).LT.0) GO TO 6

BSA=(1.-TAD)\*W\*(1.-RAD)

BSRC=BSR\*(1.-TCO(J))

ALF=BSRC+BSA+0.6\*TCO(J)

S(J)=S(J)\*TFUN1

K(J)=(K(J)\*TFUN)/(1.-AS(J)\*ALF)

D(J)=K(J)-S(J)

GO TO 10

6 K(J)=S(J)=D(J)=-99999.

20 S(J)=D(J)=K(J)=0.

21 CONTINUE

10 CONTINUE

RETURN

END

```

SUBROUTINE MACB (S,D,K,W,A,B)
MACB USES AN EXPONENTIAL TRANSMISSION FUNCTION AND A THEORETICAL
CLOUDLESS SKY GLOBAL RADIATION VALUE, GO.

      T=A/W*EXP(-B*W)/GO

DIMENSION K(24),D(24),S(24),A(16),B(16),CTRAN(4),TLAY(4),ALFA(16)
REAL K1,K
COMMON/DATA/HR(24),OPT(24),STP(24),DBT(24),TCO(24),TCA(24),
1CO(24,4),CA(24,4),ST(24),RF1(24),RF2(24),SH(24),
1SLONG,MLONG,DAY,MON,JULIAN,DEC,RSQ,ET,YR,DDAYY,MMONN
COMMON/LAYER/CT(24,4),7(24),PW(24),AMC(24),XK,EXTRA(24),
1CCA(24,4),AS(24),ZEN(9),BAA(9),TORAW(24),TOTR(24),JS,JE,
1CCO(24,4),FT(24)

C DATA STATEMENT CONTAINS CLOUD ALBEDO VALUES.
C DATA ALFA/3*.55,3*.35,10*.60/

      BSR=0.0685
      BAD=0.83
      TAD=XK**1.66

C DO 10 J=JS,JE
C AEROSOL TRANSMISSION
      TAS=XK**AMC(J)
C CLOUDLESS SKY IRRADIANCES.
      DB1=EXTRA(J)*TORAW(J)*TAS
      SR=EXTRA(J)*TOTR(J)*TAD/2.
      SA=EXTRA(J)*TORAW(J)*(1.-TAS)*W*FT(J)
      D1=SR+SA
      K1=DB1+SR+SA
      S(J)=DB1
      D(J)=D1
      K(J)=K1
C CLOUD LAYER TRANSMISSIONS.
      TFUN=1.0
      DO 5 L=1,4
      IF (CCA(J,L).EQ.0) GO TO 4
      IF (CT(J,L).EQ.0) GO TO 4
      ITYP=CT(J,L)
      CTRAN(L)=(A(ITYP)/AMC(J)*EXP(-B*AMC(J)))/K1
      TLAY(L)=1.-CCA(J,L)+CTRAN(L)*CCA(J,L)
      GO TO 3
      4 CTRAN(L)=TLAY(L)=1.
      3 CONTINUE
      TFUN=TFUN*TLAY(L)
      5 CONTINUE
      TFUN1=1.-TCO(J)
C COMPUTE EFFECT OF MULTIPLE REFLECTION BETWEEN GROUND AND
C ATMOSPHERE.
      SUMAC=0.0
      DO 400 L=1,4
      IF (CO(J,L).EQ.0.) GO TO 400
      IF (CT(J,L).EQ.0.) GO TO 400
      ITYP=CT(J,L)
      XALF=ALFA(ITYP)*CO(J,L)
      SUMAC=SUMAC+XALF
      400 CONTINUE
      ALFAC=SUMAC/TCO(J)

C IF(TCO(J).LT.0) GO TO 6
      BSA=(1.-TAD)*W*(1.-BAD)
      BSRC=BSR*(1.-TCO(J))
      ALF=BSRC+BSA+0.6*TCO(J)
      S(J)=S(J)*TFUN1
      K(J)=(K(J)*TFUN1)/(1.-AS(J)*ALF)
      D(J)=K(J)-S(J)
      GO TO 10
      6 K(J)=S(J)=D(J)=-9999.
      20 S(J)=D(J)=K(J)=0.
      21 CONTINUE
      10 CONTINUE
      RETURN
END

```



SUBROUTINE MACC (S,D,K,W,A,B)

MACC USES A LINEAR TRANSMISSION FUNCTION.

T=A+BM

DIMENSION K(24),D(24),S(24),A(16),B(16),CTAN(4),TLAY(4),ALFA(16)  
 REAL K1,K  
 COMMON/ DATA/HR(24),DPT(24),STP(24),DBT(24),TCO(24),TCA(24),  
 ICD(24,4),CA(24,4),ST(24),RF1(24),RF2(24),SH(24),  
 ISLONG,MLONG,DAY,MON,JULIAN,DEC,RSQ,ET,YR,DDAY,MHONN  
 COMMON/LAYER/CT(24,4),7(24),PW(24),AMC(24),XK,EXTRA(24),  
 ICCA(24,4),AS(24),ZLN(9),BAA(9),TORAW(24),TOTR(24),JS,JE,  
 ICCO(24,4),FT(24)

DATA STATEMENT CONTAINS CLOUD ALBEDO VALUES.

DATA ALFA/3\*.55,3\*.35,10\*.60/

BSR=0.0685  
 BAD=J.83  
 TAD=XK\*\*1.66

DO 10 J=JS,JE  
 AEROSOL TRANSMISSION

TAS=XK\*\*AMC(J)  
 CLOUDLESS SKY IRRADIANCES.  
 DB1=EXTRA(J)\*TORAW(J)\*TAS  
 SR=EXTRA(J)\*TOTR(J)\*TAD/2.  
 SA=EXTRA(J)\*TORAW(J)\*(1.-TAS)\*W\*FT(J)  
 D1=SR+SA  
 K1=DB1+SR+SA  
 S(J)=DB1  
 D(J)=D1  
 K(J)=K1

C CLOUD LAYER TRANSMISSIONS.

TFUN=1.0  
 DO 5 L=1,4  
 IF (CCA(J,L).EQ.0) GO TO 4  
 IF (CT(J,L).EQ.0) GO TO 4  
 ITYP=CT(J,L)  
 CTRAN(L)=A(ITYP)+B(ITYP)\*AMC(J)  
 TLAY(L)=1.-CCA(J,L)+CTAN(L)\*CCA(J,L)  
 GO TO 3  
 4 CTRAN(L)=TLAY(L)=1.  
 3 CONTINUE  
 TFUN=TFUN\*TLAY(L)  
 5 CONTINUE  
 TFUN1=1.-TCO(J)

C COMPUTE EFFECT OF MULTIPLE REFLECTION BETWEEN GROUND AND  
 C ATMOSPHERE.

SUMAC=0.0  
 DO 400 L=1,4  
 IF (CO(J,L).EQ.0.) GO TO 400  
 IF (CT(J,L).EQ.0.) GO TO 400  
 ITYP=CT(J,L).  
 XALF=ALFA(ITYP)\*CO(J,L)  
 SUMAC=SUMAC+XALF  
 400 CONTINUE  
 ALFAC=SUMAC/TCO(J)

IF (TCO(J).LT.0) GO TO 6  
 BSA=(1.-TAD)\*W\*(1.-BAD)  
 BSRC=BSR\*(1.-TCO(J))  
 ALF=BSRC+BSA+0.6\*TCO(J)  
 S(J)=S(J)\*TFUN1  
 K(J)=(K(J)\*TFUN)/(1.-AS(J)\*ALF)  
 D(J)=K(J)-S(J)  
 GO TO 10  
 6 K(J)=S(J)=D(J)=-9999.  
 20 S(J)=D(J)=K(J)=0.  
 21 CONTINUE  
 10 CONTINUE  
 RETURN  
 END

```

SUBROUTINE MACD (S,D,K,W,TRAN)
C
C MACD USES A CONSTANT CLOUD-TYPE TRANSMISSION.
C
C     T=TRAN
C
C     DIMENSION K(24),D(24),S(24),TRAN(16),CTRAN(4),FLAY(4),ALFA(16)
C     REAL K1,K
C     COMMON/DATA/HR(24),DPT(24),STP(24),DHT(24),TCO(24),TCA(24),
C     1CO(24,4),CA(24,4),ST(24),KF1(24),RF2(24),SH(24),
C     1SLONG,MLONG,DAY,MON,JULIAN,DEC,KSQ,ET,YR,DDAYY,MPONN
C     COMMON/LAYER/CT(24,4),Z(24),PW(24),AMC(24),XK,XTRA(24),
C     1CCA(24,4),AS(24),ZLN(9),BAA(9),TORAW(24),TOTR(24),JS,JE,
C     1CCO(24,4),FT(24)
C
C DATA STATEMENT CONTAINS CLOUD ALBEDO VALUES.
C
C     DATA ALFA/3*.55,3*.35,10*.60/
C
C     BSR=0.0685
C     BAD=0.83
C     TAD=XK**1.66
C
C     DO 10 J=JS,JE
C     C AEROSOL TRANSMISSION
C     TAS=XK**AMC(J)
C     C CLOUDLESS SKY IRRADIANCE S.
C     DB1=EXTRA(J)*TORAW(J)*TAS
C     SR=EXTRA(J)*TOTR(J)*TAD/2.
C     SA=EXTRA(J)*TORAW(J)*(1.-TAS)*W*FT(J)
C     D1=SR+SA
C     K1=DB1+SR+SA
C     S(J)=DB1
C     D(J)=D1
C     K(J)=K1
C     C CLOUD LAYER TRANSMISSIONS.
C     TFUN=1.0
C     DO 5 L=1,4
C     IF (CCA(J,L).EQ.0) GO TO 4
C     IF (CT(J,L).EQ.0) GO TO 4
C     ITYP=CT(J,L)
C     CTRAN(L)=TRAN(ITYP)
C     TLAY(L)=1.-CCA(J,L)+CTRAN(L)*CCA(J,L)
C     GO TO 3
C     4 CTRAN(L)=TLAY(L)=1.
C     3 CONTINUE
C     TFUN=TFUN*TLAY(L)
C     5 CONTINUE
C     TFUN1=1.-TCO(J)
C     C COMPUTE EFFECT OF MULTIPLE REFLECTION BETWEEN GROUND AND
C     C ATMOSPHERE.
C     SUMAC=0.0
C     DO 400 L=1,4
C     IF (CO(J,L).EQ.0.) GO TO 400
C     IF (CT(J,L).EQ.0.) GO TO 400
C     ITYP=CT(J,L)
C     XALF=ALFA(ITYP)*CO(J,L)
C     SUMAC=SUMAC+XALF
C     400 CONTINUE
C     ALFAC=SUMAC/TCO(J)
C
C     IF (TCO(J).LT.0) GO TO 6
C     BSA=(1.-TAD)*W*(1.-BAD)
C     BSRC=BSR*(1.-TCO(J))
C     ALF=BSRC+BSA+0.6*TCO(J)
C     S(J)=S(J)*TFUN1
C     K(J)=(K(J)*TFUN)/(1.-AS(J)*ALF)
C     D(J)=K(J)-S(J)
C     GO TO 10
C     6 K(J)=S(J)=D(J)=-9999.
C     20 S(J)=D(J)=K(J)=0.
C     21 CONTINUE
C     10 CONTINUE
C     RETURN
C     END

```

```

SUBROUTINE INTERP(X,Y,XX,YY,N)
DIMENSION X(N),Y(N)
K=1
8 IF(X(K)-XX)2,3,4
2 IF(K=N)5,6,6
5 K=K+1
GO TO 8
3 YY=Y(K)
GO TO 9
4 DELTA=X(K)-X(K-1)
YY=(XX-X(K-1))/DELTA*(Y(K)-Y(K-1))+Y(K-1)
GO TO 9
6 YY=Y(N)
9 CONTINUE
RETURN
END

```

```

SUBROUTINE ALBTD (TEMP,AS)
C
C CALCULATES ALBEDO VALUES FOR A STATION.
C
DATA TLOW,ALOW,THIGH,AHIGH/-6.0,0.6,3.0,0.2/
IF (TEMP.GT.TLOW) GO TO 10
AS=ALOW
RETURN
10 IF (TEMP.LT.THIGH) GO TO 20
AS=AHIGH
RETURN
20 AS=(TEMP-TLOW)/(THIGH-TLOW)*(AHIGH-ALOW)+ALOW
RETURN
END

```

Appendix E

E1. Cloud Transmission Results for Individual Stations

- (a) uncorrected data
- (b) corrected data
- T mean transmittance
- $\sigma T$  standard deviation
- $\alpha, \beta$  regression constant and coefficient
- R correlation coefficient

	Cloud	$\bar{T}$	$\sigma T$	$\alpha$	$\beta$	R
GOOSE						
(a)	AC	.438	.110	.406	.012	.114
	AS	.474	.097	.421	.017	.204
	CS	.795	.061	.864	-.024	-.456
	CI	.957	.082	.834	.044	.611
	SC	.350	.035	.370	-.007	-.238
	ST	.316	.073	.418	-.036	-.525
	F	.290	.173	-.080	.135	.805
(b)	AC	.345	.084	.365	-.008	-.096
	AS	.340	.061	.340	.0002	.003
	CS	.715	.067	.818	-.036	-.625
	CI	.895	.069	.819	.027	.447
	SC	.269	.029	.318	-.017	-.714
	ST	.243	.057	.353	-.039	-.733
	F	.241	.125	-.019	.098	.802
	Cloud	T	$\rho T$	$\alpha$	$\beta$	R
CHARLOTTETOWN						
(a)	AC	.369	.049	.405	-.013	-.319
	AS	.403	.115	.513	-.046	-.351
	CS	.733	.099	.711	.011	.074
	CI	.874	.111	1.079	-.109	-.588
	SC	.367	.023	.387	-.007	-.349
	ST	.284	.052	.318	-.012	-.276
	F	.269	.044	.269	.0001	.002

CHARLOTTETOWN  
(continued)

(b)	AC	.269	.041	.359	-.023	-.634
	AS	.304	.073	.385	-.034	-.409
	CS	.648	.094	.712	.031	-.231
	CI	.849	.112	1.062	-.113	-.611
	SC	.289	.024	.332	-.014	-.729
	ST	.231	.040	.273	-.015	-.430
	F	.230	.039	.231	.0002	-.005
	Cloud	$\bar{T}$	$\sigma T$	$\alpha$	$\beta$	R

MONTREAL

(a)	AC	.360	.067	.327	.011	.204
	AS	.414	.087	.493	-.030	-.355
	CS	.734	.034	.702	.013	.405
	CI	.846	.047	.879	-.016	-.249
	SC	.265	.061	.218	.016	.320
	ST	.224	.062	.236	-.005	-.075
	F	.406	.109	.541	-.046	-.438
(b)	AC	.287	.052	.286	.0004	.009
	AS	.320	.074	.419	-.037	-.523
	CS	.672	.038	.663	.003	.096
	CI	.795	.045	.843	-.023	-.388
	SC	.208	.053	.188	.007	.154
	ST	.176	.051	.208	-.012	-.245
	F	.343	.092	.472	-.044	-.495
	Cloud	$\bar{T}$	$\sigma T$	$\alpha$	$\beta$	R

TORONTO

(a)	AC	.380	.041	.407	-.010	-.271
	AS	.443	.074	.461	-.007	-.096
	CS	.730	.053	.820	-.036	-.660
	CI	.877	.028	.848	.013	.402
	SC	.327	.048	.348	-.007	-.179
	ST	.274	.050	.238	.014	.299
	F	.246	.062	.226	.007	.133
(b)	AC	.309	.033	.362	-.020	-.661
	AS	.345	.056	.393	-.019	-.333
	CS	.683	.054	.775	-.036	-.664
	CI	.836	.025	.838	-.001	-.021
	SC	.260	.033	.297	-.013	-.464
	ST	.216	.033	.203	.005	.168
	F	.210	.053	.195	.005	.117

	Cloud	$\bar{T}$	$\sigma T$	$\alpha$	$\beta$	R
WINNIPEG						
(a)	AC	.476	.101	.331	.051	.587
	AS	.509	.083	.429	.031	.438
	CS	.817	.054	.871	-.021	-.387
	CI	.863	.053	.845	.007	.132
	SC	.429	.058	.313	.041	.813
	ST	.392	.057	.298	.033	.673
	F	.428	.119	.441	-.005	-.035
(b)	AC	.365	.065	.284	.029	.511
	AS	.376	.044	.374	.001	.016
	CS	.752	.054	.831	-.031	-.570
	CI	.810	.051	.830	-.008	-.159
	SC	.313	.019	.287	.009	.568
	ST	.288	.026	.256	.011	.483
	F	.348	.097	.388	-.014	-.128

## Appendix E.2

Mean Seasonal Cloud Type Transmittances (uncorrected data).

	1	2	3	4 *
<u>AC</u>				
Goose	.594	.451	.211	.385
Charlottetown	.504	.339	.312	.376
Montreal	.510	.363	.284	.285
Toronto	.546	.370	.348	.288
Winnipeg	.656	.479	.267	.380
Pooled	.566	.396	.297	.337
<u>AS</u>				
Goose	.518	.477	.316	.424
Charlottetown	.519	.396	.384	.419
Montreal	.484	.371	.345	.381
Toronto	.520	.442	.330	.350
Winnipeg	.603	.530	.235	.384
Pooled	.542	.456	.314	.388
<u>SC</u>				
Goose	.429	.388	.253	.300
Charlottetown	.436	.386	.363	.304
Montreal	.291	.239	.273	.207
Toronto	.406	.302	.334	.268
Winnipeg	.592	.409	.332	.340
Pooled	.435	.353	.320	.291
<u>ST</u>				
Goose	.462	.374	.252	.285
Charlottetown	.411	.286	.276	.234
Montreal	.260	.174	.350	.205
Toronto	.315	.279	.210	.182
Winnipeg	.497	.364	.371	.309
Pooled	.412	.314	.290	.267

\* Winter  
Spring  
Summer  
Autumn

## Appendix E.3

## Mean Seasonal Cloud Type Transmittances (corrected data)

	1	2	3	4
<u>AC</u>				
Goose	.406	.360	.187	.346
Charlottetown	.354	.289	.276	.332
Montreal	.357	.304	.253	.250
Toronto	.396	.316	.311	.252
Winnipeg	.455	.376	.137	.315
Pooled	.397	.327	.264	.290
<u>AS</u>				
Goose	.353	.340	.281	.318
Charlottetown	.349	.306	.340	.358
Montreal	.338	.293	.309	.341
Toronto	.373	.355	.292	.314
Winnipeg	.409	.403	.209	.325
Pooled	.374	.348	.279	.329
<u>SC</u>				
Goose	.339	.305	.221	.242
Charlottetown	.310	.304	.318	.255
Montreal	.207	.189	.240	.174
Toronto	.300	.250	.293	.262
Winnipeg	.386	.314	.291	.262
Pooled	.304	.278	.201	.237
<u>ST</u>				
Goose	.289	.279	.221	.241
Charlottetown	.313	.237	.242	.204
Montreal	.184	.133	.307	.175
Toronto	.236	.226	.184	.156
Winnipeg	.323	.280	.327	.243
Pooled	.282	.247	.254	.217